UNIVERSIDADE ESTADUAL PAULISTA
"JÚLIO DE MESQUITA FILHO"
Campus de São José do Rio Preto

Luciana Puia Moro Zanin

Novos Peptídeos Sintéticos e Estudo da Interação com Membranas Modelo: Efeito de Modificações no N-terminal na Atividade Lítica e Antimicrobiana.

São José do rio Preto

2014

Luciana Puia Moro Zanin

Novos Peptídeos Sintéticos e Estudo da Interação com Membranas Modelo: Efeito de Modificações no N-terminal na Atividade Lítica e Antimicrobiana.

Tese apresentada para obtenção do título de Doutor, junto ao Programa de Pós-Graduação em Biofísica Molecular, do Instituto de Biociências, Letras e Ciências Exatas da Universidade Estadual Paulista "Júlio de Mesquita Filho", Campus de São José do Rio Preto.

Orientador: Prof. Dr. João Ruggiero Neto

São José do Rio Preto

2014

Zanin, Luciana Puia Moro.
Novos peptídeos sintéticos e estudo da interação com membranas modelo : efeito de modificações no N-terminal na atividade lítica e antimicrobiana / Luciana Puia Moro Zanin. – São José do Rio Preto, 2014
93 f. : il., tabs.

Orientador: João Ruggiero Neto
Tese (Doutorado) – Universidade Estadual Paulista "Júlio de Mesquita Filho", Instituto de Biociências, Letras e Ciências Exatas

1. Biologia molecular. 2. Biofísica. 3. Dinâmica molecular. 4. Peptídeos antibióticos. 5. Agentes antiinfecciosos. 6. Membranas (Biologia) I. Ruggiero Neto, João. II. Universidade Estadual Paulista "Júlio de Mesquita Filho". Instituto de Biociências, Letras e Ciências Exatas. III. Título.

CDU – 577.3

Ficha catalográfica elaborada pela Biblioteca do IBILCE
UNESP - Câmpus de São José do Rio Preto

Luciana Puia Moro Zanin

Novos Peptídeos Sintéticos e Estudo da Interação com Membranas Modelo: Efeito de Modificações no N-terminal na Atividade Lítica e Antimicrobiana.

Tese apresentada para obtenção do título de Doutor, junto ao Programa de Pós-Graduação em Biofísica Molecular, do Instituto de Biociências, Letras e Ciências Exatas da Universidade Estadual Paulista "Júlio de Mesquita Filho", Campus de São José do Rio Preto.

Banca Examinadora

Prof. Dr. João Ruggiero Neto

UNESP - São José do Rio Preto

Orientador

Prof[a]. Dr[a]. Margarete Teresa Gottardo de Almeida

FAMERP- São José do Rio Preto

Prof[a]. Dr[a]. Mara Corrêa Lelles Nogueira
FAMERP- São José do Rio Preto

Prof[a]. Dr[a]. Fátima Pereira de Souza

UNESP – São José do Rio Preto

Prof. Dr. Prof. Dr. Fernando Alves de Melo

UNESP – São José do Rio Preto

São José do Rio Preto

20/junho/2014

Agradecimentos

Primeiramente, gostaria de agradecer à DEUS pela vida, por ter me proporcionado mais esta oportunidade tão enriquecedora e por colocar no meu caminho tantas pessoas que de diferentes formas me ajudaram a chegar até aqui, e às quais algumas aqui agradeço:

Ao Professor João Ruggiero Neto pela orientação e dedicação ao trabalho e pela paciência que teve durante esse período devido ao nascimento de minhas duas filhas Rebeca e Helena;

Ao Professor Amando Siuiti Ito que se empenhou em me ajudar a produzir o primeiro artigo. Sempre muito prestativo e paciente;

Ao amigo Wallance Moreira Pazin que me ajudou nos experimentos realizados na USP de Ribeirão Preto e que sempre está de bom humor, mesmo sanando dúvidas pelo telefone;

Ao Professor e amigo Alexandre Suman de Araujo que tem um coração enorme e me ajudou a produzir o segundo manuscrito, sem ele não seria possível;

A todos os amigos do departamento pelas conversas e pelo companheirismo;

Aos Professores e amigos Sidney Jurado de Carvalho e Leandro Cristante de Oliveira pelas noites de reflexões ao som de uma boa música em um bom bar chamado Vila Dionísio;

A amiga Sabrina Costa Broggio que me ajudou a iniciar esse trabalho. Juntas também inicioamos o prazer de ser mãe, hora discutíamos sobre peptídeos hora sobre a maternidade. Obrigado pelas "férias" em Valência na Espanha;

A Professora Mara Nogueira que possibilitou os experimentos biológicos na FAMERP;

Aos amigos de laboratório em especial a Natalia Leite Bueno que sempre foi muito atenciosa comigo discutindo experimentos e dúvidas teóricas;

Aos meus PAIS, que tanto se sacrificaram para que eu chegasse onde estou e a minha irmã. Sem vocês jamais conseguiria;

Ao amor da minha vida Alexandre Zanin que sempre me apoiou com seu enorme companheirismo e compreensão;

As minhas filhas Rebeca e Helena, que são as coisas mais importantes na minha vida e a minha melhor conquista nesses anos de doutorado;

A Capes pelo apoio financeiro durante o período do doutorado;

A FAPESP pelos recursos que viabilizaram a pesquisa.

Enfim, agradeço a todos que contribuíram direta e indiretamente para que esse trabalho fosse concluído.

RESUMO

Peptídeos antimicrobianos (PAMs) são componentes do sistema imune inato, que estão presentes na maioria dos organismos vivos cujo interesse é crescente devido à sua potente atividade antimicrobiana contra uma vasta gama de microrganismos, juntamente com a sua baixa toxicidade, em geral, para as células de mamíferos. Esse trabalho teve a finalidade de desenvolver um peptídeo antimicrobiano curto com as mesmas características estruturais do peptídeo Polybia-MP1 (IDWKKLLDAALQIL-NH2) extraído da vespa *Polybia paulista* que conferem ação antimicrobiana e seletividade, tais como: o posicionamento relativo dos resíduos de aminoácidos carregados, um resíduo ácido na posição N-terminal, a hidrofilicidade e a ampla face polar. Foi idealizado e sintetizado um peptídeo denominado L1A (IDGLKAIWKKVADLLKNT-NH2) e dois análogos com modificações na região do N-terminal; um acetilado (Ac-L1A) e outro com o ácido orto-aminobenzóico (Abz), uma sonda fluorescente extrínseca, ligado covalentemente ao N-terminal, esse peptídeo teve o triptofano substituído por um resíduo de valina (Abz-L1A-W8V). Analisou-se a fluorescência estática e dinâmica do triptofano e do Abz, que apresentaram significante deslocamento quando os peptídeos são adsorvidos em vesículas lipídicas; a supressão da fluorescência por acrilamida mostrou que os fluoróforos em vesículas aniônicas estão menos expostos ao solvente do que em vesículas zwitterionicas. A atividade lítica em vesículas a partir das curvas de dose-resposta também reforça que os três peptídeos são mais eficientes em vesículas aniônicas, além disso, que os análogos foram mais eficientes. Estas observações foram compatíveis com o maior teor helicoidal (observado em dinâmica molecular e dicroísmo circular) seus fluoróforos se enterram mais profundamente em vesícula aniônica. Dados de MD e CD demonstraram uma relação entre a estabilidade da hélice e a ausência de carga no N-terminal. L1A e Ac-L1A apresentam potente ação antimicrobiana além de seletividade contra bactérias Gram negativas sem efeito tóxico para eritrócitos (não hemolítico).

Palavras-chave: Peptídeos antimicrobianos. Interações peptídeo-membrana. Atividade lítica. Dinâmica Molecular.

ABSTRACT

Antimicrobial peptides (AMPs) are components of the innate immune system, which are present in the majority of the living organisms and whose interest is growing due to their potent antimicrobial activity against a broad range of microorganisms, coupled with their usually low toxicity to mammalian cells. In an effort to develop short antimicrobial peptides with the same structural characteristics that imparted selectivity to Polybia-MP1 (IDWKKLLDAALQIL-NH2): the relative positioning of acid and basic residues, an acid residue at the N-terminus, hydrophilicity and the broad polar face. MP1 is a potent antimicrobial, antitumoral and non-hemolytic peptide. We generated a peptide named L1A (IDGLKAIWKKVADLLKNT-NH2) and two analogs with N-terminus modifications; one acetylated (Ac-L1A) and other was extrinsic fluorescent labeled with *ortho*-aminobenzoic acid (Abz) in which the tryptophan was substituted by valine (Abz-L1A-W8V). We analyzed static and time-resolved fluorescence of tryptophan and *ortho*-aminobenzoic acid were used and showed significant blue shift when peptides are adsorbed in lipid vesicles and the fluorescence quenching by acrylamide showed that fluorophores in anionic vesicles, are less exposed to the solvent than in neutral vesicles. The lytic activity in vesicles showed from dose-response curves that the three peptides were more efficient in anionic vesicles moreover that the analogs were more efficient. These observations were compatible with the higher helical content (observed in Molecular Dynamics and Circular Dichroism) and deeper burying of the fluorophores in anionic vesicle. MD and CD data demonstrated a relationship between the stability of the helix and the absence of load on the N-terminal. L1A and Ac-L1A presented potent antimicrobial selective against Gram negative bacteria without being hemolyitic while Abz -L1A -W8V was mildly hemolytic.

Keywords: Antimicrobial peptides. Peptide-membrane interactions. Lytic activity. Molecular Dynamics simulations.

Sumário

APRESENTAÇÃO

A presente tese está dividida em duas partes ou artigos, onde a ideia principal foi construir peptídeos com potencial antimicrobiano e não hemolítico. Para tal, utilizou-se como base a sequência do peptídeo antimicrobiano purificado da vespa *Polybia paulista* (MPI) I ^{1}D^{2} W^{3} K^{4} K^{5} L^{6} L^{7} D^{8} A^{9} A^{10} K^{11} Q^{12} I^{13} L^{14} - NH2 (14 resíduos de aminoácidos). Para desenvolver o trabalho foram sintetizadas três sequências de peptídeos baseados em características como: i) a importância das posições e do balanço de cargas dos resíduos de aminoácidos do MP-1 e seu momento hidrofóbico, para manter um conteúdo helicoidal; ii) a presença de resíduo ácido na região do N-terminal importante para a seletividade; resultando em um peptídeo com espectro bactericida, não hemolítico e pouco citotóxico como MP-1.

Tem-se como base que o peptídeo construído deve possuir uma fraca interação com as bicamadas zwitteriônicas e consequentemente forte interação com as bicamadas aniônicas. As membranas bacterianas caracterizam-se por serem organizadas de tal forma que a face externa da bicamada lipídica, voltada para o meio extracelular, possui alto conteúdo de fosfolipídeos carregados negativamente, enquanto a mesma face da membrana plasmática dos mamíferos (eucariotos) é composta majoritariamente por fosfolipídeos neutros, como fosfatidilcolina e esfingomielina, estando os fosfolipídeos aniônicos, como fosfastidilserina e fosfatidilglicerol, voltados para o interior da célula.

O par de peptídeos sintetizados primeiramente foi: I^{1}D^{2}G^{3}L^{4}K^{5}A^{6}I^{7}W^{8}K^{9}K^{10}V^{11}A^{12}D^{13}L^{14}L^{15}K^{16}N^{17}T^{18}-NH2 (L1A) (Figura 1A) e Abz-IDGLKAIVKKVADLLKNT-NH2 (Abz-L1A-W8V) (Figura 1B). Ambos possuem dois resíduos ácidos (D2 e D13) e quatro básicos (K5, K9, K10 e K16) formando pareamento iônico entre o terceiro e quarto resíduo vizinho, que mantem um conteúdo helicoidal. Fato importante demonstrado no MP-1 com a presença de dois resíduos ácidos (D2 e D8) concomitantemente com três resíduos ácidos (K4, K5 e K11), que somados ao C-terminal amidado resulta em uma carga Q=+2. A escolha dos resíduos e suas posições mantiveram o ângulo polar (140°) e hidrofobicidade média (<H>=-0.11) similar ao do modelo MP-1, 120 e <H>=-0.1 respectivamente, porém com diferente carga (Q=+3) devido ao acréscimo de uma lisina. Os peptídeos também possuem um acréscimo no número de resíduos (18 resíduos de aminoácidos) diferentes do MP-1.

O análogo Abz-IDGLKAIVKKVADLLKNT-NH2 (Abz-L1A-W8V) foi sintetizado para explorar o efeito de carga no N-terminal. O peptídeo possui uma sonda

extrínseca no N-terminal para neutralizar os efeitos da carga positiva do NH3 do mesmo, com isso ocorre consequentemente redução da carga do peptídeo para Q=+2 como no MP-1. A importância dessa sonda foi aprofundar nos estudos dos efeitos de carga no N-terminal: estabilidade da estrutura secundária, interação do peptídeo com bicamadas e atividade antimicrobiana do peptídeo (seletividade).

O MP-1 possui arranjo dos resíduos carregados em dois clusters, o primeiro envolvendo Asp2, Lys4, Lys5 e N-terminal o outro é formado pelo resíduo de Asp8 e Lys11, posicionados formando pareamento de íons e pontes e de hidrogênio. Esse equilíbrio de carga minimiza os efeitos eletrostáticos da carga positiva no N-terminal proporcionando maior estabilidade da estrutura helicoidal e juntamente com demais características como ângulo polar e hidrofobicidade, melhor interação e seletividade.

O ácido orto amino benzoico (Abz) está ligado covalentemente ao N-terminal. Essa molécula foi escolhida devido a suas características estruturais, de modo que não interferisse na estrutura do peptídeo (volume) e seu alto rendimento quântico (Φ= 0.6). O rendimento quântico é proporcional à intensidade do sinal, quanto maior o seu valor maior a precisão nas medidas experimentais. Outra modificação desse peptídeo é a troca do resíduo de triptofano (W8) por um de valina (V8), tentando preservar as mesmas características ao longo da cadeia e apenas avaliar a modificação em torno do N-terminal. Essa troca se fez necessária para evitar que o peptídeo tivesse duas sondas fluorescentes, uma intrínseca e outra extrínseca.

Tornou-se necessária à síntese de um terceiro peptídeo: Ac-IDGLKAIWKKVADLLKNT-NH2(Ac-L1A), com a finalidade de neutralizar o N-terminal sem modificações estruturais significativas causadas pelo mesmo e com a mesma sequência original. Nesse peptídeo a sequência é idêntica ao do L1A, porém com a ligação do acetil no N-terminal, ou seja, com neutralização da carga positiva do N-terminal como o Abz-L1A.

Os peptídeos foram sintetizados pelo grupo da Prof. Dra. Maria Aparecida Juliano na Universidade Federal de São Paulo (UNIFESP) utilizando o método em fase sólida. A concentração dos peptídeos foi determinada espectrofotometricamente utilizando o coeficiente de extinção molar ε= 5675 M^{-1} e 1998 M^{-1} para peptídeos contendo triptofano e Abz respectivamente. O Abz tem sido intensamente empregado como sonda fluorescente no estudo de peptídeos e membranas e o entendimento dos efeitos de solvente sobre suas propriedades espectroscópicas apresenta grande interesse científico.

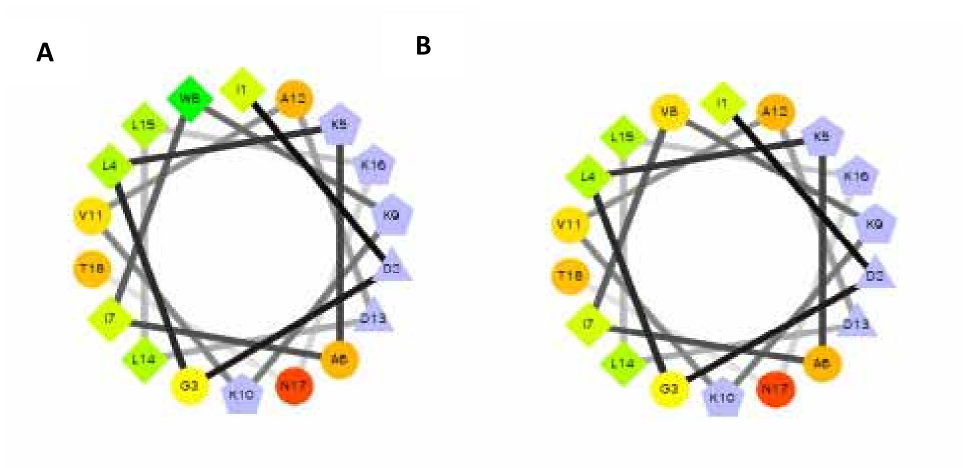

Figura 1. Projeção helicoidal do peptídeo, A) IDGLKAIWKKVADLLKNT-NH2 (L1A) e B) Abz-IDGLKAIVKKVADLLKNT-NH2(Abz-L1A-W8V).

Os filmes lipídicos que foram utilizados no trabalho são compostos por POPC (palmitoil-oleil-fosfatidilcolina) (Figura 2A) e a mistura POPC/POPG (8:2) contendo além de POPC o palmitoil-oleoil-fosfatidilglicerol (POPG) (Figura 2B).

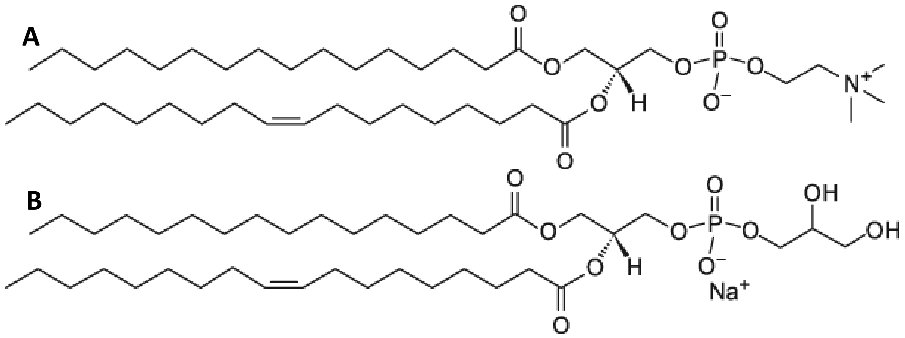

Figura 2. Estrutura do fosfolípideo, A) palmitoil-oleil-fosfatidilcolina (POPC) de caráter zwitteriônico; B) palmitoil-oleoil-fosfatidilglicerol (POPG) de caráter de caráter aniônico.

A primeira parte desta dissertação, denominada “INTERACTION OF A SYNTHETIC ANTIMICROBIAL PEPTIDE WITH MODEL MEMBRANE BY FLUORESCENCE SPECTROSCOPY”, descreve experimentos de espectroscopia de fluorescência estática e com resolução temporal. Diversos parâmetros fluorescentes são utilizados: intensidade ou rendimento quântico, espectros de emissão e excitação, anisotropia de fluorescência e cinética de decaimento. Através destes espectros também foi possível calcular o deslocamento espectral ($\Delta\lambda$) para menores comprimentos de onda (*Blue Shift*), na presença de cada concentração vesícula POPC e POPC/POPG, respectivamente. O deslocamento espectral observado na passagem da sonda de um meio aquoso para um meio menos polar (bicamada lipídica) ocorre simultaneamente a

um aumento na intensidade de fluorescência, refletindo a diminuição da ocorrência de desexcitação por processos colisionais com moléculas de água. Os três peptídeos demonstraram ser adsorvidos nas membranas modelos tanto em POPC quanto em POPC/POPG, demonstrando o importante papel da hidrofobicidade.

Para melhor caracterizar o deslocamento do peptídeo para a face hidrofóbica da bicamada foram realizados experimentos de supressão de fluorescência, para obter informações sobre a acessibilidade do supressor (Acrilamida) à sonda de intrínseca (W) e a extrínseca (Abz) na cadeia peptídica. Em tampão observou-se uma maior acessibilidade da acrilamida às sondas com discreta diferença entre os três peptídeos. Essa acessibilidade se mostra menor quando em vesículas, mais pronunciadas em POPC/POPG (aniônica) se comparada com POPC (zwitteriônica), sugerindo que os peptídeos são adsorvidos na membrana e que a carga da vesícula é um fator importante. Os peptídeos análogos com modificação no N-terminal possuem uma menor acessibilidade se comparado com o peptídeo L1A.

A anisotropia estática foi determinada por meio das componentes paralela e perpendicular da emissão quando o fluoróforo (W ou Abz) é excitado com feixe polarizado nestas direções. Se a molécula tem movimentação restrita, o grau de despolarização da radiação incidente é menor que no caso em que a grande liberdade de movimento, como demonstrado com os peptídeos em tampão. Com a adição de vesículas o meio se torna ainda mais restrito, aumentando os valores de anisotropia devido às restrições ao movimento do peptídeo. Os peptídeos análogos de menor carga apresentam uma maior restrição em vesículas zwitteriônicas (POPC) do que o L1A (Q=+3), demonstrando o feito de carga. Com exceção do L1A a anisotropia atinge valores próximos em vesícula aniônica (POPC/POPG), porém L1A tem uma queda no valor da anisotropia, reforçando os experimentos de supressão. Com a finalidade de obter as isotermas de associação do peptídeo em vesículas foram realizados experimentos de titulações fluorimétricas. O peptídeo Abz-L1A (Q=+2) apresenta significativo aumento do coeficiente de partição que o análogo Ac-L1A(Q=+2) e L1A (Q=+3), indicando ser o peptídeo mais adsorvido.

O decaimento de fluorescência e a anisotropia de fluorescência resolvida no tempo foram realizados utilizando o método de contagem de fóton único correlacionados no tempo. Os peptídeos que possuem a sonda intrinseca (W) apresentam três tempos de

vida similares em tampão (maior para L1A), porém apresentam diferenças no fator pré-exponencial e a contribuição do tempo de vida longo é maior para L1A. Diferenças no fator pré-exponencial sugere que a acetilação pode induzir mudanças estruturais que afetam a interação do fluoróforo com o solvente ou a distribuição dos rotameros de triptofano. Porém o tempo de vida médio é maior para o peptídeo acetilado, 3.8ns se comparado com 3.6ns para L1A.

O peptídeo que contém a sonda extrínseca Abz (Abz-L1A-W8V), apresentou melhor ajuste aos dados experimentais com dois tempos de vida, relacionados a dois isomeros do fluoróforo, o tempo de vida longo ocorre predominante durante 89% do total de emissao em tampão. Quando em contato com vesículas POPC ou POPC/POPG a inserção do peptídeo na bicamada lipídica não provoca mudança significativa no equilibrio dos isômeros de Abz no peptídeo, como sugerido pela similaridade do fator pré-exponencial.

A anisotropia de fluorescência resolvida no tempo reforça a observação que os peptídeos se movem de um meio polar para outro meio menos polar, além de significante aumento do tempo de correlação longo acompanhado do aumento dos valores da anisotropia residual.

O potencial zeta foi mensurado pela mobilidade eletroforética de vesículas aniônicas (POPC/POPG) na presença de diferentes concentrações de peptídeo. Utilizou-se dessa técnica não espectroscópica para melhor compreender a afinidade dos peptídeos análogos de menos carga (Q=+2) pela vesícula aniônica, corroborando com dados de fluorescência e reafirmando a importância da carga na regiao N-terminal diminuindo a repulsão do potencial dipolo da bicamada. Artigo publicado em “European Biophysics Journal”.

Na segunda parte, denominada “LYTIC AND BIOLOGICAL ACTIVITIES AND SELECTIVITY OF A NOVEL SYNTHETIC ANTIMICROBIAL PEPTIDE”, realizou-se experimentos de dinâmica molecular (MD), dicroísmo circular (CD), atividade lítica e biológica, além de fluorescência. As vesículas unilamelares grandes (LUVs) foram utilizadas na realização dos experimentos de extravasamento (atividade lítica), titulação fluorimétrica, supressão de fluorescência (W/Abz) por acrilamida e medidas de potencial zeta enquanto as vesículas unilamelares pequenas (SUVs) foram utilizadas na realização dos experimentos de dicroísmo circular para reduzir os efeitos de espalhamento de luz.

Através da dinâmica molecular podemos observar que o novo peptídeo (L1A) possui uma distribuição de seus resíduos em dois clusters. O primeiro envolve Asp2, Lys5 e o segundo composto por Asp13, Lys9, Lys10, Lys16 e Asn17, comportamento similar ao MP1. Através de ferramentas da dinâmica a nova sequencia foi criada procurando manter comportamentos do MP1, usando o posicionamento dos resíduos hidrofóbicos e hidrofílicos na cadeia peptídica, para aperfeiçoar a estrutura anfipática. A hidrofobicidade média (<H>=-0.1) e o momento hidrofóbico (μ=0.36) foram calculados usando escala de consenso de Eisenberg. A composição de hélice (40-45%) verificada em dinâmica molecular após 50ns (30% de TFE) corrobora com dados de dicroísmo circular. Analisando as distancias entre o NH de um resíduo com o CO do quarto resíduo vizinho (i, i+4) simultaneamente com o ângulo diedral da cadeia (φ,ψ) pode ser observado 7 pontes de hidrogênio estáveis durante mais de 70% do tempo de simulação.

Os análogos com modificação no N-terminal possuem acréscimo da uma ligação de hidrogênio entre I1-K, estável entre 80-90% do tempo. O peptídeo Abz-W8V-L1A apresenta ligação de hidrogênio entre Abz-Leu4, o mesmo não ocorre com Acetil em Ac-L1A. Podemos verificar que quando o N-terminal não está carregado, como é o caso dos análogos, ocorre uma estabilização da hélice com 10-11 ligações de hidrogênio mantidas por mais de 80% do tempo (50ns).

A atividade lítica dos peptídeos em vesícula aniônica e zwitteriônica foi monitorada usando espectrofluorímetro. A interação de peptídeos com vesículas contendo carboxifluoresceína (CF) foi monitorada pelo aumento da fluorescência causado pela ruptura destas vesículas; a CF, quando em alta concentração, tem sua fluorescência auto-suprimida e fluoresce mais intensamente pela diluição que sofre ao ser liberada do interior das vesículas pela ação de peptídeos ou detergentes. Portanto na razão de 50% ([P]/[L]) indica que os peptídeos são mais eficientes em vesículas aniônicas, demonstrando a importância da carga da vesícula para seletividade do peptídeo e que a redução da carga no N-terminal é favorável à permeabilização.

Espectros de dicroísmo circular foram coletados no ultra-violeta distante (abaixo de 260 nm) na ausência e presença de vesículas com a finalidade obter informações estruturais dos peptídeos, podendo estimar a porcentagem de cada elemento estrutural secundário como: hélice α, folha β e estruturas desordenadas. Podemos avaliar as modificações estruturais diante as variações do meio utilizando vesículas aniônicas e zwitteriônicas. Os dados de CD demonstram que os análogos que reduzem a carga na

região do N-terminal possuem uma maior estabilidade da hélice. Os dados de CD estão de acordo com os dados de zeta demonstrando que a afinidade dos análogos em vesículas aniônicas é maior se comparado ao L1A.

Para avaliar atividade biológica foram utilizados os seguintes micro-oganismos *Staphylococcus aureus* (ATCC 25923), *Escherichia coli* (ATCC 35218) e *Pseudomonas aeruginosa* (ATCC 27853). A concentração mínima inibitória mostra que os peptídeos são mais eficientes para bactérias Gram negativas. Utilizando *E. coli* para avaliar L1A e MP1 obtivemos valores de MICs de 4,6 e 5,0 respectivamente . Os análogos de menor carga (Q=+2) possuem menor potencial bactericida sugerindo menor interação eletrostática com bicamadas carregadas negativamente.

A atividade hemolítica dos peptídeos foi avaliada através de células do sangue humano de doadores saudáveis. A atividade hemolítica do L1A (4%) e do Ac-L1A (5%) é similar ao do MP1 (5%), baixa se comparado com 100% para melitina no controle. O aumento da atividade hemolítica em Abz- L1A (46%) pode estar relacionado à substituição do resíduo de triptofano por valina, aumentando a hidrofobicidade média da face polar ou mesmo pela ligação do Abz.

1 INTRODUÇÃO

1.1 Peptídeos Antimicrobianos (PAMs).

Durante a evolução, a capacidade de um organismo proteger-se da invasão microbiana ou de outra espécie tem sido um fator chave para a sobrevivência. Todas as espécies, desde bactérias até os seres humanos, resistem à invasão de micro-organismos através de um mecanismo simples, mas complexo em função, envolvendo peptídeos antimicrobianos (PAMs). Esses derivam de precursores de peptídeos através de um ou mais passos de ativação proteolítica (Zasloff, 2002). Prevê-se que cada espécie pode conter uma grande variedade de PAMs (Hancock e Rozek, 2002) e evidências sugerem que estes peptídeos não atuam apenas diretamente combatendo agentes patogênicos, mas também modulam a imunidade inata e ainda fazem uma ponte entre as respostas imunes inatas e adaptativas (Matsuzaki, 2009).

Peptídeos antimicrobianos são moléculas anfipáticas com amplo espectro de atividade antimicrobiana, exibindo múltiplos modos de ação, incluindo bacteriostático, propriedades microbicidas e citolítica (Figura 1) (Pasupuleti et al., 2012).

A maioria dos PAMs possui uma carga líquida entre +2 a +11, devido ao conteúdo de lisina e /ou arginina (Yeaman Yount, 2003) e da ausência ou escassez de ácido aspártico ou glutâmico (Yount e Yeaman, 2005). Possuem uma proporção substancial ($\geq$ 30%) de residuo hidrófobico (Zasloff, 2002) e é amplamente aceito que a cationicidade seja responsável pela interação inicial do PAM com a superfície da membrana bacteriana, carregada negativamente (Yount e Yeaman, 2005).

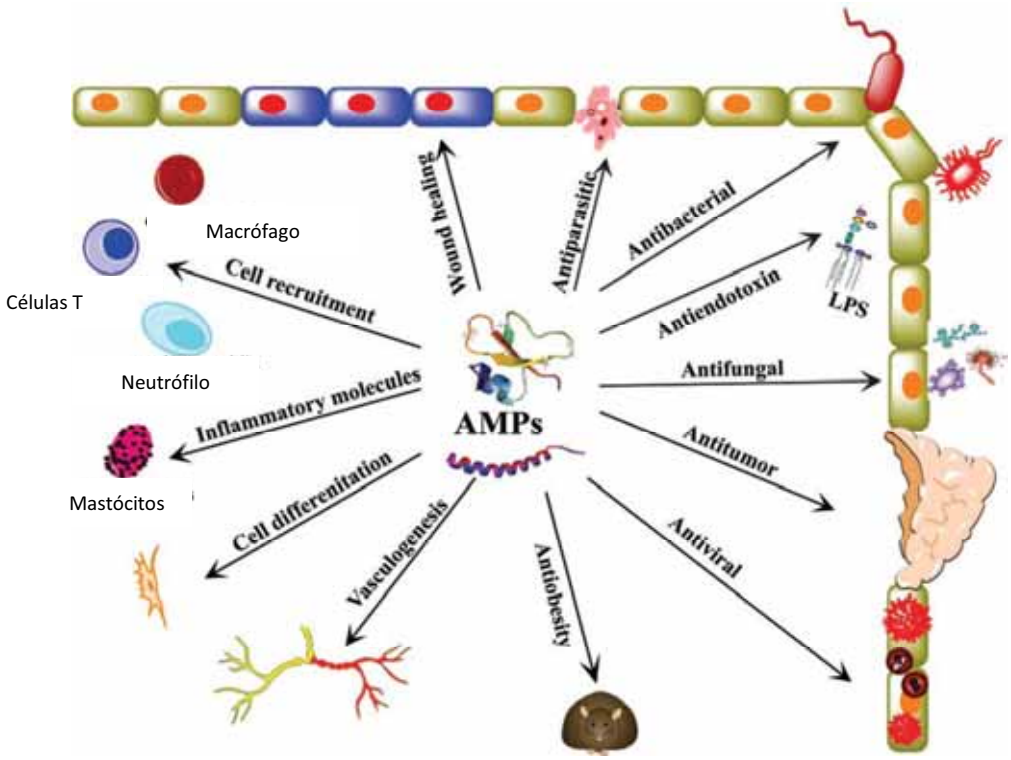

Figura 1. Diferentes funções de PAMs na proteção imunológica do hospedeiro. AMPs podem induzir um grande número de respostas tais como iniciação do mecanismo de cicatrização; genese do sistema vascular, prevenindo o desenvolvimento da obesidade; promovem o recrutamento de leucócitos no local da infecção; a indução do processo de diferenciação celular; a ligação aos LPS e prevenir as respostas pró-inflamatórias. A vantagem global de todas essas funções é a proteção contra infecções, bem como respostas pró-inflamatórias induzidas pelo hospedeiro. Retirada de Pasupuleti et al., 2012.

A diversidade de peptídeos antimicrobianos é tão grande que é difícil categorizá-los exceto, com base na sua estrutura secundária. (Um catálogo on-line dessas moléculas pode ser encontrado em http://www.bbcm.univ.trieste.it/~tossi/antimic.html). O princípio estrutural fundamental de todas as classes é a capacidade da molécula adotar uma forma em que "clusters" de aminoácidos hidrofóbicos e catiônicos são espacialmente organizados em setores discretos da molécula (*design* "anfipático") (Zasloff, 2002) (Figura 2).

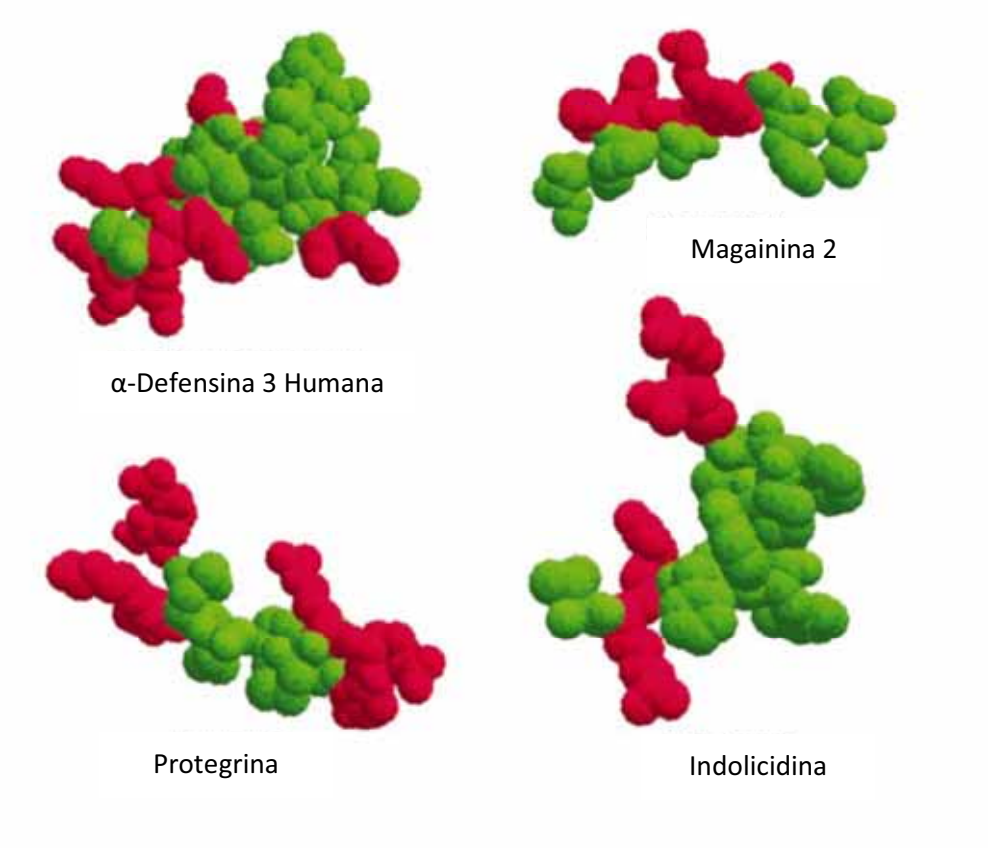

Figura 2. Conjunto de aminoácidos catiônicos e hidrofóbicos em distintos domínios de vários peptídeos antimicrobianos de diferentes classes estruturais. Este "*desing*" anfipático é evidente em muitos, mas não em todos os peptídeos antimicrobianos. Em vermelho: aminoácidos básicos (positivamente carregado); verde: aminoácidos hidrofóbicos. Outros aminoácidos não são mostrados. Magainina está representada na sua conficuração α-helicoidal. Retirada de Zasloff, 2002.

Peptídeos antimicrobianos são classificados em quatro grandes grupos de acordo com sua estrutura secundária, proposto por van't Hof et al. (2001):

Grupo I: peptídeos lineares com estrutura α-helicoidal (Figura 3A). Ex. magainina, cecropina A, além de um número de peptídeos antimicrobianos "projetados" (Mangoni et al., 2000). Esses peptídeos não possuem estruturas secundárias em solução aquosa, enquanto que após a interação com solventes hidrofóbicos ou bicamadas apresentam-se em conformação α-helicoidal. São muitas vezes considerados anfipáticos e podem adsorver sobre a superfície da membrana ou se inserem na membrana como um conjunto de feixes helicoidais. A maioria dos peptídeos anfipáticos helicoidais são catiônicos e apresentam toxicidade seletiva para os micróbios (Zhao et al., 2002). Há também peptídeos helicoidais hidrofóbicos ou ligeiramente aniônicos, por ex.

alameticina (Kikukawa e Aralso, 2002). Esses peptídeos expõe menos seletividade para os micróbios em comparação com células de mamíferos e formam clusters de hélices que atravessam a bicamada, formando um poro aquoso de transporte de íons (Sansom, 1993).

Grupo II: peptídeos conformacionalmente mais restritos (ciclicos), majoritariamente compostos por filamentos β ligados por ligações de dissulfeto intramoleculares (Figura 3B), como por exemplo, a β-defensina-2 humana (Hancock, 2001), taquiplesinas (Matsuzaki, 1999), protegrinas (Harwig et al., 1995), e lactoferricina (Jones et al., 1994), ou por ciclização do esqueleto do peptídeo, tal como no caso de gramicidina S (Prenner et al., 1999), polimixina B (Zaltash et al., 2000). Eles existem em grande parte na conformação em folha-β. Estudos detalhados indicaram que a substituição dos resíduos de cisteína por aminoácidos como Ala e Asp conduz a uma inativação do peptídeo enquanto que os análogos com resíduos aromáticos Phe, Tyr e aminoácido hidrofóbico como Met e Val retem amplo espectro de atividade antimicrobiana (Tamamura et al.,1998). Estudos com análogos da taquiplesina, em que os grupos SH foram quimicamente protegidos para evitar a ciclização ou cisteínas foram substituídos por resíduo Ala, sugeriram que a estrutura cíclica foi essencial para a atividade antimicrobiana, embora possa não ser crucial para a permeabilização da membrana (Tamamura et al., 1998).

Grupo III: peptídeos lineares com uma estrutura estendida (Figura 3C), caracterizado por ser rico em um ou mais aminoácidos específicos. Por exemplo, o peptídeo histatina, que é produzido na saliva; muito rico em resíduos His (Zhao et al., 2002). Este peptídeo transloca-se através da membrana e interage com a mitocôndria, sugerindo um mecanismo antifúngico (Helmerhorst et al., 1999). Os peptídeos produzidos por neutrófilos porcino são muito ricos em prolina e arginina ou prolina e fenilalanina. Eles pertencem à família de peptídeos antimicrobianos catelicidinas e são chamados PR-39 e profenina, respectivamente (Linde et al., 2001). O triptofano em geral, não é um resíduo de aminoácido abundante em peptídeos ou proteínas. Exemplo de peptídeo antimicrobianos rico em triptofano inclue o indolicidina (ILPWKWPWWPWRR-amida) (Selsted et al., 1992). Vários análogos têm sido sintetizados de modo a satisfazer os requisitos de carga e também a importância dos resíduos de Tyr e Pro para a atividade (Falla et al., 1996).

Grupo IV: peptídeos contendo uma estrutura em “loop” (Figura 3D). Em contraste com outros peptídeos antimicrobianos, estes são ricos em prolina e arginina e não podem formar estruturas anfipáticas. Devido à elevada concentração de resíduos de prolina tem sido proposta uma estrutura helicoidal poliprolina (tipo II) (Cabiaux et al., 1994). Lantibióticos (peptídeos produzidos apenas por bactérias Gram positivas, como Staphylococcus, para matar bactérias Gram positivas) contem pequenas estruturas de anéis fechados por ligação tioetér em sua estrutura (Montville e Chen, 1998). Um dos lantibióticos, nisina, é atualmente utilizado como um agente antimicrobiano de conservação de alimentos e este peptídeo possui elevada atividade contra bactérias Gram-positivas. Peptídeos desta classe possuem potencial considerável para combater doenças infecciosas existentes e emergentes, devido seu tamanho pequeno, serem fácil de sintetizar e proteoliticamente estável.

A) α-Hélice

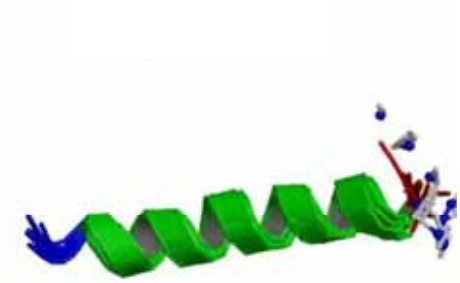

Magainina 2

DOI:10.2210/pdb2mag/pdb

B) Folha β

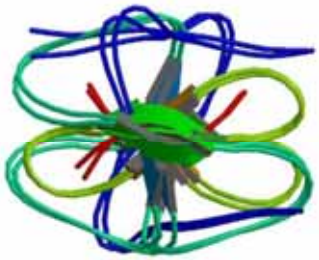

β-Defensina

DOI:10.2210/pdb1kj5/pdb

C) Estrutura Estendida

Indolicidina

DOI:10.2210/pdb1g89/pdb

D) Estrutura em “loop”

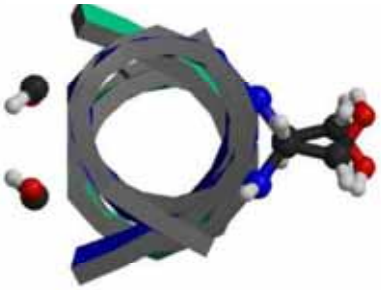

Gramicidina

DOI:10.2210/pdb1mag/pdb

Figura 3. a) Peptídeos α-helicoidals (por exemplo, LL-37, cecropinas ou magalninas); b) Peptídeos β- folhas estabilizadas por duas a quatro ligações dissulfeto (por exemplo, e α-β-defensinas humana, plectasina ou protegrinas); c) Estruturas estendidas ricas em glicina, prolina, triptofano, arginina e/ou histidina (por exemplo, indolicidina); d) Peptídeos com uma ligação de dissulfeto (por exemplo, bactenecina). Peters et al, 2010.

Os ensaios proporcionados por este grande conjunto de pesquisa têm gerado esforço comercial considerável para criar novas classes de antimicrobianos terapêuticos.

1.2 Relações entre Estrutura e Atividade antimicrobiana

A existência de uma ampla diversidade de seqüências e estruturas de peptídeos antimicrobianos ressalta que nenhuma seqüência única emergiu singularmente eficaz contra todos os agentes patogênicos em todas as configurações. Com base no baixo grau de conservação da seqüência específica de PAMs, sugere-se que a termodinâmica desempenha um papel importante na especificidade e mecanismo de ação do peptídeo, uma vez que esta abrange as energias responsáveis para estruturação do peptídeo e a sua adsorção na bicamada. (Tossi et al., 2000).

Forças eletrostáticas (tanto atração coulombiana/repulsão e interações dipolares), formação de ligações de hidrogênio e interações hidrofóbicas possuem papéis igualmente importantes. A interação do peptídeo com a membrana pode ser dividida em três passos termodinâmicos (figura 4).

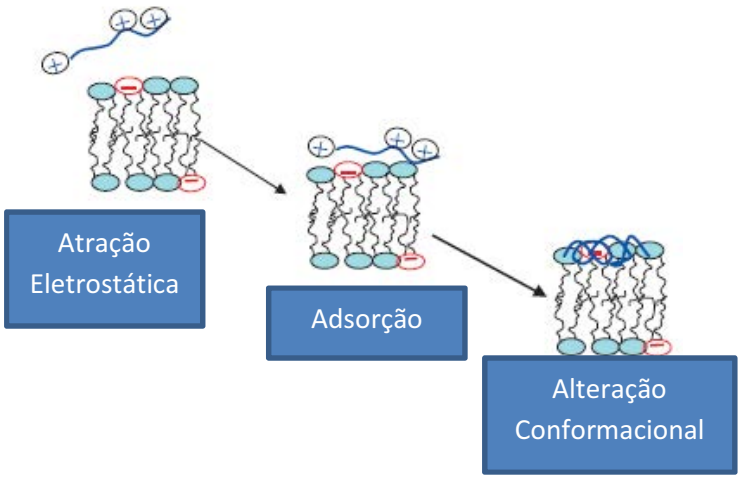

Figura 4. Diferentes fases da ligação do peptídeo na bicamada lipídica. O peptídeo carregado (Q= +3) é atraído electrostáticamente à superfície da membrana, seguido por uma mudança conformacional para α-helice (Retirada de Seelig, 2004).

Apesar de haver uma homologia de sequência limitada entre PAMs mesmo aqueles pertencentes a famílias semelhantes ou isolados a partir do mesmo animal, existe certo grau de conservação de aminoácidos específicos em posições significativas. A conservação na estrutura secundária pode ser a chave para configurações tridimensionais facilitando a atividade antimicrobiana de distintos pepídeos (Yeaman e Yount, 2003).

Peptídeos helicoidais são os mais abundantemente distribuídos e estudados entre os grupos de PAMs, constituindo em torno de 27% de todos os PAMs com estrutura secundária conhecida (Tossi et al., 2000). Muitos desses peptídeos exibem características anfifílicas distintas com cerca de 50% de resíduos hidrofóbicos, freqüentemente aparecendo em padrões repetidos. A maioria das suas atividades parece estar relacionada à interação peptídeo-lipídeo, e provavelmente são moduladas por fatores tais como: a carga elétrica líquida, a hidrofobicidade média, a propensão em formar estrutura helicoidal e o ângulo de face polar (Dathe et al., 2002). Estes determinantes moleculares são interdependentes e, portanto, a modificação de um parâmetro muitas vezes leva a alteração compensatória no outro (Yeaman e Yount, 2003) (Figura 5).

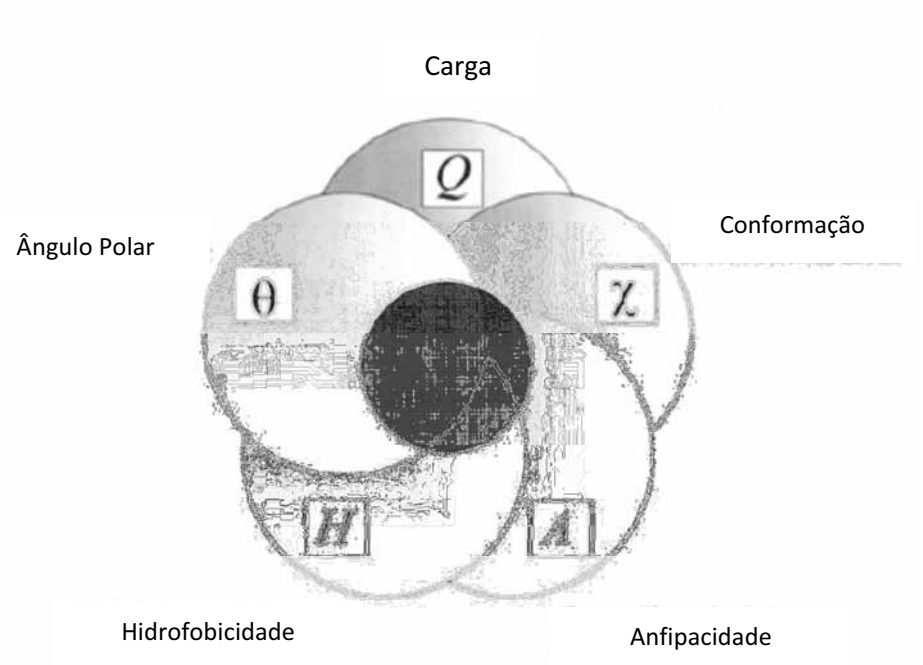

Figura 5. Inter-relação entre os determinantes estruturais dos peptídeos antimicrobianos. Composição fundamental e influências de sequências de aminoácidos não só as propriedades bioquímicas dos peptídeos [carga, (Q), anfipaticidade (A), e hidrofobicidade (H)], mas também regulam a sua configuração tridimensional [por exemplo, conformação, (χ), ângulo polar (θ), e estereogeometria]. Retirada de Yeaman Yount, 2003.

Para assegurar a seletividade do peptídeo antimicrobiano para micro-organismos um valor mínimo de carga se faz necessário, talvez tão baixo como: +2. Esta propriedade é importante para uma série de razões: 1) para uma atração inicial eletrostática de membranas microbianas carregadas negativamente, 2) potencial para deslocar cátions associados à membrana, e 3) um forte gradiente eletroquimico Δψ de diversos micro-organismos pode facilitar as transições de peptídeos catiônicos para a face polar da membrana.

Dentro de um determinado intervalo, o aumento da carga (+) do peptídeo é geralmente associado com o aumento da potência antimicrobiana. No entanto, esta relação não é totalmente linear, com exemplos diretos, indiretos, ou relações inversas entre essas variáveis (Bessalle et al., 1992; Blondelle e Houghten, 1992).

A hidrofobicidade é uma característica essencial para as interações de peptídeos antimicrobianos na membrana, uma vez que rege o quanto um peptídeo pode particionar na bicamada lipídica. Embora a hidrofobicidade seja necessária para permeabilização na membrana, acima de níveis ótimos leva a uma perda da especificidade antimicrobiana e ao aumento da toxicidade em mamíferos (Yount e Yeaman, 2003). A razão para o aumento da toxicidade, de peptídeos altamente hidrofóbicos em células eucarióticas ocorre devido a condições de solubilidade, em solução aquosa, perturbando também membranas celulares eucarióticas (Dennison et al., 2005). Desse modo, uma forte correlação é observada entre a citotoxicidade e hidrofobicidade (Pasupuleti et al., 2008). A hidrofobicidade média é dada pela média aritmética da hidrofobicidade intrínseca dos resíduos, de acordo com a escala de consenso de Eisenberg (Eisenberg et al., 1984) nesta escala o resíduo mais hidrofóbico é a isoleucina <H> = 0,73 e o resíduo menos hidrofóbico é a arginina <H> = - 1,76.

A relação entre hidrofobicidade e anfipaticidade (este último muitas vezes expresso como um momento hidrofóbico pela separação de faces opostas hidrofóbica e

hidrofílica) é o ângulo polar (Φ), uma medida da proporção relativa da face polar e não polar da conformação do peptídeo em uma hélice anfipática (Yount e Yeaman, 2005) como demonstrado na figura 5.

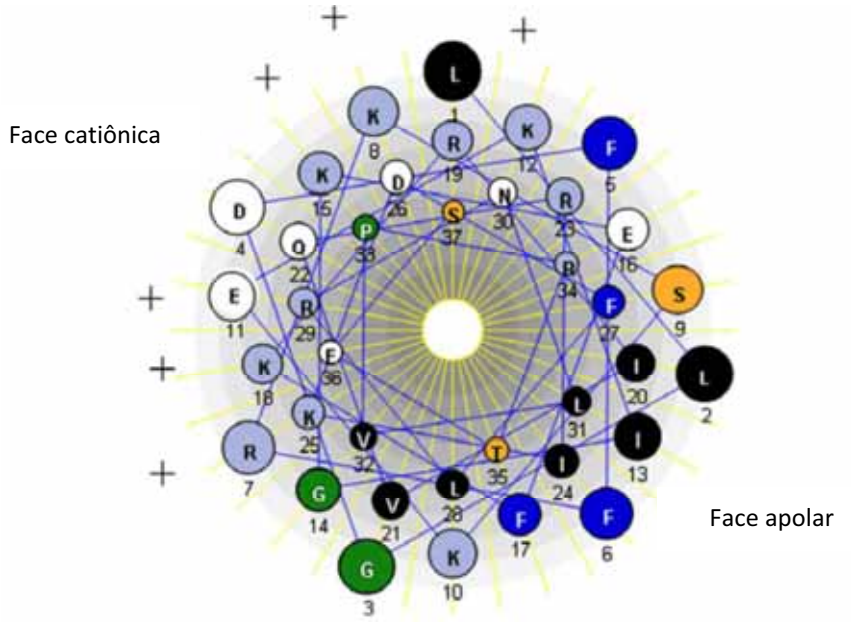

Figura 5. Hélice circular de catelicidina LL-37 em estrutura de α-hélice evidenciando a face polar composta por resíduos de aminoácidos carregados (Face catiônica) e a apolar composta por resíduos polares não carregados e apolares (Face apolar). Caracterizando uma projeção helicoidal anfipática. Retirada e modificada de Gudmundsson (2004).

Um elevado grau de elipticidade e/ou anfipaticidade produzindo uma segregação de domínio hidrofóbico, está correlacionado com o aumento da toxicidade em relação às células compostas de fosfolípidos neutros (Dathe e Wieprecht, 1999). Aumentar o momento hidrofóbico resulta num aumento significativo da permeabilização e atividades hemolíticas dos peptídeos contra a membrana (Yeaman e Yount, 2003).

Em numerosos estudos de peptídeos nativos e sintéticos, menor ângulo polar (maior superfície hidrofóbica) está, em geral, associado com o aumento da capacidade de permeabilização nas membranas (Uematsu e Matsuzaki, 2000). No entanto, pesquisas demonstram que os poros mais estáveis são aqueles formados por peptídeos com maior ângulo polar; isso pode ser resultado de maiores superfícies carregadas e/ou de mais moléculas de peptídeos por canal (Yeaman Yount, 2003).

1.3 A Biologia da Membrana Plasmática

A membrana plasmática, membrana celular ou plasmalema é a estrutura que delimita todas as células vivas, tanto as procarióticas como as eucarióticas. Ela estabelece a

fronteira entre o meio intracelular, o citoplasma, e o ambiente extracelular, que pode ser a matriz dos diversos tecidos. Universalmente, todas as membranas celulares são mosaicos fluidos de proteínas e fosfolípideos, os quais são dispostos em bicamadas com os domínios hidrofóbicos e hidrofílicos. Na matriz lipídica são encontradas moléculas de proteínas, com grande capacidade de movimentação e deslocamento, apresentando significativa importância na retenção e no transporte de outras moléculas através da membrana plasmática, tarefa que realiza de forma seletiva. Em alguns organismos, esteróis e glicerídeos também estão presentes, contribuindo para a topologia da superfície e bioquímica da arquitetura das biomembranas (Yeaman e Yount 2003).

Existem diferenças significativas de composição lipídica entre as membranas procarióticas e eucarióticas, bem como entre os tipos de células (Pasupuleti et al., 2012). Essas diferenças são à base da especifidade e a não toxicidade para mamíferos. Peptídeos antimicrobianos têm como alvo uma diferença surpreendente, mas claramente fundamental no estrutura das membranas de micro-organismos e animais multicelulares (Zasloff, 2006) (Figura 6).

As membranas de mamíferos são ricas em fosfolipídios zwitteriônicos incluindo, fosfatidilcolina (PC) e esfingomielina (SM). O colesterol que também está presente em membranas de células de mamíferos pode reduzir a atividade de PAMs, afetando a fluidez e o potencial de dipolo dos fosfolípideos. Ele estabiliza a bicamada lipídica e dificulta a ligação do peptídeo nas membranas (Matsuzaki, 1999).

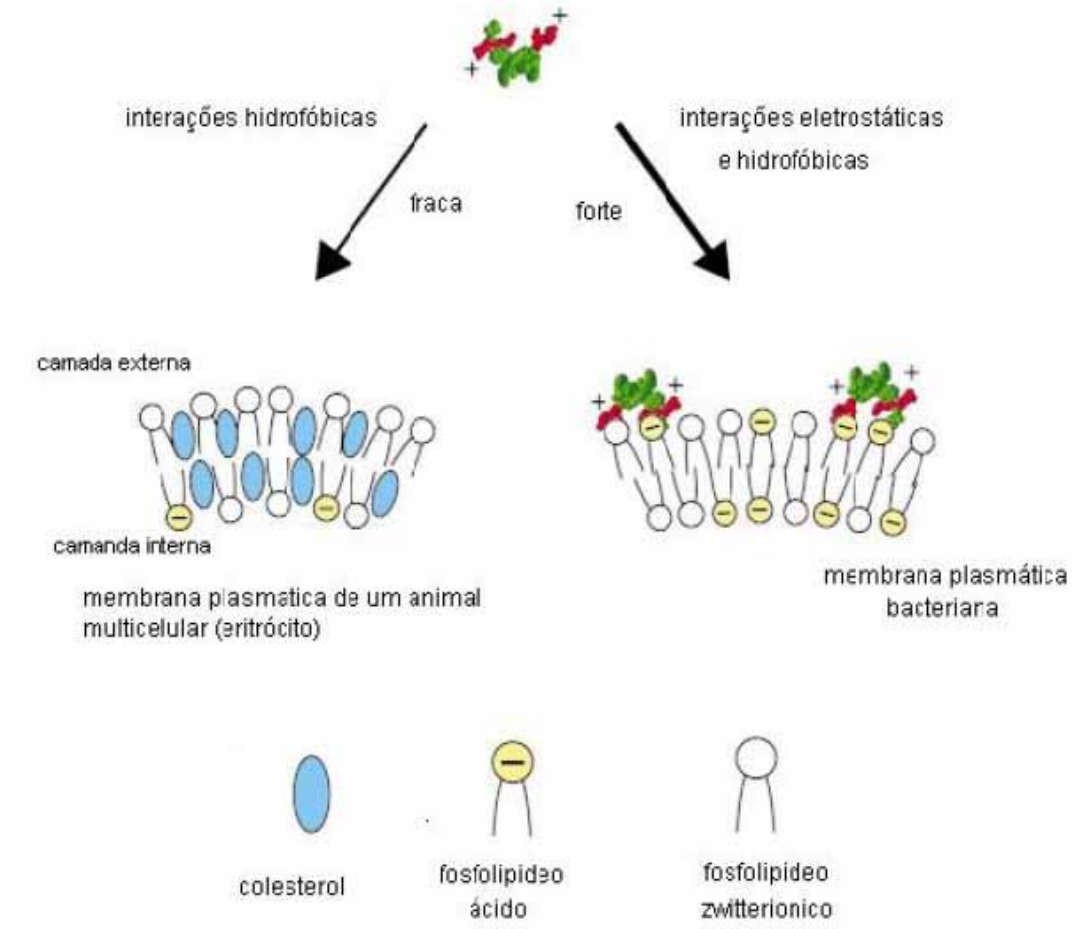

Figura 6. A membrana-alvo de peptideos antimicrobianos de organismos multicelulares e a base da especificidade. Diferenças na composição da bicamada lipídica coordenam a interação do peptídeo evitando a toxicidade para eucariotos. Retirada de Zasloff, 2002.

Membranas bacterianas são compostas de fosfolípideos carregados negativamente tais como fosfatidilglicerol (PG), cardiolipina (CL) ou fosfatidilserina (PS) (Cronan, 2003). Bactérias Gram negativas possuem uma pequena camada de peptidoglicano se comparado com as Gram positivas. Outra característica importante é uma membrana externa, para além da membrana citoplasmática, que age como barreira seletiva (Hancock, 2001), diferentes das bactérias Gram positivas. Essa membrana é mantida unida pelo equilibrio entre os íons de magnésio e cálcio que se ligam ao grupo fosfato do açucar carregado negativamente. Os peptídeos catiônicos induzem deslocamento do metal, danificando a membrana externa, e facilitam a entrada de moléculas adicionais a partir do exterior (Zasloff, 2002) (figura 7).

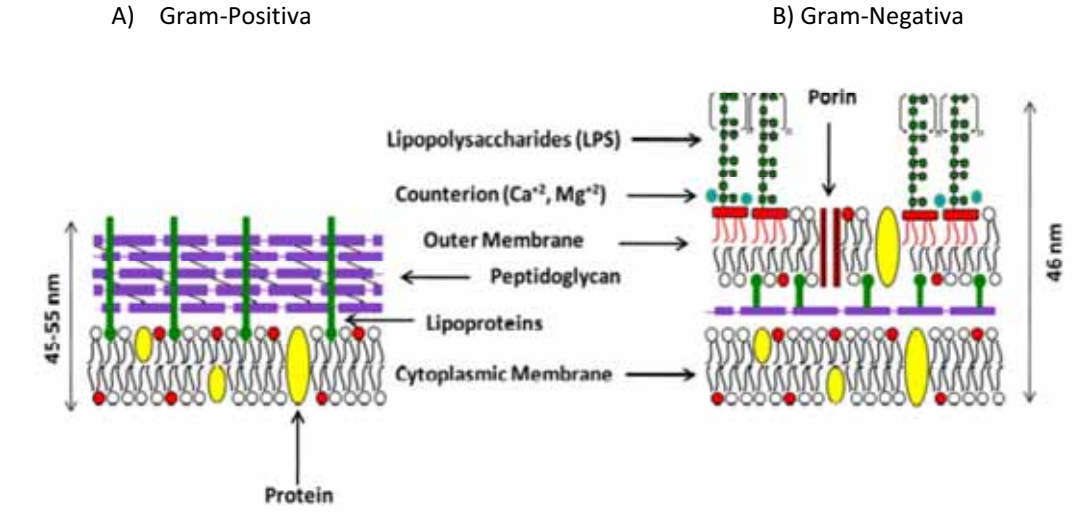

Figura 7. Em 1884, Christian Gram desenvolveu um método de coloração de bactérias que permitia sua separação em dois grupos distintos: A) As Gram positivas, que se coram em roxo, apresentam uma parede celular espessa (20 a 80 nm), de aspecto homogêneo e B) as Gram negativas, que se coram em vermelho, exibem uma parede mais delgada (9 a 20 nm) e de aspecto bastante complexo, apresentando mais de uma camada. (Figura retirada de Bagher, 2010).

1.4 Mecanismos de Ação

Peptídeos antimicrobianos interagem com os micro-organismos por meio de mecanismos diferente das citocinas (extenso grupo de moléculas envolvidas na emissão de sinais entre as células durante o desencadeamento das respostas imunes) e fagócitos (leucócitos do sangue que protegem o corpo através da ingestão, fagocitose, de partículas estranhas como, bactérias e células mortas) (Figura 8).

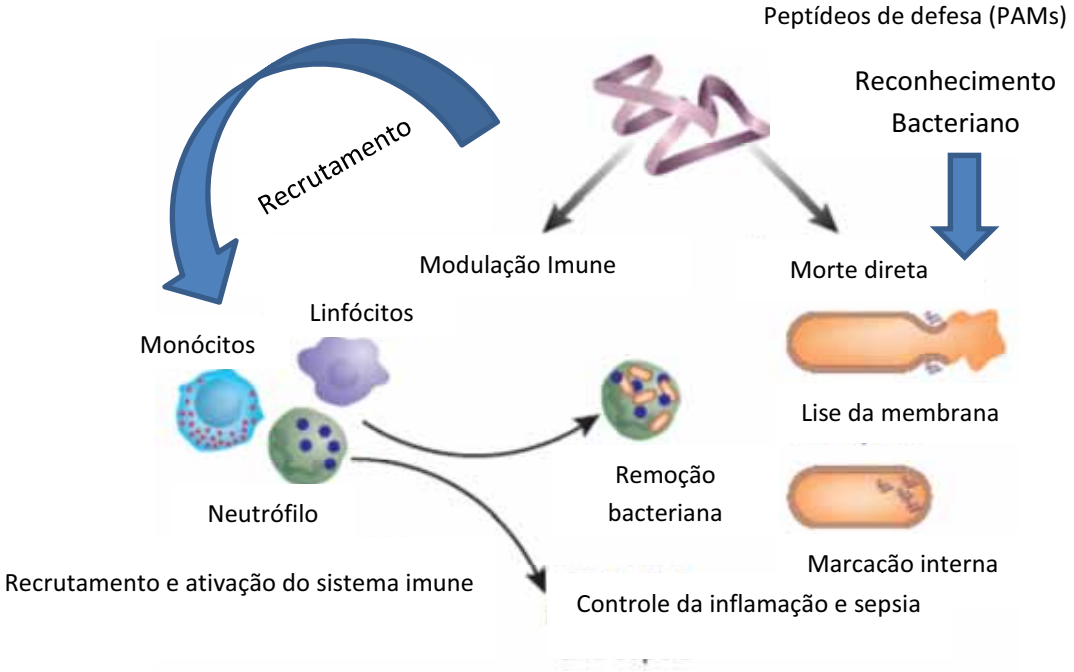

Figura 8. Papéis biológicos do peptídeo de defesa do hospedeiro. Recrutar células do sistema imune inato de defesa como os monócitos, linfócitos e neutrofilos (glóbulos brancos) para promever remoção bacteriana e/ou controle da inflamação; podendo também ocorrer reconhecimento bacteriano acarretando lise e morte celular. Retirada e modificada de Hancock and Sahl 2006.

Múltiplos mecanismos simultâneos de ação de PAMs podem ajudar a explicar o seu amplo espectro de atividade e a raridade de resistência induzível. Após a ligação de PAMs a vesículas lipídicas aniônicas por meio de interações eletrostática e hidrofóbica (figura 4), muitos tipos de perturbações podem ocorrer, incluindo a permeabilização da membrana (Wimley, 2010).

Acredita-se que o mecanismo de ação dos peptídeos varie de acordo com o micro-organismo alvo, devido às propriedades físicas das membranas (p.ex. fosfolipídeos) e concentração dos peptídeos (Jenssen et al., 2006). Estudos apontam que, para além de colesterol, o potencial de membrana e a distribuição assimétrica de fosfolípidos em membranas eucariotas contribuem para a prevenção de PAMs (Matsuzaki, 1999).

A maioria dos PAMs interage e influencia a integridade das membranas microbianas, porém não se sabe se a permeabilização da membrana é sempre um caso letal ou ainda se a membrana é o único local de ação. Outros alvos intracelulares de PAMs têm sido propostos, incluindo DNA e chaperonas. Há PAMs que podem ter modos alternativos de ação translocando através das membranas microbianas, e às vezes podem fazer assim, sem permeabilização extensiva (Wimley, 2010).

1.4.1 Modelos de Poros Transmembrânicos

No modelo poro barril *(Barrel-stave),* mecanismo hidrofóbico, peptídeos helicoidais ligam-se a superfície da bicamada lipídica orientando-se com sua face polar do peptídeo voltada para os grupos fosfato presentes na superfície da bicamada lipídica (figura 9).

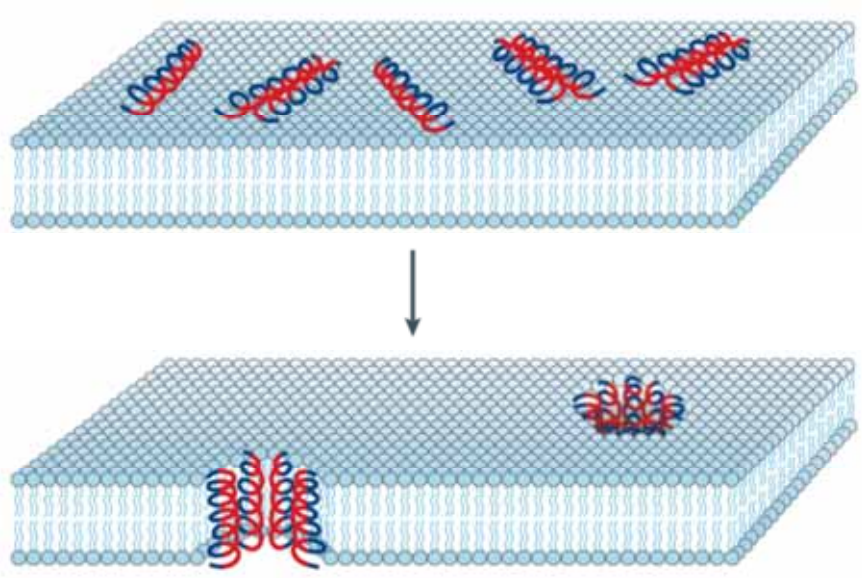

Figura 9. Representação esquemática do Modelo Barril-Stave. Regiões hidrofóbicas do peptídeo estão representadas em azul e a região hidrofílica em vermelho. Figura retirada de Brogden (2005).

A interação de uma única α-hélice anfipática com a bicamada é energeticamente desfavorável devido à baixa constante dielétrica da membrana e a incapacidade do peptídeo de estabelecer ligações de hidrogênio. Portanto tais monômeros de pepttídeo devem associar-se na superfície da membrana antes da sua inserção perpendicular, onde suas regiões hidrofílicas ficam expostas ao solvente para facilitar o fluxo livre de íons e moléculas pequenas através da bicamada lipídica. O tamanho dos poros formados pode variar consideravelmente de acordo com a concentração de monômeros de peptídeo na membrana (Pukala et al., 2006). Um poro formado pela alameticina pode conter de 3-11 monômeros de hélice para formar um poro com diâmetro interno de 1.8 nm e externo de 4.0nm respectivamente. (Brogden, 2005)

O modelo de carpete (figura 10) foi proposto pela primeira vez para descrever o modo de ação da dermaseptina S (Pouny et al., 1992), e, mais tarde, foi utilizado para descrever o modo de ação de outros peptídeos antimicrobianos.

De acordo com este mecanismo de ação, as moléculas de peptídeo são adsorvidas paralelamente na superfície da membrana, formando um agregado que cobre a superfície da bicamada lipídica, como um “tapete” de moléculas.

Em seguida, o peptídeo se reorienta, direcionando as cadeias laterais de resíduos hidrofóbicos para o interior da bicamada lipídica (região hidrofóbica da membrana),

momento em que ocorre uma redistribuição dos lipídeos, resultando em uma tensão na curvatura da membrana (Figura 10).

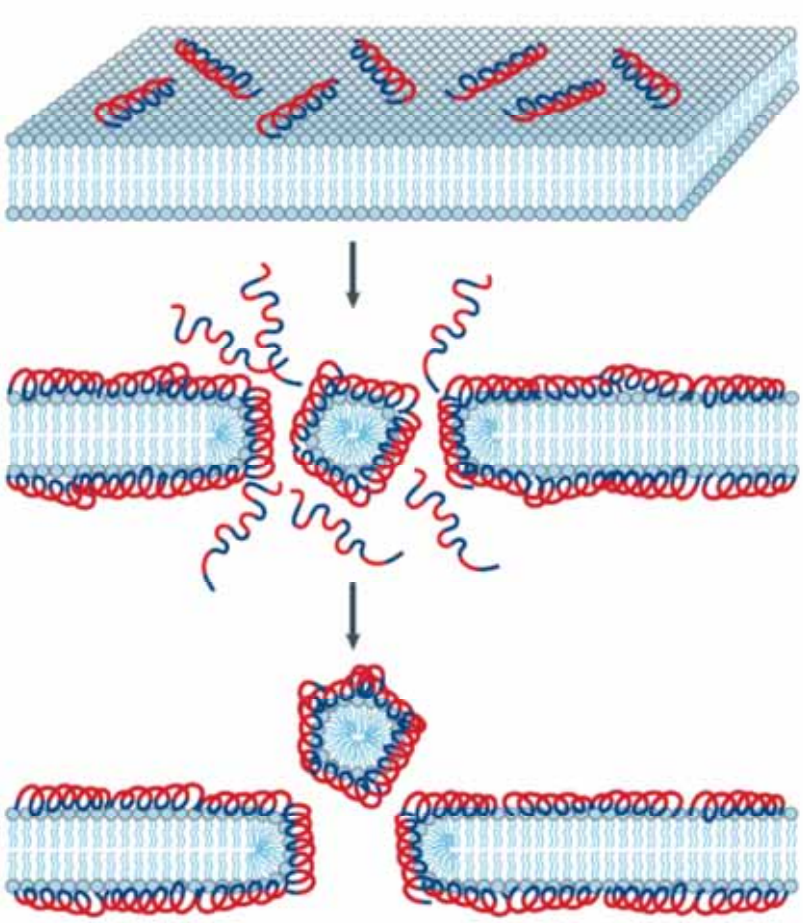

Figura 10. Representação esquemática do Modelo Carpet-like. A região hidrofílica do peptídeo está representada em vermelho e a hidrofóbica em azul. Figura retirada de Brogden (2005).

O peptídeo que permeia a membrana através deste mecanismo pode adotar diferentes estruturas secundárias, comprimentos, e pode ser linear ou cíclico após a sua ligação à membrana. Sua carga líquida precisa ser altamente positiva e distribuida ao longo da cadeia peptídica, se ligam muito pouco, ou não ligam a membranas zwitteriônicas. Peptídeos antimicrobianos altamente carregados positivamente podem lisar os eritrócitos e formar oligômeros em soluções (Shai e Oren, 2001).

No modelo de formação do poro toroidal (figura 11), o peptídeo é adsorvido paralelamente à superfície da membrana (Huang, 2009). Esse modelo explica tanto a

organização de poros aquosos quanto a manutenção das interações entre peptídeos e lipídeos. Peptídeos formadores de α-hélices são dispostos perpendicularmente na bicamada e permanecem fortemente ligados aos grupos lipídicos por toda sua extensão, devido ao rearranjo dos lipídeos. Como resultado tem-se a formação de poros aquosos por onde os íons fluem.

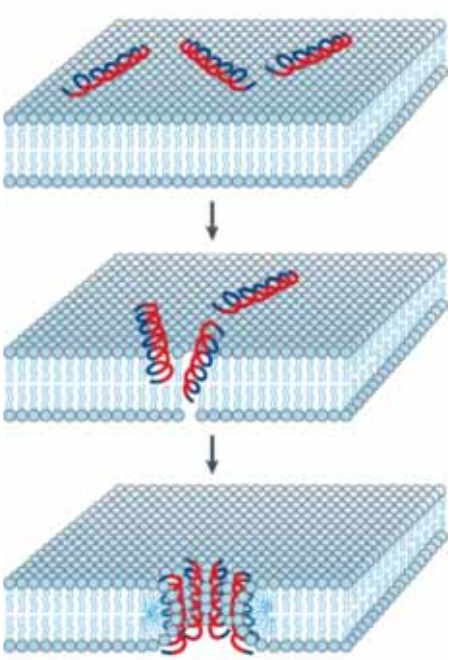

Figura 11. Representação do modelo de poro toroidal. A região hidrofífica do peptídeo está representada em vermelho e a hidrofóbica em azul. Figura retirada de Brogden (2005).

O aumento da concentração de peptídeos em simultâneo com a formação do poro toroidal, dois cenários podem acontecer: (1) eventualmente causar micelização de uma forma de detergente. (Shai, 2002), embora a formação de poros inicial não seja um pré-requisito para esta ação; (2) o potencial químico através da bicamada desequilibra devido à adsorção de peptídeos e ocorre translocação de peptídeos da monocamada externa para a membrana interna, o qual pode realizar-se através de poros transientes toroidais ou sem a formação de poros (Pokorny e Almeida, 2004).

Outro modelo, o Shai-Matsuzaki-Huang (SMH) aplica-se a grande parte dos peptídeos antimicrobianos, inclusive a peptídeos menores, os quais seriam incapazes de formar poros segundo um mecanismo *Barrel-stave*. Este propõe modos de ação distintos para peptídeos antimicrobianos, sendo por rompimento da bicamada lipídica

ou ainda por interação com alvos intracelulares (Wang et al., 2005). O modelo SMH pode ser explicado como uma combinação de interações superficiais e formação de poros. O peptídeo interage com a superfície da membrana como ocorre no mecanismo de "carpete" e desloca as moléculas de fosfolipídeos, levando a uma desorganização da estrutura da membrana (Shai, 2002; Huang, 2006) e a formação de poros transientes (figura 12).

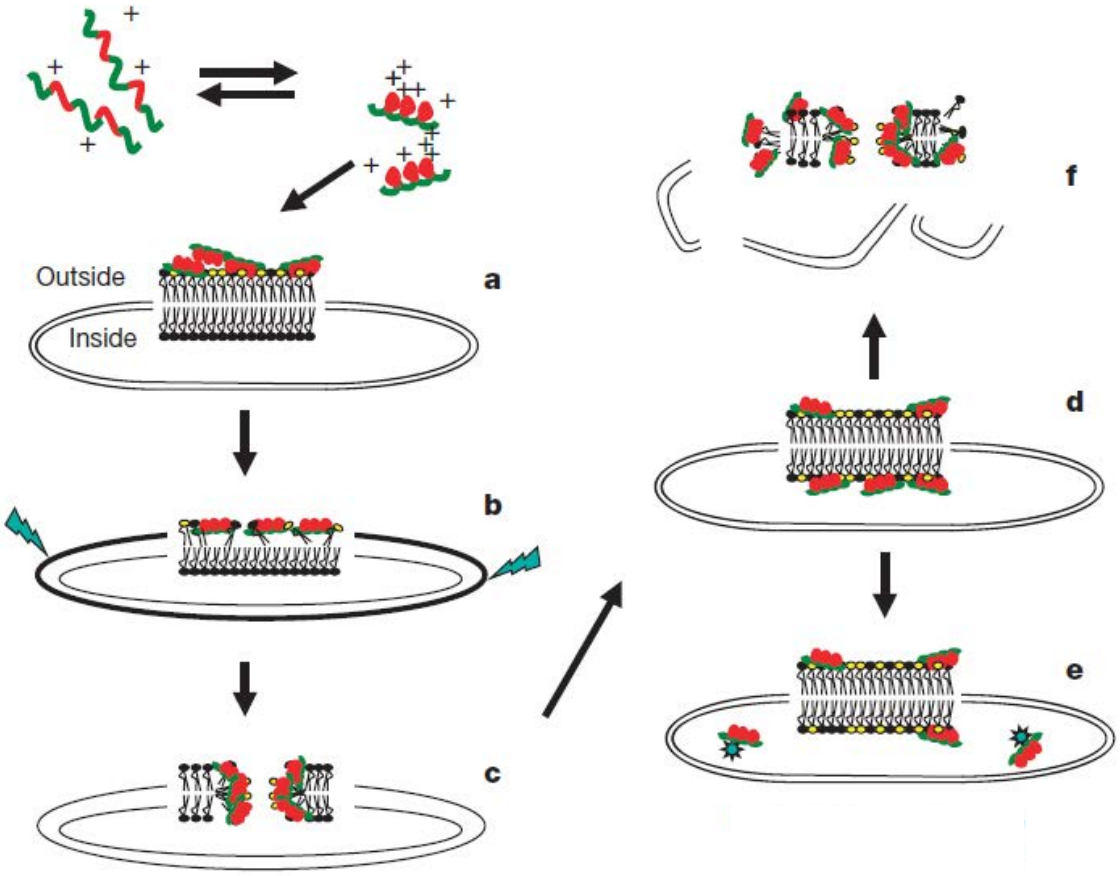

Figura 12. Representação esquemática do mecanismo de ação Shai-Matsuzaki-Huang. Mecanismo de um peptídeo em hélice é descrito. a) interação do peptídeo com a superfície da membrana; b) integração do peptídeo na membrana ocasionando afinamento da sua face externa; c) formação de poros transientes; d) difusão de peptídeos; e) em alguns casos peptídeos atuando como marcador molecular; f) Lise da membrana. Lipídeos de cabeça amarela são ácidos, ou negativamente carregados e lipídeos com cabeça preta não são carregados.

O mecanismo de detergente *(detergent-like)* baseia-se na intercalação de peptídeos em bicamadas lipídicas e representa um mecanismo mais geral para a atividade de moléculas anfipáticas (Figura 13). Sabe-se que moléculas de detergente acima da concentração micelar crítica (CMC) interagem com membranas lipídicas,

formando um estado micelar bastante complexo. Da mesma forma, peptídeos antimicrobianos podem agregar-se formando estruturas oligoméricas que interagem de forma diferente dos seus monômeros e de modo similar a um detergente (Bechinger e Lohner, 2006). Estes oligômeros formados pelos peptídeos agregados ao chocarem-se com a membrana adsorvem algumas moléculas de fosfolipídeos e podem ainda formar um agregado micelar na própria bicamada.

No mecanismo de detergente, oligômeros de peptídeos podem ser formados na região hidrofóbica da bicamada lipídica, ou seja, no seu interior. De fato, estudos recentes mostram que a formação de agregados é termodinamicamente mais favorável no interior da bicamada fosfolipídica do que em solução, e contribuem para a compreensão deste mecanismo (Babakhani et al., 2008).

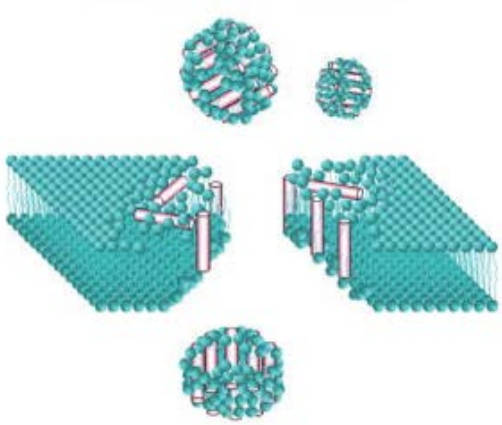

Figura 13. Mecanismo de detergente. Retirada de Wimley 2010.

2 OBJETIVOS

Os principais objetivos deste estudo foram:

- Desenhar e sintetizar peptídeos com potencial antimicrobiano e não hemolítico com dezoito resíduos de aminoácidos, utilizando peptídeos já previamente estudados como meio de selecionar características favoráveis.
- Compreender a importância de alterações no N-terminal (ligação covalente do ácido orto amino benzoico (Abz) e a inserção do Acetil) na comformação, interação com vesículas, atividade lítica e biológica.
- Explorar o efeito de parâmetros estruturais, biofísicos e biológicos utilizando membranas modelo para evidenciar efeitos de carga elétrica líquida, da hidrofobicidade média e das mudanças estruturais por meio de experimentos de dicroísmo circular, vazamento, mobilidade eletroforética e espectroscopia de fluorescência utilizando vesículas aniônicas (POPC/POPG) e zwitteriônicas (POPC).
- Ensaios biológicos como ensaios in vitro com culturas de bactérias para verificar o potencial antimicrobiano e ensaios de hemólise para verificar a toxicidade do peptídeo sobre o eritrócito.

3 ARTIGOS

3.1 INTERACTION OF A SYNTHETIC ANTIMICROBIAL PEPTIDE WITH MODEL MEMBRANE BY FLUORESCENCE SPECTROSCOPY

Luciana Moro Puia Zanin[a], Dayane dos Santos Alvares[a], Maria Aparecida Juliano[b], Wallance Moreira Pazin[c], Amando Siuiti Ito[c], João Ruggiero Neto[a*]

[a] Department of Physics - IBILCE- São Paulo State University- São José do Rio Preto- Brazil

[b] Department of Byophysics - UNIFESP - São Paulo - Brazil

[c] Department-of Physics - FFCLRP, University of São Paulo, Ribeirão Preto, SP, Brazil

.

* Corresponding author: email jruggiero@sjrp.unesp.br. Departamento de Física, IBILCE-UNESP, Rua Cristovão Colombo 2265, São José do Rio Preto SP, Brazil, CEP 15054-000. Phone (+5517) 3221-2444, Fax (+5517) 3221-2496

ABSTRACT

Static and time-resolved fluorescence of tryptophan and *ortho*-aminobenzoic acid were used to investigate the interaction of the synthetic antimicrobial peptide L1A (IDGLKAIWKKVADLLKNT-NH2) with POPC and POPC:POPG. N-acetylated (Ac-L1A) and N-terminus covalently bonded *ortho*-aminobenzoic acid (Abz-L1A-W8V) were also used. Static fluorescence and quenching by acrylamide showed that the peptides adsorption to the lipid bilayers was accompanied by spectral blue shift and by a decrease in fluorescence quenching, indicating that the peptides moved to a less polar environment probably buried in the lipidic phase of the vesicles. These results also suggest that the loss of the N-terminus charge allowed deeper fluorophore insertion in the bilayer. Despite the local character of spectroscopic information, conclusions can be drawn about the peptides as a whole. The dynamic behaviors of the peptides are such that the mean intensity lifetimes, the long correlation time and the residual anisotropy at long times increased when the peptides adsorb in lipid vesicles, being larger in anionic vesicles. From steady-state increase in fluorescence intensity and anisotropy, we observed that the partition coefficient of peptides L1A and its Abz –analog in both types of vesicles are higher than the acetylated analog and moreover the affinity to anionic vesicle is higher than to zwitterionic.

Keywords: antimicrobial peptides, extrinsically labeled peptide, model membranes, static fluorescence, time-resolved fluorescence.

1. INTRODUCTION

The search for new antibiotic compounds has deserved attention in the last decades due to the increase in microorganism strains resistant to conventional antibiotics (Hancock and Sahl 2006). Host defense peptides belong to the innate immune system of many living organisms from plants to mammals (Zaslof 2002). Among these peptides the short linear cationic peptides have been shown to constitute an important class. Besides cationic residues, these peptides are rich in non-polar and hydrophobic residues forming an amphipathic helical structure capable of disturbing lipid bilayer and cell membrane (Matsuzaki 2009). Due to their cationicity they have affinity to anionic bilayer which is a characteristic of the membrane of bacteria while the outer leaflet of eukaryotic cells is zwitterionic. This electrostatic contribution, however, does not per se determine the selectivity of cationic peptides. Some of them are also able to disturb neutral membranes resulting in an undesirable cytotoxic activity (Jiang et al. 2008). The selectivity to antimicrobial activity has been shown to involve a complex and delicate balance between peptide net charge and hydrophobicity (Dathe et al. 2001, Chen et al. 2005). Some structural parameters, such as, helix propensity, mean residue hydrophobicity, hydrophobic moment, angle of peptide polar face, have been used to quantify the peptides amphipathicity (Wieprecht et al. 1996; Dathe et al. 1999). These parameters are frequently evoked to study the charge-hydrophobicity balance and consequently the selectivity.

The synthetic peptide L1A (IDGLKAIWKKVADLLKNT-NH2) was designed to have some structural features which are present in the tetradecapeptide Polybia MP-1 (or MP-1), extracted from a Brazilian wasp. MP-1 is a highly selective peptide with broad spectrum bactericidal activity without being hemolytic and cytotoxic. This peptide showed inhibitory effect on proliferating cell culture of prostate and blade cancer cells (Wang et al 2008) and in multidrug resistant leukemic cells (Wang et al 2009). Previous work on molecular dynamics simulation in TFE (dos Santos Cabrera et al. 2008) suggested an important role played by the acidic residue in the N-terminus as well as the relative positioning of acidic and basic residues on the charge-hydrophobic balance. Those simulations showed that each acidic residue is ion-paired with two

amines: D2 with N-terminus NH3 and K5 and D8 with K4 and K11. Besides the relative positioning of acidic and basic residues, other structural characteristics which are believed to be responsible for the selectivity are the hydrophilicity, mean residue hydrophobicity <H>=-0.1; one of the aspartic acids at the N-terminus and the broad polar angle (Leite et al 2010). In L1A, the acidic residues were, however, designed to be farther apart in comparison with MP-1 and to achieve the same relative positioning between each acidic residue at ion-pairing positioning with two amine groups the new sequence is four residues longer than MP-1 and has four lysine residues with a net charge Q=+3. Besides L1A two analogs with N-terminus modification were synthesized. In one of them the N-terminus was acetylated and the analog was named Ac-L1A. In the other the fluorescence probe ortho-aminobenzoic acid (Abz) was covalently attached to the amino group. In the Abz analog the tryptophan residue was substituted by valine to avoid fluorescence energy transfer and the analog was named Abz-L1A-W8V.

A previous biophysical characterization of these peptides seeking for structure function correlations revealed that L1A and the acetylated analog are selective to Gram negative bacteria and are non hemolytic, while the attachment of the fluorescent moiety Abz in the N-terminus impaired antibacterial activity and increased the hemolytic activity (manuscript submitted). The biophysical characterization showed that the adsorption to zwitterionic and anionic vesicles is accompanied by a conformational transition to the helical conformation, with higher helical content in anionic vesicles, and the lytic efficiency in lipid vesicles correlated with helical content. Even the analogs with smaller net charge (Q=+2), due to the N-terminus modification, showed increased helical content and increased permeabilization to anionic bilayer compared to L1A with net charge Q=+3, which is unusual between cationic peptides to which the electrostatic contribution should play important role on the selectivity and affinity. To understand the origin of this unusual behavior an investigation using steady state and time resolved fluorescence spectroscopy was carried out with the aim of determine the peptides affinities to model membranes and the complex steps that occur in the lipid-solvent interface by the determinations of partition coefficients, lifetimes and rotational correlation times of these peptides in zwitterionic and anionic vesicles.

2. MATERIALS AND METHODS

2.1 Chemicals. Lipids: 1-palmitoyl-2-oleoyl-*sn*-glycero-3-phosphocholine (POPC) and 1-palmitoyl-2-oleoyl-*sn*-glycero-3-phosphoglycerol (POPG) were purchased from Avanti Polar Lipids (Alabaster, AL) and tris(hydroxymethyl) aminomethane (Tris) and sodium chloride were purchased from Merck. Unless otherwise indicated other chemicals were of high quality analytical grade.

2.2 Peptide Synthesis. The peptides IDGLKAIWKKVADLLKNT-NH2 (L1A), Ac-IDGLKAIWKKVADLLKNT-NH2 (Ac-L1A) and Abz-IDGLKAIVKKVADLLKNT-NH2 (Abz-L1A-W8V) were obtained in an automated bench-top simultaneous multiple solid-phase peptide synthesizer (PSSM 8 system from Shimadzu) using the solid-phase synthesis by the 9-fluorenylmethoxylcarbonyl (Fmoc) procedure. The final deprotected peptides were purified by semi-preparative high performance liquid chromatography (HPLC) using an Econosil C-18 column (10 µm, 22.5 x 250 mm) and a two-solvent system: (A) trifluoroacetic acid (TFA)/H2O (1:1000) and (B) TFA/acetonitrile (ACN)/H2O (1:900:100). The column was eluted at a flow rate of 5 ml/min with a 10 (or 30) to 50 (or 60)% gradient of solvent B over 30 or 45 min. Analytical HPLC was performed using a binary HPLC system from Shimadzu with a SPD-10AV Shimadzu uv-vis detector and a Shimadzu RF-535 fluorescence detector, coupled to na Ultrasphere C-18 column (5µm , 4.6 x 150 mm), which was eluted with solvent systems A1 (H3PO4/H2O, 1:1000) and B1 (ACN/ H2O/H3PO4, 900:100:1) at a flow rate of 1.7 mL/min and a 10–80% gradient of B1 over 20 min. The HPLC column eluate was monitored by absorbance at 220 nm. The molecular weight and purity of synthesized peptides were checked by MALDI-TOF (Brucker Daltons) or electron spray LC/MS-2010 (Shimadzu).

2.3 Vesicle preparation. Lipid films of POPC and mixture POPC:POPG at (8:2) molar ratio were obtained from phospholipids solutions in chloroform or chloroform: methanol (2:1) in round-bottom flask. The solutions were dried under N_2 and traces of

organic solvent were removed under vacuum for at least three hours. The lipid films were afterward hydrated with TRIS buffer (Tris/HCl 10 mM, 1mM Na_2EDTA, pH 7.5, containing 150 mM NaCl). The final total lipid concentration was around 5 mM. Large unilamellar vesicles (LUVs) were obtained by two extrusion steps using an Avanti Mini-Extruder (Alabaster, AL) and double stacked polycarbonate membrane (Nuclepore Track-etch Membrane, Whatman): firstly 6 times through 0.4 μm and then 11 times through 0.1 μm membranes. Vesicles were used immediately after preparation. The lipid concentration was determined by phosphorus analysis (Rouser et al. 1970). The vesicle size was determined by dynamic light scattering with Zeta Sizer Nano NS-90 (Malvern Instruments, Worcestershire, U.K.). Three dynamic light scattering measurements of 15 consecutive runs of 10 s were performed. The correlation function was fitted with cummulants expansion up to second order to obtain the intensity size distributions. A typical diameter 105 nm showed polydispersity index around 0.2 or width distribution of 20 nm. The average of these three measurements leads to diameter of 105 ± 5 nm.

2.4 Peptides solutions: Stock solutions of peptides were prepared in Milli-Q water. Peptides concentrations were determined from the absorbance spectra, obtained with Cary 2300 spectrophotometer (Varian Palo Alto). For tryptophan and Abz containing peptides the molar absortivities used were ε= 5675 M^{-1} and 1998 M^{-1}, in aqueous phase.

2.5 Steady-state Fluorescence Spectroscopy. Tryptophan and Abz emission fluorescence spectra were collected using quartz cell with 1 cm path length, at 25ºC using ISS PC1 spectrofluorometer (Urbana Champaign USA). The spectra were recorded from 290 to 450 nm with excitation at 279 nm and from 350 to 550 nm with excitation at 314 nm for tryptophan and Abz containing peptides respectively. The emission spectra were recorded after one hour of sample preparation. Excitation and emission slits varied from 0.5 to 2.0 nm and bandpass filters were used, depending on the samples fluorescence intensities. Blue shifts ($\Delta\lambda_{max}$) were calculated as the differences in wavelength of the maxima in emission spectra of the peptide collected in the absence or presence of vesicles. Standard deviation for the blue shift was 1 nm. The

steady-state fluorescence anisotropy was measured using Glan-Thompson polarizers in L-format configuration.

2.6 Fluorescence Quenching. A 2.0 M stock solution of acrylamide was prepared in Tris/HCl 10.0 mM buffer. Aliquots of this solution were added to 5.0 μM solution of Trp containing peptides or 2.0 μM of that containing Abz, in the absence and in the presence of 500 μM lipid vesicles at 25°C and the solution was constantly stirred. Tryptophan emission fluorescence spectra were collected from 320 to 450 nm, excited at 295 nm. Abz emission fluorescence spectra were recorded from 350 to 550 nm with excitation at 314 nm. The fluorescence quenching data were analyzed according to the Stern-Volmer equation for collisional quenching:

$$I/I_0 = 1 + K_{sv}[Q] \quad (1)$$

where I_0 and I are fluorescence intensities measured in the absence and in the presence of quencher respectively. K_{SV} is Stern-Volmer constant for collisional quenching process and [Q] is the quencher concentration.

2.7 Fluorescence decays and time-resolved anisotropy. Fluorescence decays and time-resolved anisotropy were measured using the time-correlated single photon counting method. The excitation source was a Tsunami 3950 Spectra Physics titanium-sapphire laser, pumped by a Millenia X Spectra Physics solid state laser. The repetition rate of the pulses was set to 8.0 MHz using 3980 Spectra Physics pulse picker. The laser was tuned so that a third harmonic generator BBO crystal (GWN-23PL Spectra Physics) gave the 297, 279 and 308 nm excitation pulses that were directed to an Edinburgh FL900 spectrometer for L1A, Ac-L1A and Abz-L1A-W8V respectively. The spectrometer was set in L-format configuration, the emission wavelength was selected in 350 and 416 nm for tryptophan and Abz respectively by a monochromator, and emitted photons were detected by a refrigerated Hamamatsu R3809U microchannel plate photomultiplier. Soleil-Babinet compensator in the excitation beam and Glan-Thompson polarizer in the emission beam were used in anisotropy experiments. The FWHM of the instrument response function was typically 100 ps and time resolution

was 12 or 24 ps per channel. Software provided by Edinburgh Instruments was used to analyze the individual decays, which were fitted to multiexponential curves:

$$I(t) = \sum_i b_i e^{-\frac{t}{\tau_i}} \tag{2}$$

where b_i and τ_i are the pre-exponential factor and the lifetime of the component i of decay respectively. The quality of the fit was judged by the analysis of the statistical parameter reduced-χ2 and by inspection of the residuals distribution. Average lifetimes τ_{av} were calculated applying the statistical definition of averages to the multi-exponential intensity decay, resulting in the expression:

$$\tau_{av} = \frac{\sum_i b_i \tau_i^2}{\sum_i b_i \tau_i} \tag{3}$$

The anisotropy decay data, in the non-associative model as discussed by Loura and Ramalho (2007), were fitted to the theoretically derived expression by Kawato et al (1978)

$$r(t) = (r_0 - r_\infty)\sum_i f_i e^{-\frac{t}{\phi_i}} + r_\infty \tag{4}$$

where r_o is the initial anisotropy, Φ_i is the rotational correlation time of component *i* of anisotropy decay, which has the fractional contribution f_i, and r_∞ stands for the residual anisotropy at long time *t*. Restricted rotational motion was characterized by the residual anisotropy at long times (r_∞) and the maximum angle (θ_m) allowed for the local rotational diffusion of the emission dipole, measured from the azimutal axis in spherical coordinates, was calculated from:

$$\frac{r_\infty}{r_0} = \left[\frac{1}{2}\cos\theta_m(1+\cos\theta_m)\right]^2 \tag{5}$$

2.8 Partition Coefficients Partition coefficients were obtained from peptide-vesicle titrations. In these experiments aliquots of LUV suspension were added to a peptide solution and the fluorescence spectra were monitored. Corrections of the vesicular

scattering effects in the fluorescence spectra were accounted using the fluorescence of the tryptophan zwitterion as proposed by Ladokhin et al. (2000):

$$I_{pep}^{corr} = I_{pep}\frac{I_{trp}^{buff}}{I_{trp}([L])} \quad (6)$$

where I_{trp} and I_{pep} are the fluorescence intensities of the tryptophan zwitterion and the peptide at a given lipid concentration [L] and I_{trp}^{buffer} is the fluorescence intensity of the tryptophan zwitterion in the buffer. The partition coefficients were obtained from the plots of the fluorescence intensities (I) as a function of the total lipid concentration [L] by fitting the experimental points to the equation similar to that proposed in Coutinho and Prieto (1995):

$$I = I_W + \frac{(K_p[L]\gamma_L)}{(1+K_p[L]\gamma_L)}(I_L - I_W) \quad (7)$$

where I_W and I_L are the limit fluorescence intensities with all the peptide in water and in the lipid phase, respectively, Kp is the partition coefficient, γ_L = 0,76 is the lipid molar volume.

The partition coefficients were also determined from the steady-state fluorescence anisotropy, r, once this parameter presented a significant change between both phases and comparable fluorescence intensities in the two phases. Using the same experimental approach for the fluorescence intensity, the data are fitted using eq. proposed by Castanho and Prieto (1992):

$$r = \frac{\left\{\left[\frac{1}{(\gamma_L[L])}-1\right]r_W + r_L K_p {}^{\phi_L}/_{\phi_W}\right\}}{\left[\frac{1}{(\gamma_L[L])}-1+K_p {}^{\phi_L}/_{\phi_W}\right]} \quad (8)$$

where, r_i are the anisotropies in the lipid (i = L) or aqueous phase (i = W), φ_L/φ_W is the ratio between the fluorescence quantum yields of the peptides in the lipid and aqueous phases, $\gamma_L$is the molar volume of the lipid in the membrane which was taken to be γ_L = 0.76 and [L] is the total lipid molar concentration.

2.9 Electrophoretic Mobility and Dynamic Light Scattering Measurements. Electrophoretic mobilities of anionic POPC:POPG (8:2) large unilamellar vesicles, at 40 μM total lipid concentration, in the absence and in the presence of different concentrations of peptides, were determined from three measurements of 30 consecutive runs using DTS1060 (Malvern) disposable cells with golden electrodes at 25°C.

3. RESULTS

3.1 Fluorescence emission spectra. The interaction of peptide L1A (Fig. 1a) and its acetylated analog with lipid vesicles resulted in a significant blue shift of the peak of the emission band, from 350 nm in buffer to around 320 nm vesicles. Besides the spectral shift, the intensity of fluorescence emission increased significantly indicating that the tryptophan in both L1A and in the acetylated analog moves to a less polar environment when the peptide is adsorbed in the lipid membrane. The wavelength shift observed for L1A and the acetylated analog was approximately the same for both zwtterionic and anionic vesicles (Table 1), indicating that the environment around the fluorescent moiety in the peptides has similar polarity, independent on the surface vesicle charge. Blue shift of the maximum emission wavelength was also observed for the Abz-analog, from 416 in buffer to 410 nm in the presence of POPC and POPCPOPG vesicles with small increase in emission intensity (Fig. 1. b). Although the value of the blue shift is smaller than observed in the tryptophan containing peptides, it is comparable to that obtained for Abz labeled oligopeptides in SDS micelles and vesicles (Turchiello. et al 1998, 2002).

3.2 Fluorescence Quenching. Fluorescence quenching experiments were performed to better characterize the extent of the peptides penetration in the hydrophobic phase of the bilayer, Water soluble acrylamide was used as quencher and the loss of fluorescence intensity was analyzed with Stern-Volmer plots. In buffer the plots were linear (Fig.2 left) and well fitted with the eq. 1 from which the Stern-Volmer constants K_{SV} were obtained. The degree of exposure of the tryptophan residue in L1A and Ac-L1A is

almost the same and slightly higher than the exposure of Abz in Abz-L1A-W8V peptide. In the presence of lipid vesicles, the tryptophan containing peptides showed Stern-Volmer linear plots. For the Abz-analog, however, the fluorescence quenching was not complete and non-linear plots were obtained suggesting two fluorophore populations with different accessibilities to the quencher. In these cases the Stern-Volmer constants were obtained from the initial linear segment fitted with the eq.1.

Compared to the quenching in buffer, interaction of peptides with vesicles of POPC (Fig. 2, center) and POPC/POPG (Fig. 2, right), resulted in decrease of K_{SV} showing reduced accessibility of acrylamide to tryptophan and Abz. The changes are less pronounced in POPC compared to POPC/POPG: the extent of decrease of K_{SV} for L1A in anionic vesicles (3.6) is more than twice the decrease in zwitterionic vesicles (1.5). Similar decreases were also observed for the two analogs (Table 1). The results show that the reduction in the K_{SV} constants of the Abz-analog in both vesicles is well above the reduction for L1A and Ac-L1A suggesting that the Abz moiety is more screened from the solvent than the tryptophan residue (Table 1). It is noteworthy that, even in the zwitterionic vesicle, where a positive dipole potential would act against the insertion of N-terminus in the lipid phase, it was observed that Abz is buried in the bilayer.

3.3 Time-resolved fluorescence intensity decay. Fluorescence intensity decay profiles of tryptophan in L1A (Fig. 3-a) and Ac-L1A in buffer were best fitted to triexponential functions. The presence of three lifetime components for Trp in peptides has been attributed to the occurrence of different rotational conformers of the indole ring around the C_α-C_β bond of the alanyl side chain. Theoretical calculations (Goldman et al. 1995) showed that in g^- rotamers of Trp the electron transfer process competes with fluorescence as a deactivation route for the excited state and in g^+ rotamers electron transfer rate is high, predominating over the fluorescence. However, the fluorescence decay heterogeneity does not have a unique interpretation and dipolar relaxation of a simple molecule in a bulk phase can produce similar complex decay even in the absence of any rotamers (Ladokhin, 2001).

The three lifetimes for L1A and Ac-L1A peptides in buffer were quite similar, around 5.0, 3.0 and 1.0 ns, and the values were slightly higher for L1A (Table 2). However the pre-exponential factors were not the same and the contribution of the long lifetime is lower in L1A, so that the calculated average lifetime was greater in the acetylated peptide (3.8 ns for Ac-L1A and 3.6 ns for L1A, Table 2). The values of average lifetimes are comparable to those observed in α-melanocyte stimulating hormone (α-MSH) and adrenocorticotropin peptide (ACTH), (Romani et al. 2009). Differences in the pre-exponential factors of L1A and Ac-L1A reveal that the acetylation may induce structural changes affecting the interaction of the fluorophore with the solvent or the distribution of Trp rotamers.

In the presence of both POPC and POPC/POPG vesicles, the lifetimes of L1A peptide increased significantly, as observed in the interaction of many peptides with model membranes (Romani et al. 2006, 2009, 2010). At high lipid concentration (1 mM) the average lifetime for the emission of L1A at 350 nm increased from 3.62 to 3.85 ns in POPC vesicles and to 4.7 ns in POPC/POPG vesicles (Table 2). It is noticeable that for the emission at 350 nm the intermediate lifetime presented the highest pre-exponential factor and the contribution of the long lifetime drastically decreased. The result is similar to that reported for MSH in the presence of phospholipid vesicles (Ito, 1993): due to the interaction with the bilayer, the emission from tryptophan was blue shifted, the contribution of the long lifetime became more important at short wavelengths and less significant at 350 nm. In Ac-L1A in the presence of vesicles an even more drastic reduction in the pre-exponential factor associated to the long lifetime was observed, compared to the decay in buffer solution. In the acetylated analog the pre-exponential factor corresponding to the intermediate lifetime of the decay at 350 nm did not show pronounced changes and the contribution of the short lifetime increased. As this increase in the contribution of short lifetime was larger in the presence of POPC/POPG vesicles the calculated average lifetime was slightly lower than the value obtained in POPC (Table 2).

The Abz-L1A-W8V peptide, containing the *ortho*-aminobenzoic (Abz) group, presented decay curves best fitted to a bi-exponential function. In buffer a long lifetime (8.57 ns) predominates, accounting for 89% of the total emission, and it was necessary a short lifetime (4.51 ns) to fit adequately the data. Results are similar to those observed in Abz containing peptides (Ito et al. 1998; Turchiello et al. 1998; Turchiello et al.

2002) and the two lifetimes are related to the two isomers of the fluorophore, originated from rotation around the bond linking the carboxyl and benzyl groups (Takara et al. 2009). Addition of POPC LUV's caused increase in lifetimes and at 1 mM lipid concentration the average lifetime increased from 8.32 to 8.62 ns. In the mixed POPC/POPG vesicles at the same total lipid concentration, average lifetimes raised even more, to 8.97 ns (Table 2). The pre-exponential factors showed only small changes in the presence of vesicles, indicating that the insertion in the bilayer did not change significantly the isomer equilibrium of the fluorophore Abz in the Abz-L1A-W8V peptide.

3.4 Fluorescence Anisotropy decay. Steady state fluorescence anisotropy of the peptides in buffer was close to zero, showing that the peptides have large rotational diffusion. With addition of vesicles and insertion of the peptides in the bilayer, the anisotropy increased due to the restrictions imposed by the neighbor lipid molecules to the rotation of the peptides, leading the steady state anisotropy to values above 0.20 in high concentration of lipids (Table 3).

Anisotropy decay curves were measured at emission wavelength 350 nm for L1A and Ac-L1A and 415 nm for Abz-L1A-W8V peptide (Figure 4). The anisotropy of free Trp or Abz in aqueous medium decays fast to zero and using equation (4) data were fitted to mono-exponential curves, with rotational correlation times below 50 ps. In the anisotropy decay of Abz-L1A-W8V peptide in aqueous solution two rotational correlation times were obtained, and the result can be interpreted ascribing the short correlation time to local Abz motion, and the long correlation time (around 1.0 ns for the peptides in buffer) to overall tumbling of the whole peptide (Souza et al. 2000; Romani et al. 2006). In the experiments with L1A and Ac-L1A in buffer we could not discriminate two components in the anisotropy decay, which was fitted to a monoexponential curve with rotational correlation times near to 0.50 ns (Table 3).

For the peptides in interaction with the vesicles, the anisotropy experiments were performed in the presence of lipid dispersions in an aqueous environment. In this case we are not able to discriminate populations with positioning in distinct planes in the bilayer and anisotropy decay curve was fitted to the expression (4), where the intensity decay and the anisotropy decay are non-associated (Rapson et al, 2011). Two

correlation times were observed in the presence of vesicles, and the short correlation times, at sub-nanoseconds range, are affected by scattering effects, more pronounced in the presence of the vesicles, and by the relative increase in the contribution of the short lifetime of the intensity decay. These transient effects at very short times are less informative than the long rotational correlation time (Φ_1) and the residual anisotropy at long times (r_∞). The rotation of peptides in the vesicles comes from the movement of the molecule, or a segment of the molecule to which the fluorophore is bound, subjected to the restrictions imposed by the lipid arrangement, combined with the rotation of the vesicle as a whole. However the typical rotation times of vesicles with 100 nm diameters in aqueous medium are in the domain of microseconds and could not be measured in the experiments of fluorescence anisotropy decay. Thus, the long rotational correlation times, in the range of nanoseconds obtained in our measurements, can be ascribed to the rotation of the segment of the peptide containing the flurophore, inside the vesicles. In the peptides L1A and Ac-L1A, the long rotational correlation times in POPC/POPG vesicles are more than twice higher than the values measured in POPC vesicles (Table 3) showing that the structural restrictions to the rotation of the peptides are more pronounced in the charged vesicles compared to the neutral ones. Even more pronounced changes were observed in Abz-L1A-W8V where the long correlation time increased to circa 7.5 ns in POPC/POPG vesicles. Therefore the peptide as a whole experiences larger restriction to its movement compared to the other peptides, as revealed also by the significantly high values of the residual anisotropy r_∞ , mainly in the negative charged POPC/POPG vesicles. The residual anisotropy reflects the occurrence of hindered rotation limiting the rotational diffusion to a wobbling in a cone (Kawato 1978), characterized by the angle θ_{max} which can be calculated according to equation (5). We observed that the rotations in the bilayers are limited to angles below 60^o, with the lowest values, around 40^o, observed for Abz-L1A-W8V in POPC/POPG vesicles (Table 3).

3.5 Determination of the partition coefficient between the aqueous and lipid phase..

Partition coefficients were obtained from titration experiments in which the peptides were titrated with POPC and POPC/POPG (8:2) LUVs using fluorescence intensity and static anisotropy are displayed in the fig.5 and fig. 6 respectively. These plots were

analyzed by non-linear regression using eq. 7 and 8 and the fitted K_p values are displayed in the table 4.

The affinities of the peptides to neutral POPC vesicles are characterized by partition coefficients in the range of 6000 to 9000$M^{-1}$with the same magnitude order as observed in mastoparan peptides (Almeida et al. 2009; Arbuzova and Schwarz 1999). The affinity of the native peptide L1A (Q=+3) was slightly higher compared to the acetylated analog which has smaller net charge (Q=+2), while the partition constant of the Abz – analog (Q=+2) was the highest. Roughly the same affinity order, Abz-L1A-W8V>> L1A≥AcL1A, was observed monitoring the static anisotropy, considering the experimental error. The values of the affinity constants obtained from the anisotropy data are somewhat different from those obtained from the fluorescence intensities. This difference could be due to the scattering induced by the vesicles in the anisotropy data that were not corrected. The same affinity order was also observed in anionic POPCPOPG vesicles. In these vesicles, the native peptide L1A and the Abz-analog showed higher affinity than in neutral vesicles suggesting the importance of the electrostatic interactions in the peptides adsorption. The increase in the partition coefficients, in transferring the peptides to anionic bilayer in relation to neutral vesicles, does not depend on the peptides net charges. While for L1A was observed an increase of 20% in the partition constant, for the Abz-analog K_p was more than three times higher, suggesting that the adsorption of this analog is also driven by non-electrostatic interactions. Interestingly the adsorption of the acetylated analog seems to be roughly independent on the vesicle charge suggesting also the importance of the role played by the non-electrostatic interactions.

Aiming to check the unusual higher preference of the less charged peptides Ac and Abz- analogs to anionic vesicles we used a different and non-spectroscopic technique. Suspensions of anionic vesicles, at 40 μM total lipid concentration, were titrated with the peptides and the electrophoretic mobility was monitored in the absence and in the presence of peptides. The plots of electrophoretic mobility as a function of the peptide concentration, fig.7, show that the mobility decreases monotonically with the peptide concentration up to the vesicle neutralization with further increase in mobility. The peptides concentrations to induce vesicle charge neutralization increase in the order L1A > Ac-L1A > Abz-L1A-W8V. It should be expected lower amount of the most charged peptide L1A to neutralize the vesicle charge, suggesting that the smaller

net charge of Abz-analog was compensated by higher partition constant of this peptide, in good agreement with the fluorescence data.

4. DISCUSSION

The interaction of the lytic peptides with model membranes is an important way to understand the physicochemical bases of the mechanism of action and also the peptides selectivity. Different models have been proposed for the mechanism of action of antimicrobial peptide (Wimley and Hristova 2011). Independent of the mechanism of action of the peptide its partition to the solvent-lipid bilayer interface is common to these mechanisms. We have used fluorescence spectroscopy to explore the photophysical properties of the unique tryptophan and of *ortho*-aminobenzoic acid as intrinsic and extrinsic labels to obtain information about affinity, penetration, orientation and conformational dynamics of these peptides in zwitterionic (POPC) and anionic (8POPC:2POPG) LUVs.

Two of the peptides studied have a tryptophan as eighth residue which was observed, in previous work by molecular dynamic simulation, to be in the region of the helical structure in TFE and probably also in lipid bilayer. The third peptide has the extrinsic fluorescent probe *ortho*-aminobenzoic acid covalently bonded to the N-terminus.

The partition of the tryptophan containing peptides to lipid vesicles is accompanied by a significant spectral shift compared to their emission spectra in buffer. The shift to shorter wavelength is a characteristic of change of the tryptophan to a less polar environment as observed with other antimicrobial peptides (Zhao and Kinunnen 2002; Ferre et al. 2009). Compatible with the change in environment, it was observed that the tryptophan accessibilities to the aqueous soluble quencher acrylamide was reduced to 66% and 31% for the native and the acetylated analog respectively in zwitterionic vesicles, using the accessibility in buffer as reference. The reduction in the accessibility indicates that the fluorescent moiety is buried in a region of the bilayer which is screened from the solvent (Gazzara et al. 1997). In anionic vesicles the screening of the tryptophan is even more drastic and the accessibility decreased to 28%

and 15% for the native and the acetylated analog respectively. Although the spectral shifts of the *ortho*-aminobenzoic acid showed low sensibility to discriminate the changes in the environment polarity between the two types of vesicles, assays of fluorescence quenching showed that the accessibility of the Abz-analog was much more reduced compared to the tryptophan containing peptides.

The fit of the time-resolved intensity decay to three exponential functions is a common feature of tryptophan containing peptides (Engelborghs 2001; Romani et al. 2009, 2010). A multi-exponential decay kinetic model based on the indole side chain dynamics was employed to establish structure-fluorescence correlations in protein solution structure (Moncrieffe et al. 2000) and an identification was made for lifetimes and corresponding rotamers in proteins, from comparison of fluorescence with crystallographic and 1H-NMR data (Clayton and Sawyer, 1999; Pan and Barkley, 2004). On the other hand, the partitioning of the fluorophore into a complex environment as the bilayer interface may substantially influence its fluorescence (Ladokhin 2001), so that the meaning of the individual decay component of membrane peptides and proteins is ambiguous, and data processing using continuous lifetime distributions would be relevant, as reported in studies on gramicidin in lipid vesicles (Haldar et al, 2012) . We observed that the three lifetimes for L1A and Ac-L1A are similar, however differences in the pre-exponential factors indicate that acetylation of the peptide leads to conformational changes that can be related to modifications in rotamers distribution or in relaxation process of tryptophan. Upon interaction with the vesicles, lifetimes increase, as expected from the increase in the intensity of emission, without further differentiation between the original peptide and its acetylated analog. Concerning the Abz-L1A-W8V peptide, the intensity decay profile, best fitted to a bi-exponential function, shows that the fluorescent group linked to the N-terminal have deeper insertion into the bilayer of mixed POPC/POPG vesicles, which occurs without significant changes in the isomer equilibrium of the Abz fluorophore.

The anisotropy decay profiles were analyzed considering that the peptides are randomly oriented when free in buffer solutions and, in the presence of lipid vesicles, interact with the lipid aggregates which also do not display any preferential orientation in the aqueous environment. When peptides are adsorbed into the lipid bilayer the rotational freedom in buffer was lost, and rotational diffusion of the fluorophores were subjected to the local constraints resulting in a significant increase in steady-state anisotropy. Parallel to that, for the peptides in the bilayer, the average lifetime of both

Trp and Abz fluorophores increased reinforcing the observation that they move to a less polar environment (Raghuraman and Chattopadhyay 2007). In addition, the anisotropy decay of the peptides in the lipid bilayers also presented significant raise in the long correlation times, accompanied by high values in the residual anisotropy. Altogether, the time-resolved data reveal the restrictions imposed by the lipid bilayers to the peptides as a whole, consistent with the information obtained by steady-state anisotropy measurements.

The decrease in accessibility of the fluorophores to quencher molecules dispersed in water, and the higher values of the long correlation times observed for the two analogues, suggest that the N-terminus modification lead to different positioning of the peptides in the vesicle surface compared with the native peptide. Probably this is favored by the loss of N-terminus positive charge and, therefore, by the decrease of repulsion from the bilayer dipole potential (Brockman 1994, Zhan and Lazaridis 2012). Judging from the intensity decay lifetimes, correlation times and accessibility to the quencher, these analogues, specially the Abz-analogue, have the N-terminus more deeply inserted into the bilayer leading to more restricted motion. The restriction to motion seems to be closely related to the lipid packing perturbation induced by the peptide and its consequent effect on the lytic activity. The fraction of peptide bound per lipid to achieve 50% of dye release from vesicles ($[P_b]/[L]_{EC50}$), after 1 min. of action, has been used as a parameter to quantify the lytic efficiency (Dathe et al. 2001). The peptide to lipid ratios to induce 50% of leakage in lipid vesicles (EC50) and the respective $[P_b]/[L]_{EC50}$ fractions of bound peptide are shown in the table 4. L1A and both analogs were more efficient in anionic vesicles, indicating selectivity to charged bilayers and suggesting a modulatory effect of the electrostatic interactions on the selectivity. The reduction of the peptides net charge, due to the N-terminus acetylation, led to the decrease of lytic efficiency in both vesicles compared to the native peptide, which probably is due to reduced perturbation to the lipid package and consistent with the reduced residual anisotropy compared to the other two peptides. Despite the reduction in the lytic efficiency and of the similarity in the affinity of the acetylated analog to the two types of vesicles, this analog is almost 5 times more efficient in anionic than in zwitterionic vesicles. The Abz-analog with higher affinities to both bilayers induced higher perturbation in the lipid packing, consistent with the higher correlation time and residual anisotropy, resulting in higher efficiency in the lytic

activity. Despite the enhancement in the lytic efficiency this analog has similar selectivity to anionic vesicles observed for the native peptide.

The mechanism of action of these peptides is not yet known, however, considering that the sequence was derived from Polybia MP1 they may have similar mechanism of this peptide. Previous work (dos Santos Cabrera et al 2011) showed evidences that MP1 has an interfacial action on lipid vesicles. Visualization of giant unilamellar vesicles (GUVs) by fluorescence and phase contrast microscopies showed that L1A and analogues (manuscript submitted) and MP1 (dos Santos Cabrera et al 2011) at low concentrations induced gradual loss of phase contrast while the integrity of the vesicles was maintained even after the complete vesicle leakage. The peptide accumulates in the outer monolayer, without evidence of self-aggregation, up to a critical concentration. The perturbation induced in the bilayer by the peptide accumulation is relieved by the formation of defects leading to the leakage. The results above show that the peptide penetration in the non-polar membrane environment and consequent lipid packing perturbation are well correlated with the peptide to lipid ratios inducing vesicle leakage. The higher lytic efficiency of L1A and analogues in mixed anionic compared to zwitterionic vesicles were also observed in the biological activities. L1A and its acetylated analog was efficient against Gram negative bacteria (MIC= 5.0 and 9.0 μM in *E.coli*) without being hemolytic at 150 μM). The Abz-analog with the same efficiency of the acetylated analog against *E. coli* induced almost 30% of hemolysis at the same concentration. The N-terminus modifications lead to deeper penetration and higher lytic efficiency in model membrane. These modifications however impaired the bactericidal activity. Their decreased net charges hampers that they cross the outer membrane of these bacteria rich in anionic lipopolysaccharides. On the other hand, their lower efficacy against Gram positive bacteria suggest that their lytic mechanism could involve segregation of zwitterionic from the anionic lipids once the lipid membrane of these bacteria is composed only by anionic lipids (Epand and Epand 2009).

5. CONCLUSIONS

The fluorescence of tryptophan or Abz is informative about the local environment of the eighth residue in L1A and Ac-L1A or the amino-terminal in Abz-

L1A-W8V peptides. The adsorption of the peptides into lipid bilayers of zwitterionic (POPC) and (8POPC:2POPG) LUVs was assessed by fluorescence spectroscopy. Peptide adsorption was accompanied by spectral blue shift of fluorescence emission due to the displacement of the fluorophores to a less polar environment. In addition the decrease in fluorescence quenching by acrylamide evidences the burying of these fluorophores in the lipid phase of the vesicles.

Despite the local character of spectroscopic information, conclusions can be drawn about the peptides as a whole. The peptides behave so that the mean intensity lifetimes, the long correlation time and the residual anisotropy at long times increased when the peptides adsorb in lipid vesicles, being larger in anionic vesicles. From steady-state increase in fluorescence intensity and anisotropy, we observed that partition coefficient of peptides L1A and its Abz –analog in both types of vesicles are higher than the acetylated analog and moreover the affinity to anionic vesicle is higher than to zwitterionic ones. The spectroscopy data are in agreement with the observation that the Abz-analog has more lytic efficiency while the acetylated analog was even more selective than the native peptide that has higher net charge.

Acknowledgements: JRN acknowledges the financial support from Sao Paulo Research Foundation (FAPESP) grant # 2011/11640-5. ASI thanks the Brazilian agencies FAPESP, CNPq and INCT-FCx for financial support. Support from INCT. ASI and JRN are researchers of CNPq. LMPZ and WMP are recipient of PhD grant from CAPES. DSA acknowledges Sao Paulo Research Foundation (FAPESP) for PhD fellowship # 2012/08147-8

Figures

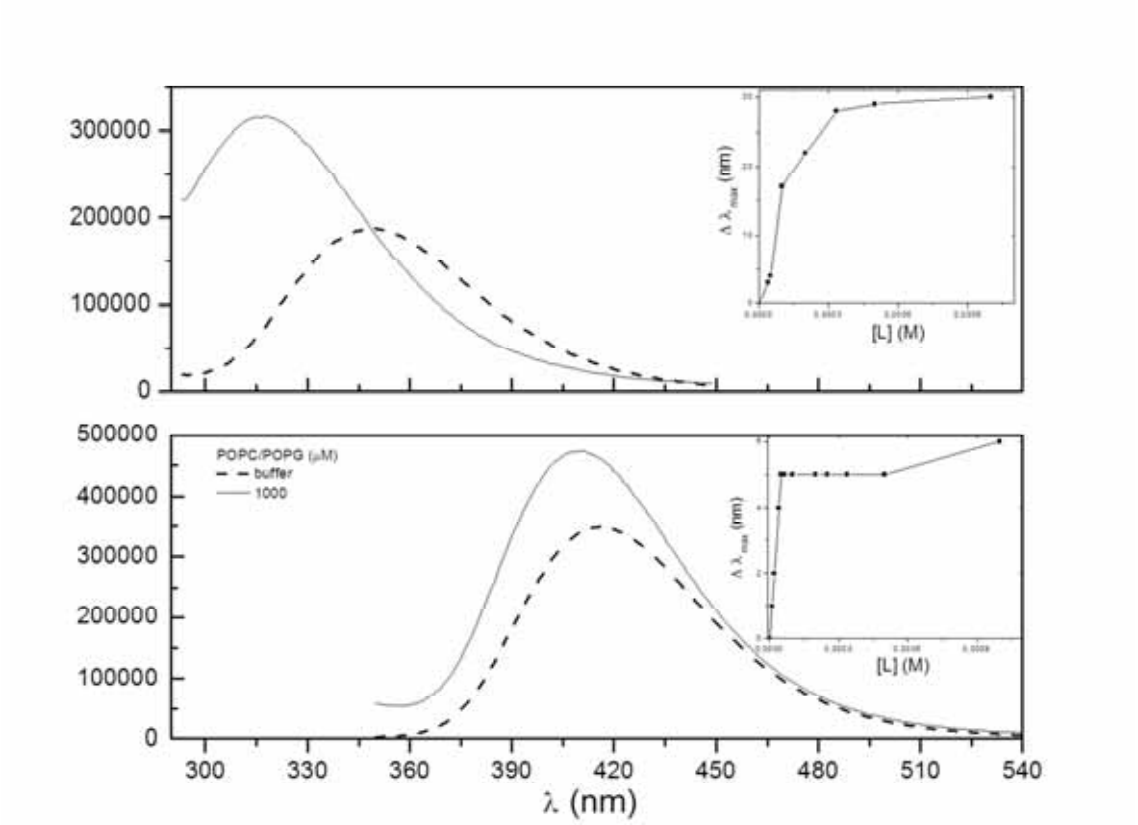

Fig. 1. Emission fluorescence spectra of (a) L1A and (b) Abz-L1A-W8V in buffer and in the presence of POPCPOPG vesicles at 1 mM total lipid concentration. Tryptofan and Abz were excited at 279 nm and 314 nm respectively. Inset: blue shifts as the difference between the wavelengths at the maximum emission in the absence and in the presence of lipids ($\Delta\lambda = \lambda_0 - \lambda$) displayed as a function of the total molar lipid concentration.

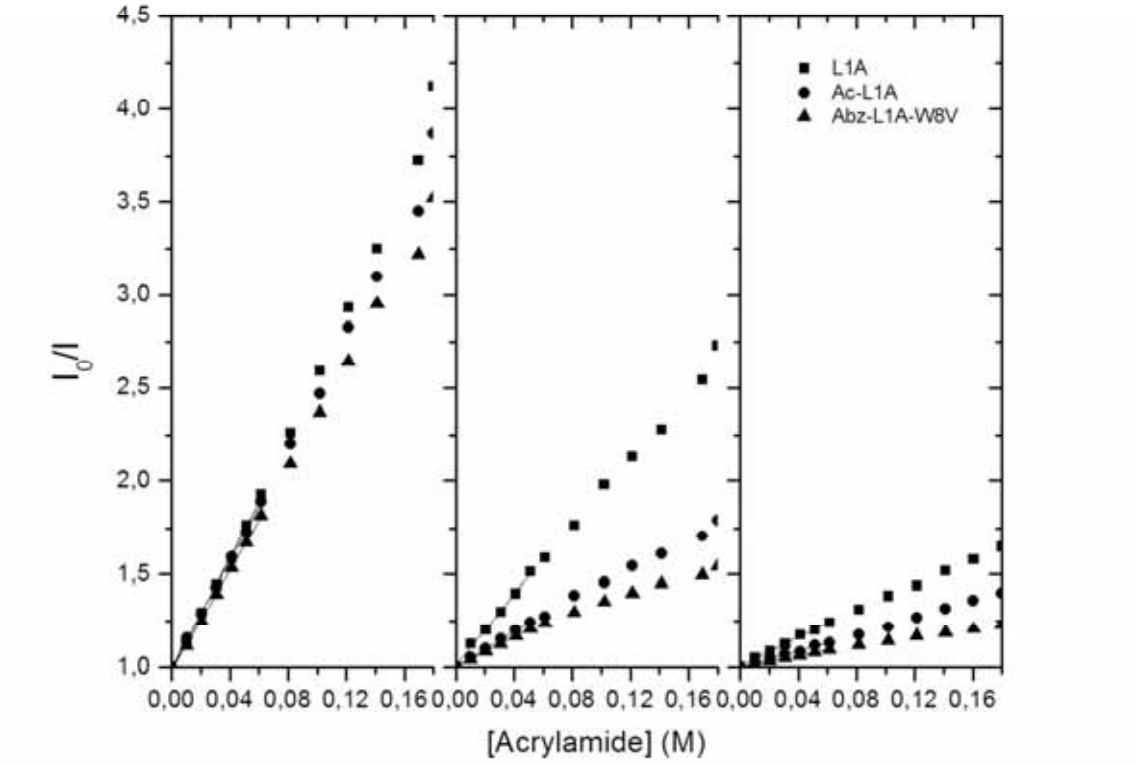

Fig. 2. Stern-Volmer plots for the quenching of three peptides by acrylamide in Tris buffer (left) and in the presence of zwitterionic (POPC) vesicles (center) and anionic (8POPC:2POPG) vesicles (right). Concentrations of the trp and Abz containing peptides were 5.0 μM and 2.0 μM respectively, both in the absence and in the presence of 500 μM lipid vesicles.

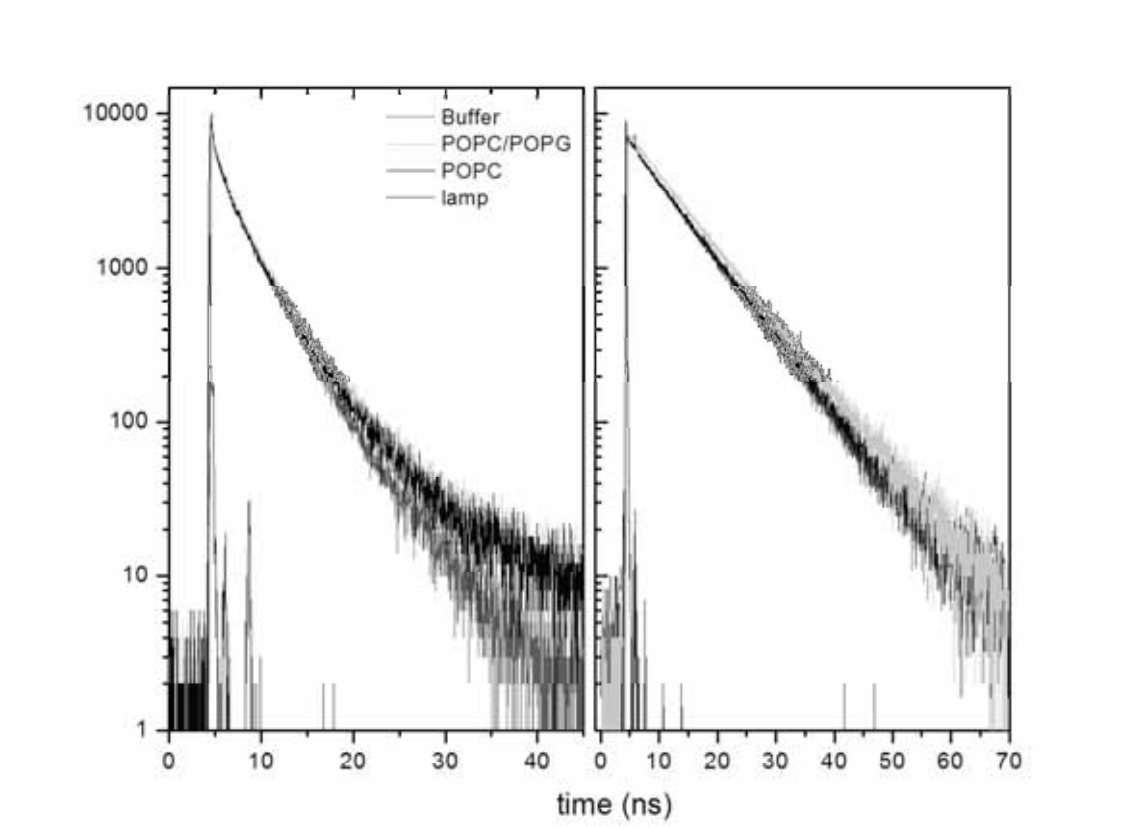

Fig. 3. Fluorescence intensity decays of Trp emission at 350 nm and excitation 295 nm of L1A (left) and Abz- L1A-V8W emission 415 nm and excitation 315 nm (right) in buffer and in the presence of 1 mM POPC and (POPC/POPG) (8:2) LUVs. Also shown the lamp profile (black). Decays were fitted with three exponential function and the fit parameters are shown in table 2.

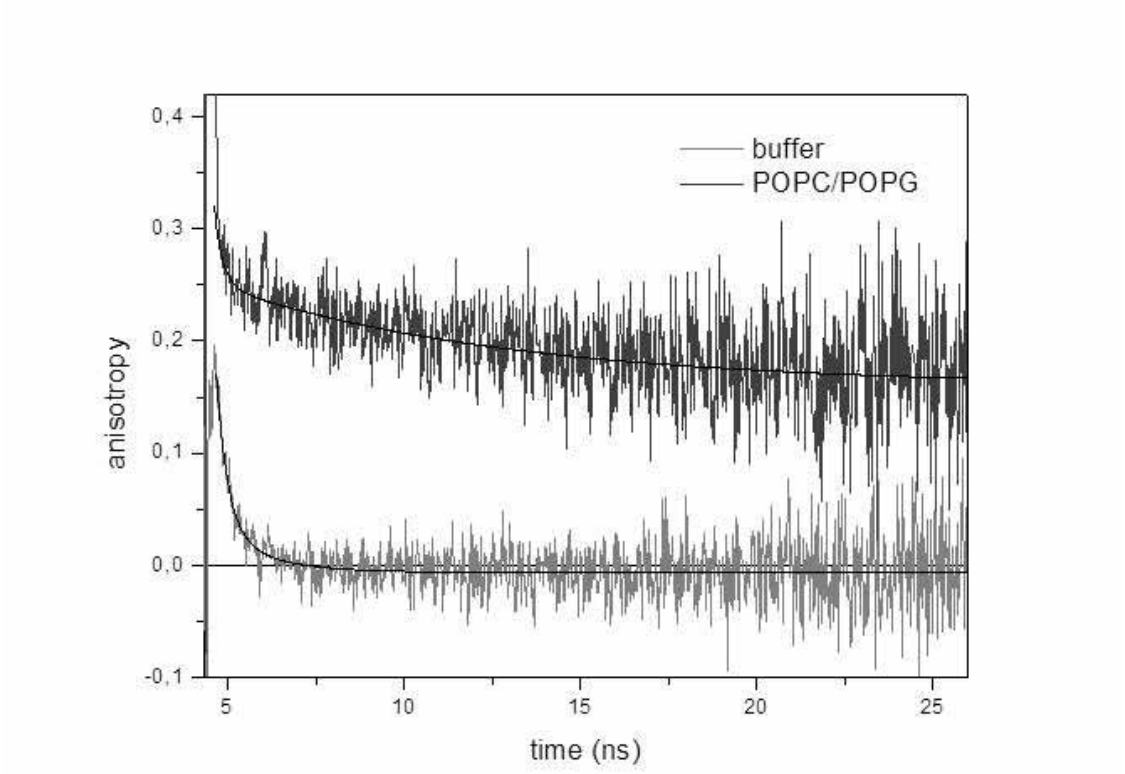

Fig. 4. Anisotropy decay curves for Abz-L1A-W8V peptide in buffer (black) and in the presence of POPC/POPG (8:2) vesicles (gray) at 1 mM total lipid concentration. Excitation 315 nm and emission 415 nm. Lines represent best fit with two exponential function and parameters are shown in table 5.

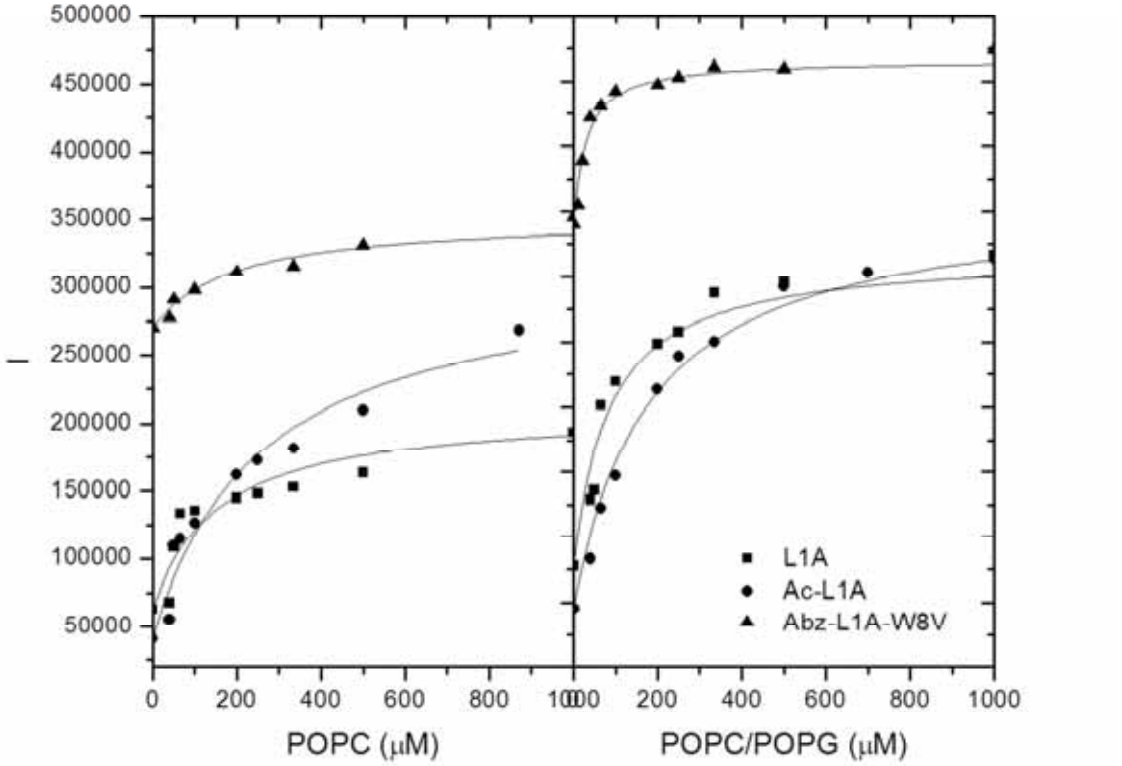

Fig. 5. Equilibrium binding isotherms for peptides titrated with LUVs of POPC (left) and POPC/POPG (8:2) (right). Fluorescence intensities of L1A (square), Ac-L1A (circles) and Abz-L1A-W8V (up-triangles) were plotted as a function of total lipid concentration. Concentration of tryptophan containing peptide 5μM and Abz-L1A-W8V 2 μM. Fluorescence intensities were corrected using eq. 4. Solid lines are best fitting using eq.5.

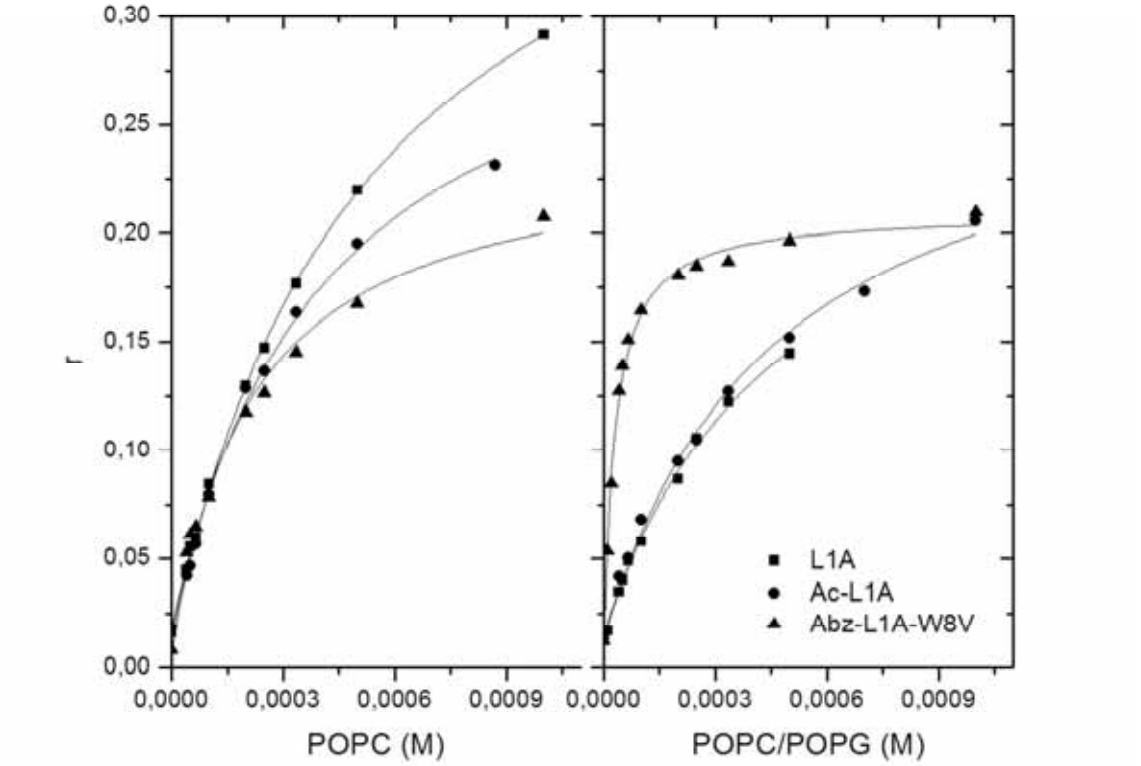

Fig. 6. Equilibrium binding isotherms for peptides titrated with LUVs of POPC (left) and POPC/POPG (8:2) (right). Static anisotropy of L1A (squares), Ac-L1A (circles) and Abz-L1A-W8V (up-triangles) were plotted as a function of the total lipid concentration. Concentration of tryptophan containing peptide 5μM and Abz-L1A-W8V 2 μM. Solid lines are best fitting using eq.6.

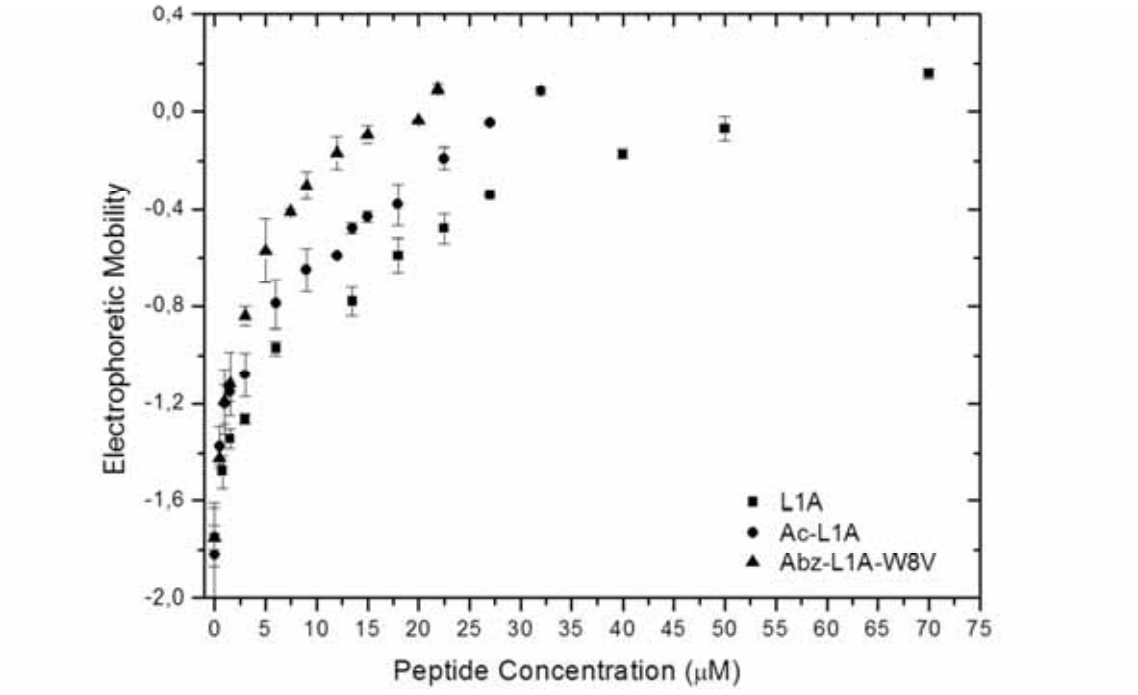

Fig. 7. Zeta potential titrations of POPC:POPG vesicles at 40 μM total lipids in TRIS buffer with L1A (triangles), Ac-L1A (circles) and Abz-L1A-W8V (squares).

Tables

Table 1. Maximum emission wavelengths and Stern-Volmer constants in buffer and in vesicles. The ratios between K_{SV} values in buffer and in the presence of vesicles ($K_{SV\ buffer}/K_{sv\ vesicle}$) are shown in parenthesis.

		L1A	**Ac-L1A**	**Abz-L1A-W8V**
λ_{max}(nm)	Buffer	350	348	416
	POPC	322	314	410
	POPCPOPG	318	313	410
$K_{SV}(mol^{-1})$	Buffer	14.3	14.7	13.0
($K_{sv\ buf}/K_{sv\ ves}$)	POPC	9.4 (1.5)	4.6 (3.2)	3.7 (3.5)
	POPCPOPG	4.0 (3.6)	2.2 (6.7)	1.5 (8.7)

Table 2. Time-resolved parameters for decay of L1A, Ac-L1A and Abz-L1A-W8V in buffer and in the presence of the vesicles (1mM). τ_i and b_i are lifetime and pre-exponential factors for component *i*. For L1A and Ac-L1A, excitation wavelength was 295 nm and emission was recorded at 350 nm. For Abz-L1A-W8V, excitation at 310 nm and emission at 410 nm.

	τ_1	τ_2	τ_3	b_{1n}	b_{2n}	b_{3n}	τ_{av}	τ_m
L1A								
buffer	5,57	3,04	1,17	0,16	0,59	0,25	3,62	2,98
POPC	6,34	3,23	1,14	0,13	0,60	0,27	3,85	3,1
POPC/POPG	10,10	3,83	1,18	0,06	0,63	0,31	4,7	3,38
Ac-L1A								
buffer	5,34	2,56	0,7	0,26	0,50	0,24	3,81	2,84
POPC	6,17	3,78	1,63	0,17	0,55	0,27	4,22	3,57
POPC/POPG	6,75	3,75	2,03	0,12	0,54	0,35	4,09	3.54
Abz-L1A-W8V								
buffer	8,57	4,51	--	0,89	0,11	--	8,32	8,12
POPC	8,76	2,39	--	0,93	0,07	--	8,62	8,31
POPC/POPG	9,07	2,15	--	0,94	0,06	--	8,97	8,65

Table 3. Steady state anisotropy (r), rotational correlation times (Φ_i), initial anisotropy (r_o), fractional pre-exponential parameter (f_i) residual anisotropy (r_∞) and maximum wobbling cone angle (θ) obtained from fitting of experimental anisotropy decay curves to bi-exponential function. Excitation and emission wavelengths were 296 nm and 350 nm for L1A and AcL1A peptides and 315 nm and 415 nm for Abz-L1A-W8V. Results for LUV's, at 1 mM total lipid concentration.

	r	Φ_1 (ns)	Φ_2 (ns)	r_o	f_1	f_2	r_∞	Θ_{max}
L1A								
buffer	0.002	0.49	-	0.222		-	-0,003	79
POPC	0.29	1.16	0.024	0.304	0.20	0.80	0.063	56
POPC/POPG	0.20	2.18	0.044	0.305	0.28	0.72	0.108	46
Ac-L1A								
buffer	0.003	0.47	-	0.215		-	0.002	80
POPC	0.23	1.68	0.043	0.284	0.18	0.82	0.034	62
POPC/POPG	0.21	3.98	0.037	0.279	0.18	0.82	0.039	60
Abz-L1A-W8V								
buffer	0.001	1.19	0.31	0.257	0.24	0.76	-0.006	77
POPC	0.20	2.46	0.12	0.302	0.22	0.78	0.098	47
POPC/POPG	0.20	7.58	0.098	0.334	0.35	0.65	0.161	39

Table 4. Partition coefficients determined from the fluorescence intensities and anisotropy, EC50 the peptide to lipid ratio to induce 50% of dye entrapped release from vesicles, at 100 µM total lipid concentration, after 1 minute of contact time and ratio of bound peptide per lipid ($[P_b]/[L]$) at EC50.

Partition Coefficients $K_p \times 10^3$ (M^{-1})

	POPC			POPCPOPG		
	L1A	Ac-L1A	Abz-L1A-W8V	L1A	Ac-L1A	Abz-L1A-W8V
Intensity	6.6 ± 0.2	6.1± 0.4	9.3± 0.2	8.2 ± 0.3	6.0± 0.6	38.7±0.6
Anisotropy	2.3± 0.5	2.5± 0.4	5.9 ± 0.7	2.4± 0.3	2.7±0.3	39.5± 3.0
EC50	0.24	0.37	0.06	0.09	0.08	0.026
$[P_b]/[L]_{EC50}$	0.08	0.2	0.03	0.04	0.03	0.02

REFERENCES

Arbuzova A, Schwarz G (1999) Pore-forming action of mastoparan peptides on liposomes: a quantitative analysis. Biochim Biophys Acta 1420:139-152.

Almeida PF, Pokorny A (2009) Mechanism of antimicrobial, cytolytic and cell-penetrating peptides: From kinetics to thermodynamics. Biochemistry 48:8083-8093.

Brockman H (1994) Dipole potential of lipid-membranes. Chem. Phys. Lipids 73:57–79.

Castanho MARB, Prieto MJE (1992) Fluorescence study of the macrolide pentaene antibiotic filipin in aqueous solution and in a model system of membranes. Eur. J. Biochem. 207: 125-134.

Clayton AHA, Sawyer WH (1999) Tryptophan rotamer distributions in amphipathic peptides at a lipid surface. Biophys J 76:3235-3242.

Chen Y, Mant CT, Farmer SW, Hancock REW, Vasil ML, Hodges RS (2005) Rational design of alpha-helical antimicrobial peptide with enhanced activity and specificity/therapeutic index. J. Biol. Chem 280:12316-12329.

Coutinho A, Prieto M (1995) Self-association of the polyene antibiotic nistatin in dipalmitoylphosphatidylcholine vesicles: a time-resolved fluorescence study. Biophys. J 69:2541-2557

Dathe M, Wieprecht T (1999) Structural features of helical antimicrobial peptides: their potential to modulate activity on model membranes and biological cells. Biochim Biophys Acta 1462:71-87.

Dathe M, Nikolenko H, Meyer J, Beyermann M, Bienert M (2001) Optimization of the antimicrobial activity of magainin peptides by modification of charge. FEBS Lett. 501:146-150.

Engelborghs Y (2001) The analysis of time resolved protein fluorescence in multi-tryptophan proteins. Spectrochim Acta, 57:2255–2270.

Epand RM, Epand RF (2009) Lipid domains in bacterial membranes and the action of antimicrobial agents. Biochim. Biophys. Acta 1788: 289 - 294.

Ferre R, Melo MN, Correia AD, Feliu L, Bardaji E, Planas M, Castanho M (2009) Synergistic effects of the membrane actions of ceropin-melittin antimicrobial hybrid peptide BP100. Biophysical J. 96:1815-1827.

Gazzara JA, Philips MC, Lund-Katz S, Palgunachari MN, Segrest JP, Anantharamaiah GM, Snow JS (1997) Interaction of class A amphipathic helical peptides with phospholipid unilamellar vesicles. J. Lipid Res. 38:2134-2146.

Goldman C, Pascutti PG, Piquini P, Ito AS (1995) On the contribution of electron transfer reaction to the quenching of tryptophan fluorescence. J. Chem. Phys**.**, 103:10614-10620.

Haldar S, Chaudhuri A, Gu H, Koeppe RE, Kombrabail M, Krishnamoorthy G, Chattopadhya A (2012) Membrane Organization and Dynamics of “Inner Pair” and “Outer Pair” Tryptophan Residues in Gramicidin Channels. J. Phys. Chem. B, 116: 11056-11064

Hancock REW, Sahl H-G (2006) Antimicrobial and host-defense peptides as new anti-infective therapeutic strategies. Nat. Biotechnol. 24:1551–1557.

Hellings M, De Maeyer M, Verheyden S, Hao Q, Van Damme EJM, Peumans WJ, Engelborghs Y (2003) The dead-end elimination method, tryptophan rotamers, and fluorescence lifetimes. Biophys. J. 85:1894-1902.

Ito AS, Castrucci AML, Hruby VJ, Hadley ME, Krajcarski DT, Szabo AG (1993) Structure activity correlations of melanotropic peptides in model lipids by tryptophan fluorescence studies. Biochemistry, 32:12264-12272.

Ito AS, Turchiello RF, Hirata IY, Cezari MH, Meldal M, Juliano L (1998) Fluorescent properties of amino acids labeled with orthoaminobenzoic.Biospectroscopy 4:395-402.

Jiang Z, Vasil AI, Hale JD, Hancock RE, Vasil ML, Hodges RS (2008) Effects of net charge and the number of positively charged residues on the biological activity of amphipathic alpha-helical cationic antimicrobial peptides. Biopolymers (Peptide Science) 90:369–383

Kawato S, Kinosita Jr K, Ikegami A (1978) Effect of cholesterol on the molecular motion in the hydrocarbon region of lecithin bilayers studied by nanosecond fluorescence techniques. Biochemistry 17:5026-5031.

Ladokhin AS, Jayasinghe S, White, SH (2000) How to measure and analyze the tryptophan fluorescence in membrane properly and why bother. Anal Biochem. 285:235- 245.

Ladokhin, AS (2001) On the interpretation of decay-associated fluorescence spectra in proteins. Biopolymers Cell. 17:221–224.

Leite NB, da Costa LC, Alvares DS, Dos Santos Cabrera MP, De Souza BM, Palma MS, Ruggiero Neto J (2010) The effect of acidic residues and amphipathicity on the lytic activities of mastoparan peptides studied by fluorescence and CD spectroscopy. Amino Acids 40:91–100.

Loura LMS, Ramalho JP (2007) Location and dynamics of acyl chain NBD-labeled phosphatidylcholine (NBD-PC) in DPPC bilayers. A molecular dynamics and time-resolved fluorescence anisotropy study. Biochimica et Biophysica Acta 1768: 467–478

Makovitzki, A, Avrahami, D, Shai, Y (2006) Ultrashort antibacterial and antifungal lipopeptides Proc Natl Acad Sci USA 103:15997–16002

Matsuzaki K. (2009) Control of cell selectivity of antimicrobial peptides. Biochim. Biophys. Acta 1788: 1687– 1692

Moncrieffe MC, Juranic N, Kemple MD, Potter JD, Macura S, Prendergast FG (2000) Structure-fluorescence correlations in a single tryptophan mutant of carp parvalbumin: solution structure, backbone and side-chain dynamics. J Mol Biol 297:147-163.

Pan C-P, Barkley MD (2004) Conformational effects on tryptophan fluorescence in cyclic hexapeptides. Biophys J 86:3828-2835.

Raghuramanan H, Chattopadhyay A (2007) Orientation and dynamics of melittin in membranes of varying composition utilizing NBD fluorescence. Biophysical J 92:1271-1283.

Rapson AC, Hossain MA, Wade, JD, Nice EC, Smith TA, Clayton AHA, Gee ML (2011) Structural dynamics of a lytic peptide interacting with a supported lipid bilayer. Biophys. J. 100: 1353-1361.

Romani AP, Marquezin CA, Soares AEE, Ito AS (2006) Study of the interaction between *Apis mellifera* venom and micro-heterogeneous systems. J Fluorescence 16:423-430.

Romani AP, Ito, AS (2009) Interaction of adrenocorticotropin peptides with micro-heterogeneous systems.A fluorescence study. Biophysical Chemistry 139:92-98.

Romani AP, Marquezin CA, Ito AS (2010) Fluorescence spectroscopy of small peptides interacting with microheterogeneous micelles. Int J Pharmaceutics 383:154-156.

Rouser G, Fleischer S, Yamamoto A (1970) Two Dimensional Thin Layer Chromatographic Separation of Polar Lipids and Determination of Phospholipids by Phosphorus Analysis of Spots. Lipids 5:494-496.

Souza ES, Hirata IY, Juliano L, Ito AS (2000) End-to-end distribution distances in bradykinin observed by fluorescence energy transfer. Bioch Biophys Acta 1474:251-261.

Souza BM, Silva AR, Resende VMF, Arcuri HA, dos Santos Cabrera MP, Ruggiero Neto J, Palma MS (2009) Characterization of two novel polyfunctional mastoparan peptides from the venom of the social wasp Polybia paulista. Peptides 30:1387–1395

Turchiello RF, Lamy-Freund MT, Hirata IY, Juliano L, Ito AS (1998) Ortho-aminobenzoic acid as a fluorescent probe for the interaction between peptides and micelles. Biophys Chem 73:217-225.

Turchiello RF, Lamy-Freund MT, Hirata IY, Juliano Land Ito AS (2002) Ortho-Aminobenzoic Acid-Labeled Bradykinins in Interaction with Lipid Vesicles: Fluorescence Study. Biopolymers 65:336-346.

Takara M, Eisenhut JK, Hirata IY, Juliano L, Ito AS (2009) Solvent Effects in Optical Spectra of ortho-Aminobenzoic Acid Derivatives. Journal of Fluorescence 19:1053-1060.

Wang KR, Zhang BZ, Zhang W, Yan JX, Li J, Wang R (2008) Antitumor effects and cell selectivity and structure-activity relationship of a novel antimicrobial peptide Polybia-MP1. Peptides 29:2320-2327.

Wang K, Yan J, Zhang B, Song J, Jia J, Jia P, Wnag R (2009) Novel mode of action of polybia-MP1 a novel antimicrobial peptide in multidrug resistant leukemic cells. Cancer Lett 278:65-72.

Wimley WC, Hristova K (2011) Antimicrobial peptides: Success, Challenges and Unanswered Questions. J Membrane Biol 239:27-34.

Wieprecht T, Dathe M, Schümann M, Krause E, Beyermann M, Bienert M (1996) Conformational and functional study of magainin 2 in model membrane environments using the new approach of systematic double-D-amino acid replacement. Biochemistry 35(33):10844–10853

Yandek, LE, Pokorny A, Almeida PFF (2009) Wasp mastoparan follow the same mechanism as cell-penetrating peptide Transportan 10. Biochemistry 48:7342-7351.

Zasloff M (2002) Antimicrobial peptides of multicellular organisms. Nature 415: 389-395.

Zhan H, Lazaridis T (2012) Influence of the membrane dipole potential on peptide binding to lipid bilayers. Biophys Chem 161:1-7.

Zhao Kinnunen PJ (2002) Binding of the antimicrobial peptide Temporin L to liposomes assessed by trp fluorescence. J Biol Chem 277:25170-25177.

3.2. LYTIC AND BIOLOGICAL ACTIVITIES AND SELECTIVITY OF A NOVEL SYNTHETIC ANTIMICROBIAL PEPTIDE

Luciana Puia Moro Zanin[a], Alexandre Suman de Araujo[a], Maria Aparecida Juliano[b], Tiago Casella[c], Mara Correa Lelles Nogueira[c] and João Ruggiero Neto[a]

[a] Department of Physics - IBILCE- São Paulo State University- São José do Rio Preto- Brazil

[b] Department of Byophysics - UNIFESP - São Paulo - Brazil

[d] FAMERP - Department of Dermatological, Infectious and Parasitary Diseases – (CEP) São Jose do Rio Preto (SP) - Brazil

.

* Corresponding author: email jruggiero@sjrp.unesp.br. Departamento de Física, IBILCE-UNESP, Rua Cristovão Colombo 2265, São José do Rio Preto SP, Brazil, CEP 15054-000. Phone (+5517) 3221-2240, Fax (+5517) 3221-2247

ABSTRACT

A wide variety of microbial peptides have been designed based on the amphipathic motif, resulting in hight activities. The octadecapeptide L1A (IDGLKAIWKKVADLLKNT-NH2) was designed to have the same structural characteristics which imparted selectivity to the peptide Polybia MP1: the relative positioning of acidic and basic residues as third and fourth neighbors, the presence of an acidic residue at the N-terminus, its hydrophilicity and its broad polar face. The tetradecapeptide polybia MP1 is a potent antimicrobial, antitumoral and non-hemolytic peptide. The present work analyzes the conformation and evaluate the peptides adsorption and lytic activity in zwitterionic and anionic vesicles as well as the bactericidal and hemolytic activities. Two analogs of L1A with N-terminus modifications were also synthesized. One of them with N-terminus acetylation (Ac-L1a) and the other with the fluorescent moiety ortho-amonibenzoic acid (Abz) covalently incorporated at its N-terminus. In the Abz - analog the tryptophan was changed by valine (Abz-L1A-W8V). L1A were more efficient to induce release of fluorescent dye entrapped in anionic vesicles. The observed order of lytic efficiency in zwitterionic and anionic vesicles was Abz-L1A-W8V>Ac-L1A>L1A. These observations were compatible with the higher helical content (observed in MD and CD) and deeper burying of the fluorophores in anionic vesicle. L1A and Ac-L1A were selective against Gram negative bacteria without being hemolyitic. The N-terminus modifications impaired bactericidal activity and the Abz-analog was mildly hemolytic. In conclusion the acidic and basic residues distribution imparted to L1A similar selectivity observed for MP1. The decrease of the inhibitory growth effect on Gram positive bacteria was attributed to the increase of the larger separation of acidic residue in L1A compared to MP1.

Key words: antimicrobial peptide, peptide selectivity, lytic activity.

1. INTRODUCTION

Helical cationic peptides constitute an important class of lytic and antimicrobial peptides, which are broadly distributed among many living species and belong to the innate immune systems of these species [Hamil et al., 2008; Zasloff, 2002]. Generally, antimicrobial peptides are composed of 10–50 amino acids that are rich in positive charges and hydrophobic residues which are distributed in such way that they form an amphipathic helical structure when in contact with lipid bilayer or membrane mimetic environment [Zasloff, 2002]. Several studies have indicated that formation of amphipathic and stable structures on bacterial membranes is responsible for the peptides antimicrobial activity.

The mastoparan peptide Polybia-MP1 (IDWKKLLDAAKQIL-NH2) or shortly MP1, is a helical peptide extracted from the native Brazilian wasp *Polybia paulista*. This peptide has in its sequence the unusual presence of two acidic residues (D2 and D8) concomitantly with three basic residues (K4, K5 and K11), that besides the amidation of the C-terminus, resulted in relatively low net charge Q=+2. Notwithstanding its low net charge MP1 has a broad spectrum bactericidal activity being virtually non-hemolytic and non-cytotoxic [Souza et al., 2009]. Besides antimicrobial activity, MP1 showed selective inhibitory effect on proliferating bladder and prostate cancer cells [Wang et al., 2008] and efficacy against multidrug resistant leukemic cells [Wang et al., 2009]. Recently we have observed that this peptide is cytotoxic against leukemic T lymphocytes and very selective in recognizing these cells compared to the primary line lymphocytes [dos Santos Cabrera et al., 2012].

Acidic residues are of very low occurrence in antimicrobial peptides [Fjell et al., 2007, Wang and Wang, 2004], however, in the case of MP1 it seems that the acidic residues play important roles in modulating its selectivity. The substitution of the aspartic residue in the N-terminus by an asparagine (D2N) increased significantly the hemolytic activity (EC50=26 μM) leading to a less selective peptide [Leite et al., 2010]. In addition, the substitution of the aspartic residues by lysines and the glutamine by arginine in the MP1 resulted in higher toxicity to human cells [Wang et al., 2010]. Molecular dynamics simulation in 40% TFE [dos Santos Cabrera e al., 2008] suggested an important role played by the acidic residue in the N-terminus as well as the relative

positioning of acidic and basic residues on the charge-hydrophobic balance. Those simulations showed that each acidic residue is ion-paired with two amines: D2 with N-terminus NH_3 and K5 and D8 with K4 and K11. These simulations showed that the charged residues, arranged in two clusters, one involving Asp 2, Lys4, Lys5 and N-terminus and the other formed by Asp8 and Lys 11 are closely positioned to ion pair and hydrogen bonding. The O^- of Asp 2 is about around 0.75 nm far from NH3+ (N-terminal), 0.72 nm far from NH3+ of Lys 4 and 0.6 nm far from NH3+ of Lys 5 and is part of the hydrogen bond with N of Lys 5 backbone during 90% of the simulation time.

It was observed an electrostatic equilibrium relating Asp 2 and NH_3 groups of N-terminus and Lys 4 and Ly5 minimizing the electric field of the positive charge. The O^- of Asp 8 plays a similar role with NH_3 of Lys 11 and NH_2 of Gln 12. The charge equilibrium involves also NH_3 groups of Lys4 and Lys 5. The three cationic and polar groups form approximately a tetrahedron with O^- of Asp 8 at the apical position. The close positioning of the two aspartic residues provides extensive ion-pairing in its hydrophilic face. Besides charge balance these ion-pairings contribute to the stabilization of the helical structure. In addition, the low mean residue hydrophobicity (<H>= -0.11) and the wider polar face (Φ=120) of MP1 are also believed to contribute to the Polybia MP1 selectivity to antimicrobial activity compared to hemolysis.

In this paper, aiming to investigate how determinant are these characteristics to the peptides selectivity we designed a new sequence (L1A) with 18 residues: IDGLKAIWKKVADLLKNT-NH2, two acidic residues (D2 and D13) and four basic (K5, K9, K10 and K16) as third and fourth neighbors (i, i+4), in such way that each acidic residues can ion-pair two amines. The new sequence is four residues longer than MP1 and has more possesses a lysine giving a charge of Q=+3 due to C-terminus amidation, with the same mean residue hydrophobicity (<H>= -0.1) of MP1 and with slightly broader polar face (Φ=140).

To better understand the importance of the load in the region of the N-terminal, stabilization of the peptide conformation and on the lytic and biological activity two peptides were synthesized with modifications. First analog, Ac-L1A, the N-terminus was acetylated and the other the fluorescent moiety *ortho*-aminobenzoic acid (Abz) was covalently bonded to the N-terminus, resulting a charge Q= +2. In the Abz-analog, (Abz-L1A-W8V) the tryptophan residue was substituted by a valine to avoid intra-peptide energy transfer.

In this work the MD simulations and the biophysical characterization of these peptides are presented in association to their antimicrobial and hemolytic evaluations. The MD simulations indicate that L1A assumes an amphipathic α-helical conformation from residue 3 to 14, in TFE/water mixture, while analogs already have the first residue in helix. The peptides Ac-L1A possess also the fifteen residue and Abz-W8V-L1A presented Abz in helix. Conformational information obtained from the simulations is in good agreement with the α-helical contents determined in CD spectra. The conformational analysis by circular dichroism revealed higher helical content in anionic compared to zwitterionic vesicles and that both N-terminus modifications increased the helical fractions in these vesicles. These data are well correlated with higher preference to anionic vesicles and increased lytic efficiency in these vesicles with the analogs inducing higher vesicle permeabilization. The evaluation of the antimicrobial activities showed higher efficacy of L1A and its acetylated analog against Gram negative bacteria being virtually non-hemolytic.

2. MATERIALS AND METHODS

2.1 Matetials. Lipids: 1-palmitoyl-2-oleoyl-*sn*-glycero-3-phosphocholine (POPC) and 1-palmitoyl-2-oleoyl-*sn*-glycero-3-phosphoglycerol (POPG) were purchased from Avanti Polar Lipids (Alabaster, AL); carboxyfluorescein (CF), Chloramphenicol and triphenyltetrazolium chloride (TCC) from Sigma Chemical Co (S. Louis, MI). Tris(hydroxymethyl) aminomethane (Tris) were purchased from Merck. Unless otherwise indicated other chemicals were of high quality analytical grade.

2.2 Synthetic peptides. The peptides IDGLKAIWKKVADLLKNT-NH2 (L1A), Ac-IDGLKAIWKKVADLLKNT-NH2 (Ac-L1A) and Abz-IDGLKAIVKKVADLLKNT-NH2 (Abz-L1A-W8V) were obtained in an automated bench-top simultaneous multiple solid-phase peptide synthesizer (PSSM 8 system from Shimadzu) was used for the solid-phase synthesis of all the peptides by the Fmoc-procedure [Korkmaz et al., 2008]. The final peptides were deprotected in TFA and purified by semi-preparative HPLC using an Econosil C-18 column (10 μ, 22.5 x 250 mm) and a two-solvent system: (A) trifluoroacetic acid (TFA)/H_2O (1:1000) and (B) TFA/acetonitrile (ACN)/H_2O (1:900:100). The column was eluted at a flow rate of 5 ml/min with a 10 (or 30) - 50 (or 60)% gradient of solvent B over 30 or 45 min. Analytical HPLC was performed using a binary HPLC system from Shimadzu with a SPD-10AV Shimadzu uv-vis detector, coupled to an Ultrasphere C-18 column (5 μ, 4.6 x 150 mm) which was eluted with solvent systems A_1 (H_3PO_4/H_2O, 1:1000) and B_1 (ACN/ H_2O/H_3PO_4, 900:100:1) at a flow rate of 1.0 ml/min and a 10-80% gradient of B_1 over 20 min. The HPLC column eluates were monitored by their absorbance at 220 nm. The molecular weight and purity of synthesized peptides were checked by MALDI-TOF mass spectrometry (Bruker Daltons) or eletron spray LC/MS-2010 (Shimadzu).

2.3 Vesicle preparation. Lipid films of POPC or mixture POPC POPG at molar ratio (80:20) were obtained from lipids dissolved in chloroform or chloroform : metanol (2:1) in round-bottom flasks and the solvent was first dried under a N_2 flow and placed

under vacuum overnight to remove traces of organic solvents. The lipid films were afterwards hydrated with TRIS buffer (Tris/H_3BO_3 5 mM, 1mM Na_2EDTA, pH 7.5 or with Tris/HCl 10 mM, 1mM Na_2EDTA, pH 7.5, either containing 25 mM carboxyfluorescein (CF) for leakage experiments or 150 mM NaCl for fluorescence spectroscopy or 150 mM NaF for circular dichroism (CD) experiments. The final total lipid concentration was 5 mM. Small unilamelar vesicles (SUVs), for CD experiments, were obtained by sonication of the lipid suspension under N_2 flow, in ice/water bath, for 50 min, or until clear. Titanium debris has been removed by centrifugation. Large unilamellar vesicles (LUVs ~ 5-10mM) used in dye leakage experiments and zeta potential titrations were obtained by two extrusion steps using an Avanti Mini-Extruder (Alabaster, AL) and double stacked polycarbonate membrane (Nuclepore Track-etch Membrane, Whatman): firstly 6 times through 0.4 μm and then 11 times through 0.1 μm membranes. For the dye-entrapped LUVs the free dye was separated by gel filtration on a Sephadex G25M column (Amersham Pharmacia, Upsala, Sweeden). Vesicles were used within 24 hours of preparation. The lipid concentration was determined by phosphorus analysis [Rouser et al., 1970]. Laser light scattering measurements with Zeta Sizer Nano NS-90 (Malvern Instruments, Worcestershire, U.K.) have revealed homodisperse LUV suspensions, with an average diameter of 105 ± 5 nm among several preparations.

2.4 Peptide solution. Stock solutions of peptides were prepared in Milli-Q water. Peptides were dissolved in TRIS buffer (tris/HCl 10 mM, 1mM Na_2EDTA, 150 mM NaCl, pH 7.5 for Zeta experiments and dye leakage or tris/H_3BO_3 5 mM, 1mM Na_2EDTA, 150 mM NaF, pH 7.5 for CD experiments), under gentle agitation. Peptide concentration was determined spectrophotometrically with a Varian 2200 (Palo Alto, USA) spectrophotometer in 280 nm using molar extinction coefficient ε= 5675 M^{-1} and 1998 M^{-1}.

2.5 MD simulations. The MD simulations were performed in TFE/water (~30% v/v) mixture. System was made up, by about 200 TFE molecules, 1890 water molecules and 2 or 3 chlorine (Cl^-) counterions, which neutralize the net charge of each peptide. For all peptides the C-terminus was amidated. For L1A the N-terminus was treated as a

positively charged group (NH_3^+), in Ac-L1A the N-terminus was acetylated and in Abz-W8V-L1A we attached an o-amino-benzoic acid (Anthranilic acid, or Abz) to N-terminus. The MD simulations were performed in GROMACS 4.5.6 [Pronk et al., 2013] package, with GROMOS 96 [Schuler et al., 2001] force field. Simple Point Charge (SPC) model [Berendsen et al., 1981] was used for water while for the TFE the model proposed by Fioroi [Fioroni et al., 2000] was used. The Abz molecule were modeled using Automated Topology Builder (ATB) website [Malde et al., 2011]. The system minimizations was carried out in 8000 steps conjugate gradient and a steepest descent cycle was performed every 500 steps. Position restriction dynamics, for solvent and ions relaxation ran for 1 ns with 2 fs time-step for the integration of the equations of motion. The constraints were then removed and the system underwent a 50 ns MD simulations. Periodic boundary conditions have been imposed in the system simulation with a cutoff radius of 1.4 nm. The LINCS [Hess et al., 1997] algorithm was used to constraint all bond lengths and SETTLE [Miyamoto; Kollman, 1992] to constraint water geometry. Simulations ran in the canonical ensemble (NTP) 300 K and 1 atm. Temperature and pressure were modulated using coupling techniques [Berendsen et al., 1984] with coupling and isothermal compressibility constants of 0.01 ps and 65 μBar^{-1} respectively. Long-range electrostatic interactions were treated using Particle Mesh Ewald (PME) method. The cutoff radius for the Lenard-Jones was 1.4 nm. The atomic positions were recorded every 10 ps throughout each trajectory.

2.6 Circular dichroism (CD). CD spectra were collected over the range 190-250 nm, using a Jasco-710 spectropolarimeter (JASCO International Co.Ltd., Tokyo, Japan) coupled to a Neslab RTE111 circulating water bath. The wavelength was calibrated using d-10-camphorsulfonic acid. *Spectra* were obtained at 25°C using 0.5 cm path length cell, averaged over six scans, at a scan speed of 20 nm/min, bandwidth of 1.0 nm, 0.5 s response and 0.1nm resolution. CD spectra were obtained at 20 μM peptide concentration in different environments: Tris/H3BO3 buffer, trifluoroethanol (TFE)/water mixture (40% v/v), sodium dodecyl sulfate solution (8 mM) and, in the presence of SUVs, zwitterionic POPC and anionic POPC:POPG (80:20). Following baseline correction, the observed ellipticity, θ (mdeg), was converted to mean residue ellipticity [Θ] (deg cm^2/dmol), using the relationship [Θ] =100 θ /(l c n) where "l" is the path length in centimeters, "c" is the millimolar concentration and "n" is the number of

residues in the peptide. The observed mean residue ellipticity in 222 nm (Θ_{222}^{obs}) was converted to α-helix fraction (f_H) using the method proposed [Deber and Li, 1995]:

$$f_H = \frac{\Theta_{222}^{obs} - \Theta_{222}^{0}}{\Theta_{222}^{100} - \Theta_{222}^{0}} \quad (1)$$

Θ_{222}^{0}=0 and Θ_{222}^{100} is given by:

$$\Theta_{222}^{100} = -39500(1 - 2.57/n) \quad (2)$$

n is peptide length, n = 18 in the present study.

2.7 Steady-state Fluorescence Spectroscopy. Tryptophan and Abz emission fluorescence spectra were collected with ISS PC1 spectrofluorometer (Urbana Champaign USA), using quartz cell with 1 cm path length, at 25ºC. The spectra were recorded from 290 to 450 nm with excitation at 280 nm for L1A and Ac-L1A and from 350 to 550 nm with excitation at 314 nm for Abz-L1A-W8V. The emission spectra were recorded after one hour of sample preparation. Excitation and emission slits varied from 0.5 to 2.0 nm and bandpass filter were used, depending on the samples fluorescence intensities. Correction for scattering was carried out by using cross polarization, parallel at emission and perpendicular at excitation [Ladokin et al., 2000], and/or by subtracting spectra obtained at each vesicle concentration as blank. Blue shifts ($\Delta\lambda_{max}$) were calculated as the differences in wavelength of the maxima in emission spectra of the peptide in the presence and in the absence of vesicles. Standard deviation for the blue shift was 1 nm.

2.8 Zeta Potential Measurements. Zeta potential of anionic POPC/POPG (80:20) large unilamellar vesicles, at 40 μM total lipid concentration, in the absence and in the presence of different concentrations of peptides, were determined from the electrophoretic mobility using a ZetaSizer Nano ZS90 (Malvern Instruments Ltd, Worcestershire, U.K.). Vesicles were prepared in tris buffer Tris/HCl 10 mM, 1mM Na_2EDTA, pH 7.5, 150 mM NaCl, and measurements were carried out with a DTS1060 (Malvern) disposable cells with golden electrodes at 25°C.

2.9 Lytic activity. Aliquots of LUV suspension were added to 1 cm quartz cuvettes containing magnetically stirred peptide solutions to give a final volume of 1.2 ml. Release of CF from LUVs causes decrease in its self-quenching that was followed with a ISS PC1 spectrofluorometer (Champaign, IL, USA) at 520 nm, 0.5 nm slit width, (excited at 490 nm, 1 nm slit width) at 25°C, during 30 min for POPC/POPG (80:20) or POPC LUVs respectively. At regular intervals % leakage is calculated as 100 x (F - F_0)/(F_{100} - F_0), where F is the measured fluorescence intensity, F_0 and F_{100} correspond, respectively, to the fluorescence intensities in the absence of peptides and to 100 % leakage, determined by the addition of 33 μL of 6% Triton X-100 solution. F_{100} has been corrected for the corresponding dilution factor.

2.10 Antimicrobial activity. The minimal inhibitory concentrations (MIC) of the peptides were determined based on methods described [Meletiadis et al., 2000]. The following microorganisms' strains were used: *Staphylococcus aureus* (ATCC 25923), *Escherichia coli* (ATCC 35218) and *Pseudomonas aeruginosa* (ATCC 27853). The experiment was performed in 96 well plates. Bacterial cells were suspended in sterile culture medium; the inoculum size was 1 x 10^4 cells m/L in Müller–Hinton broth (DIFCO), confirmed by the use of McFarland scale. From this culture, 50 μL was spread onto the micro-plate previously containing 50 μL of Müller–Hinton broth, resulting in a final cell density of the 2.5 x 10^3 cell/mL. Cells were incubated at 37 °C for 18 h in the presence of 100 μL of each peptide solution, in a concentration range from 2.3 to 150 μg/ mL. After incubation, 10 μL of a triphenyltetrazolium chloride (TTC) solution (final concentration 0.05%, w/v) was added to each well plate. The plate was incubated at 37 °C for 2 h. Alive colonies reduce TTC to a dark red color, while those with reduced respiratory function are unable to do this and it remains without color change. Thus, the results were expressed as the minimal concentration that inhibits all colony forming units. Chloramphenicol in a concentration ranging from 0.078 to 40 μg/mL was used as standard antibiotic and the negative controls were considered those wells containing only the culture medium. Results were expressed as the mean of three experiments.

2.11 Hemolytic activity. The hemolytic activities of peptides were assessed using human blood cell collected in vacuplast contain EDTA.K3 from healthy donors. The

fresh blood were rinsed three times in PBS-1 (10 mM Na_2HPO_4/KH_2PO_4, 136 mM NaCl, 3 mM KCl, pH7.4), collected by centrifugation for 5 min at 845xg and re-suspended at 8% in PBS-2 (50 mM Na_2HPO_4/KH_2PO_4, 100mM NaCl, 0.5 mM EDTA, pH7.4) and incubated with sample for 60 min at 37°C with final concentration of the 300 μg. After incubation the samples then centrifuged for 5 min at 845xg. The absorbance of the supernatants was assessed at 540 nm and expressed as percentage of lysis. The controls for zero (blank) and 100% hemolysis were blood cell suspended in PBS-2 and 1% Triton X-100, respectively.

3. RESULTS

3.1 Peptide design and MD simulations. The new sequence named L1A possess two acidic (D2 and D13) and four basic residues (K5, K9, K10 and K13). It was designed to distribute these residues into two charge clusters, one involving O^- from Asp 2, Lys 5, and the N-terminus NH_3 group; the other involving O^- Asp13, NH_3^+ from Lys9, Lys10, and Lys16. The six polar groups and the amidation of C-terminus lead to a peptide net charge Q= +3. In search of achieve the separation of these charge clusters, as seen in MP1 (dos Santos Cabrera et al. 2008), the new sequence was constructed with eighteen amino acid residues in length. It enabled the residues positioning according to neighborhood i, i+4 by favoring the helical stabilization.

The starting L1A sequence was projected by using the positioning of the hydrophilic and hydrophobic residues in the helical wheel projection of MP1. MD simulation of the L1A sequence was performed to estimate the helical content, charge balance by ion pairing, and solvation, as had been done previously for MP1 [dos Santos Cabrera et al., 2008]. Various MD simulations were performed with changes in the sequence with the objective of enhance the interactions among lateral chains by keeping a significant helical content and suitable backbone hydration. If the change impaired these aspects, it was rejected and new changes were made and checked until obtain the final sequence.

The final sequence (fig. 1A) is characterized by a mean residue hydrophobicity <H> = -0.1, mean hydrophobic moment μ=0.36, both calculated using Eisenberg consensus sequence [Eisenberg, 1984]. The hydrophobic moment is slightly larger than that of MP1 for which μ=0.29. In the helical wheel projection the acidic residues are inserted in the polar face limited by the basic residues defining a polar face angle (Φ=140°) slightly higher than in MP1 (Φ=120°). Aiming to get information about the peptide-bilayer interaction, the tryptophan residue was inserted in the 8th position. It is in the structured portion of the peptide, which is different from MP1 in which the tryptophan is the third residue in a flexible and non-helical segment.

Trying to understand the role played by the N-terminus charge on the helix stability and on the lytic and biological activities two analogs was synthesized. In one analog, Ac-L1A (fig. 1B), the N-terminus was blocked by acetylation, a modification that has been emphasized to reduce the repulsive charge – dipole interaction stabilizing the helical structure [Fairman et al., 1989, Marqusee and Baldwin, 1987]. In the other analog (fig. 1C) the fluorescent probe *ortho*-aminobenzoic acid was covalently bonded to the N-terminus. In this analog the tryptophan residue was substituted by a valine residue (W8V) to avoid energy transfer. This substitution does not resulted in significant change in the amphipathic characteristics of the peptide, see fig. 1. The Abz was chosen due to its high quantum yield (Φ=0.6) (Ito., et al 1998) which provide results more need to use a lower concentration of peptide. The free energy for transferring the peptide from water to the bilayer, estimated using Mpex computer package [Jaysinge et al., 2010 and using interface scale is ΔG = -2.6 Kcal/mol for L1A and ΔG = -2.9 Kcal/mol. The transfer is more favorable compared to MP1 (ΔG = -2.3 Kcal/mol) using the same helix fractions.

The MD data showed that after 50 ns simulation the peptides have a significant helical content. Analyzing the distances between the NH of a residue with the CO of its fourth neighbor residue (i, i+4) simultaneously with the backbone dihedral angles (φ, ψ) for the timeframes throughout the simulations, we observe for L1A that in average 7 hydrogen bonds are stable for more than 70% of the simulation time as shown in the fig. 2. Hydrogen bonds were formed by atoms O (oxygen) and N (nitrogen) in the residues, D2-A6 (3), G3-I7(4), L4-W8(5), K5-K9(6) and, I7-V11(8) on average 80% of the timeframe, indicating that these residues contribute to the stabilization of the helical conformation.

The analogs with modified N-terminal showed the addition of one hydrogen bond between the residues I1-K5(2) around 80-90% of the timeframe; besides the interaction between Abz and Leu4 in the peptide Abz-L1A-W8V. The modification at the N-terminal left the helix more stable with 10 and 11 hydrogen bonds that were maintained, on average, for more than 80% of the timeframe for Abz-W8V-L1A and Ac-L1A respectively, the higher stability of the helix can be observed, more pronunced for Ac-L1A fig.3.

The distances among charged and polar groups as well as its standard deviation were evaluated and the results are shown in the table 1. These ion pairs contribute to stabilize or to sustain the helical conformation in these regions.

3.2 Circular Dichroism Analysis. The circular dichroism spectra of the peptides in water or buffer showed a negative band near 200 nm and only a slight drift from the base line in 220 nm indicating random coil conformation. In contact with zwitterionic and anionic vesicles the peptides present a conformational transition to helical structures and the CD spectra are characterized by two negative dichroic bands at 222 and 208 nm as shown in the fig. 4 for Abz-L1A-W8V. The intensities of these bands increase with the total lipid concentration up to 400 μM where the maximum spectral change was observed. These spectra show that the 208 nm band is more intense than 222 nm suggesting that up to this lipid to peptide molar concentration ratio ([L]/[P] =20) the peptides are in the monomeric form in the vesicles. The helical fractions calculated from the CD spectra are shown in the table 2. Their helical contents in anionic vesicles are those obtained in zwitterionic vesicles; however the N-terminus modified analogs are more structured than the most charged peptide L1A. The helix fractions shown in this table 2 indicate that the effect of the N-terminus modifications were slightly higher in zwitterionic vesicles.

3.3 Zeta potential titration. The peptide adsorption to POPC/POPG (80:20) vesicles was also monitored by changes in the zeta potential. The zeta potential values of vesicles, at 40 μM total lipid concentration, in the absence and in the presence of increasing peptide concentrations were shown in the fig. 5. In the absence of peptide the zeta potential of vesicle was around -22 mV and with peptide addition the zeta potential increased smoothly up to its reversion to positive values. Unexpectedly the

peptide concentrations to achieve potential reversion were lower for the analogs with lower net charges when the opposite was expected. This result suggests that the affinities of the analogs to anionic vesicle are higher in comparison to L1A in good agreement with the results obtained from CD and fluorescence spectroscopies.

3.4 Lytic activity in liposomes. The membrane permeabilization activities of the peptides L1A and its analogs Ac-L1A and Abz-L1A-W8V were investigated in dye leakage experiments. In these experiments aliquots of vesicles containing entrapped fluorescent dye carboxyfluoresceine are added to a peptide solution and the de-quenching of the dye was monitored as a function of the elapsed time. The addition of vesicles was followed by an exponential growth in the fluorescence intensity; such that, after just 1 minute the leakage was almost complete. The dose-response curves, percentage of leaked dye (% leakage) vs the peptide to lipid molar concentration ratios ([P]/[L]), obtained after 1 min of vesicle addition are shown in the fig. 6. The [P]/[L] ratios to achieve 50% of dye release ($[P]/[L]_{50}$) indicate that these peptides are more efficient in anionic vesicle. The $[P]/[L]_{50}$ values obtained in zwitterionic vesicle after 1 min of peptide action for L1A, Ac-L1A and Abz-L1A are 0.24, 0.37 and 0.06M and in anionic vesicles 0.09, 0.075 and 0.027M respectively. After 5 min of action in zwitterionic vesicles the $([P]/[L])_{50}$ were 0.15, 0.20 and 0.046M and in anionic vesicles 0.062, 0.048 and 0.018M respectively. Although these results emphasize that the vesicles charge is important to the peptide selectivity the $([P]/[L])_{50}$ values reveal, however, that the analogs, with lower net charges, were more efficient to permeabilize vesicles. Besides the lower $([P]/[L])_{50}$ the Abz analog has the most cooperatives dose-response.

3.5 Biological Activities. The biological activities of L1A and analogs were assessed by estimating their minimum inhibitory concentrations and the hemolytic efficiency, whose values are displayed in the table 3. This table shows also the MIC for the control, chloramphenicol, and includes the ratios of MIC of MP1 and chloramphenicol. The antimicrobial activities of these peptides showed that they were more efficient against the two Gram negative bacteria strains and displayed lower efficacy against *S. aureus*. Considering the Gram negative bacteria, however, the comparison of the ratios between the MICs of peptides and those of the control for L1A and for MP1 shows that the

efficiency of L1A is similar to MP1. The decreased efficacy observed for the analogs is probably related to their lower net charge that could result in weaker electrostatic interaction with the anionic lipopolysaccharides of the outer membrane of Gram negative bacteria. The hemolytic activity was evaluated at a peptide concentration which is twice the largest concentration used to kill bacteria. It was observed only 4-5 % of hemolysis for L1A and the acetylated analog, which are very low compared to the almost 100% for mellitin used as control. This low hemolytic activity is comparable to those of MP-1. The hemolytic activity of Abz analog was, however, surprisingly very high, around ten times the observed to L1A and Ac-L1A. The analogs have the same physicochemical parameters which describe the peptides amphipathicity and the same net charges (Q=+2) due to the N-terminus modification. The unique difference in their sequence is the W8V substitution in the Abz analog, which result in a slight increase of the mean hydrophobicity of the hydrophobic face, from 0.41 to 0.43. This increase seems to be very small to be responsible for the increased hemolytic activity.

4. DISCUSSION

The simulations have also shown that the acidic, basic and polar residues suggesting ions pairing among D2 with K5 and, D13 with K9, K10, K16 and N17. These two groups of ion pairing stabilize the helical structure and provide hydration of part of the backbone. In addition to the electrostatic interactions, the backbone hydration, modulate both the preference of the peptide to anionic vesicles and the perturbation imposed to the lipid bilayer upon peptide adsorption. We can observe through the molecular dynamics that the interaction between the group NH3 of N-terminal and O^- of Asp2 does not exist. Really are a considerable distance to occurrence of a salt bridge, but this distance is due to close in sequence and not by attraction.

MD simulations data in TFE/water mixture for 50 ns showed possible pairs of hydrogen bonding involving the backbone CO of i^{th} and NH $i+4^{th}$ residues were stable and can be compared to data obtained by CD at the same TFE concentration, indicate a helical content of 45%. For these residues the dihedral angles are characteristics of helical conformation. This implies that the helical content obtained from MD simulations is 40 to 45% for L1A, it is very near to that measured from the CD spectra

in the same TFE conditions fig.2. In SDS 8mM data from CD show an increased 62% of the helicoidal content of L1A to Abz-W8V-L1A, 0.36% and 0.58% equivalent 6-7 and 10 hydrogen bound for L1A and L1B respectively, corroborating the data of MD.

The conformational analysis by CD showed that, besides the stabilization of helical structure due to the C-terminus amidation [Sforça et al., 2004], the N-terminus modifications, in the analogs, also resulted in the increase in the helical content in lipid vesicles. The effects of these end modifications associated with the acidic residue in the second position at N-terminus contribute to the reduction of the repulsive interaction between N terminus and the helix macrodipole [Fairman et al., 1989]. As a consequence the helical content of the analogs are higher compared to L1A even in anionic vesicles. It is noteworthy that in the Abz-analog the tryptophan was substituted by valine that has slightly lower helix propensity than tryptophan nevertheless Abz-L1A-W8V was more structured than the acetylated analog. This stabilizing effect could be due to the increase of the hydrophobicity of the non-polar face in the Abz-analog, suggesting that hydrophobic interactions play a dominant role in the helix stabilization of the peptide by the lipid bilayer as also observed [Dathe et al., 2001].

The conformational change of the peptide due to the adsorption to zwitterionic and anionic vesicles is followed by the insertion of the peptides in the lipid bilayer as suggested by the fluorescence experiments. The spectral shift to lower wavelength observed upon the peptide adsorption to the lipid bilayer is characteristic of the change of the fluorophore environment from a polar to a less polar one. This environmental change of the fluorophore was also suggested by the fluorescence quenching experiments. The Stern-Volmer constants of tryptophan containing peptides, in zwitterionic and anionic vesicles, are in good agreement with the observed spectral shifts. The Stern-Volmer plots for the Abz-analog present a slight drift from linear as observed for L1A and Ac-L1A, suggesting two populations with different accessibilities to the quencher [Zanin et al., 2013]. The K_{SV} obtained for L1A and its two analogs in POPC/POPG are about half the value obtained in POPC indicating the strong preference for anionic vesicles compatible with CD results.

Besides the helix stabilizing effect, the N-terminus modifications also enhanced the peptides affinities to anionic vesicles assessed by zeta potential titrations. Surprisingly the peptide concentration to reverse the vesicle potential was larger for the most charged peptide indicating that the affinities of the modified peptides increased compared to

L1A. These results indicate that Abz-L1A-W8V has the highest affinity to anionic vesicle, in good agreement with the results from spectroscopy experiments. Besides higher affinity the N-terminus acetylation induced increase of the peptides penetration to the bilayer. The tryptophan and Abz fluorophores were more deeply buried and consequently inducing more perturbation on the lipid package of the membranes. The sequence designed induced leakage in lipid vesicle very quick and efficiently. The peptide concentrations to induce 50% of leakage after one minute indicate that they are more selective to anionic vesicles than MP1 [Leite et al., 2010]. The N-terminus modifications, acetylation or covalent bond of Abz, have improved the lytic efficiency and preserved the selectivity observed to L1A.

The improved selectivity observed for L1A and its acetylated form in vesicle leakage was also observed in their biological activities. These peptides showed significant bactericidal activity without being hemolytic. L1A and analogs were more efficient against Gram negative bacteria while MP1 showed broad spectra bactericidal activity [Souza et al., 2009]. Despite the increase of the peptides net charge, the efficacy of L1A in inhibiting growth of Gram positive bacteria decreased compared to MP1. Some structural factors could contribute for this effect for instance the broader polar angle in L1A, the higher hydrophobic moment and/or to the positioning of the acidic residues that in L1A are farther apart than in MP1. Determining which of these parameters is responsible for the differences observed is very difficult because these parameters act in a concerted way and they should be analyzed for the same net charges which means compare MP1 with the L1A analogs. The reduced net charges of the analogs were obtained by the modification of the N-terminus which is known to enhance the helix propensity of the peptide [Fairman et al., 1989, Marqusee and Baldwin et al., 1987]. The increase in the polar face angle in model peptide from 120º to 140º with concomitant increase of the hydrophobic moment of a hydrophilic peptide derived from magainin was observed to increase the lytic efficiency in zwitterionic and in less extension to anionic vesicle [Wieprecht et al., 1997]. This same modification led to reduction of the MIC to Gram negative and Gram positive bacteria [Wieprecht et al., 1997]. We have observed that Ac-L1A showed higher lytic efficiency in anionic vesicle than in zwitterionic and that it was more efficient than MP1. The acetylated analog showed also the same efficiency of MP1 to inhibit the growth of the *E. coli* (ATCC 35218) strain used and the this analog showed reduced efficacy to *P. aeruginosa* (ATCC 27853) and to *S. aureus* (ATCC 25923). This comparison suggests that the

lesser efficacy against Gram positive bacteria could be due to the separation of acidic residues in L1A preventing the extensive ion-pairing in the hydrophilic face.

L1A and the acetylated analog were virtually non- hemolytic as MP1 [Souza et al., 2009]. The increase in the hemolytic potency observed for the Abz analog is similar to that observed for the NBD labeled melittin [Raghuramanan and Chattopadhyay, 2007]. They observed increased hemolytic activity for the NBD covalently bonded at the N-terminus of melittin compared to the native peptide.

In conclusion taking into account those features which we have judged to provide selectivity in the antimicrobial peptide of MP1, the relative positioning of acidic and basic residues as third and fourth neighbors, allowing that each acidic residue can ion-pair with two amines; one of the acidic residues at the N-terminus, the hydrophilicity and width of the polar face, on the design of the new sequence resulted in a lytic selective peptide to anionic vesicles. The modifications of the N-terminus, reducing the microdipole-charge electrostatic repulsion, lead to higher α-helix content and consequently to a more stable amphipathic structure. In addition the N-terminus modifications resulted in deeper burying of tryptophan and Abz in the apolar region of the lipid bilayer with consequent higher perturbation of the lipidic packing leading to higher lytic activity in model membrane. The new sequence L1A and its acetylated analog showed to be selective peptides with potent bactericidal activities in Gram negative bacteria without being hemolytic.

Figures

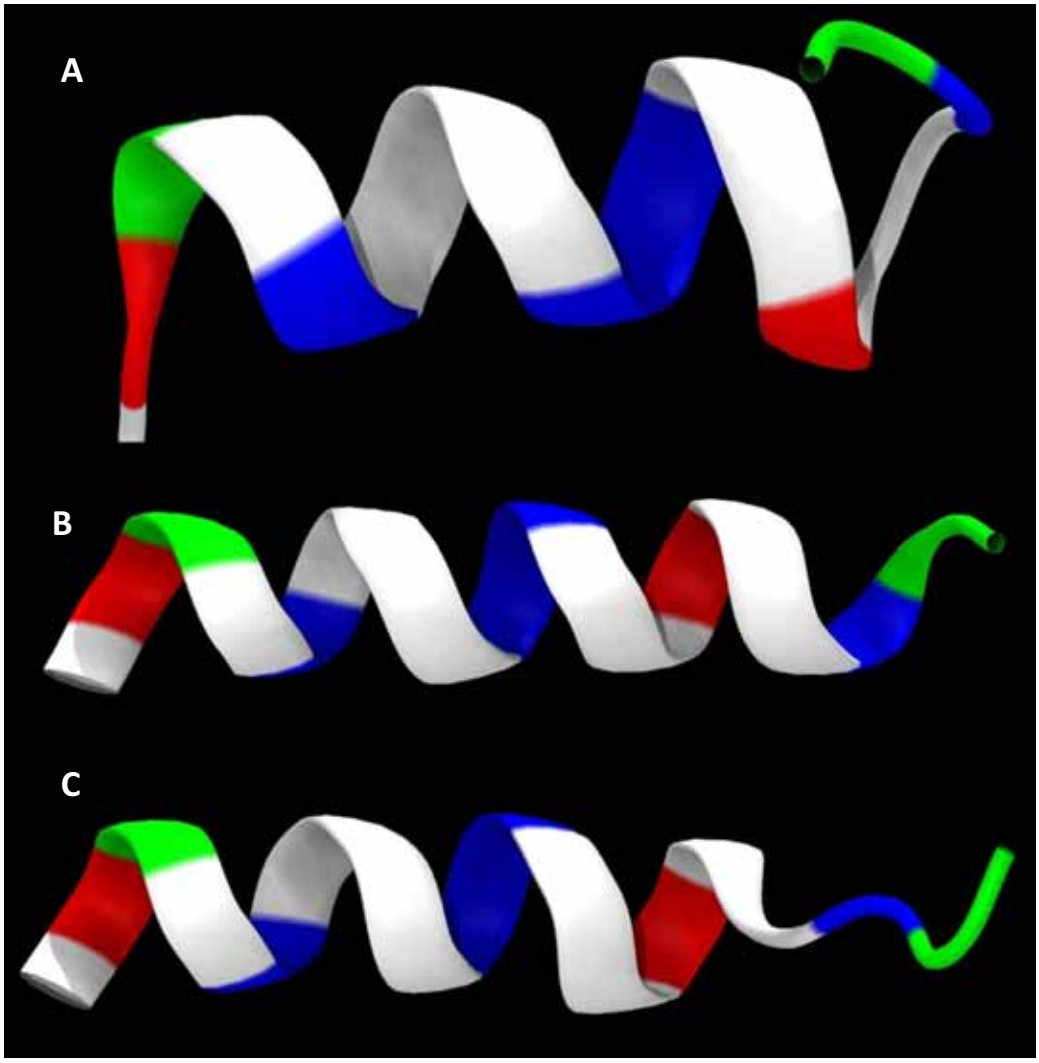

Fig. 1. Amphipathic α -helical structure of the peptides: L1A (A), Ac-L1A (B) and Abz-L1A-W8V (C) by molecular dinamics. Show hydrophilic residues (green), hydrophobic residues (white), potentially negatively charged (red), and potentially positively charged (blue).

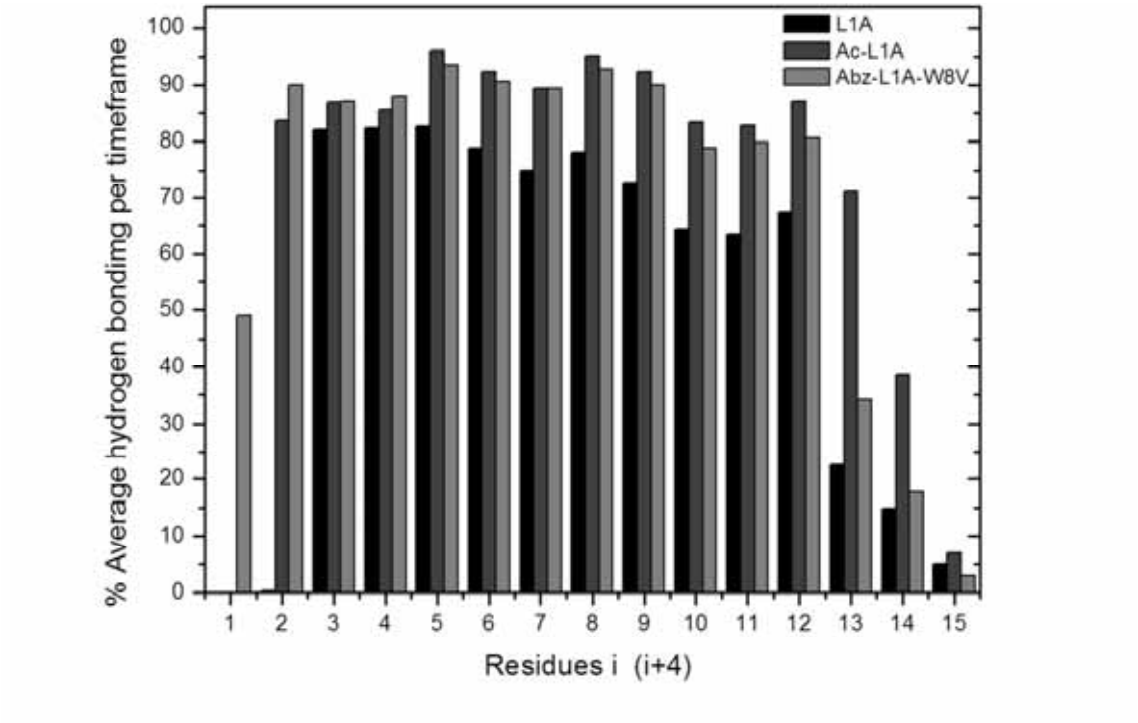

Fig. 2. The average number of hydrogen bonds of type i, i +4 over the 50 ns molecular dynamics.

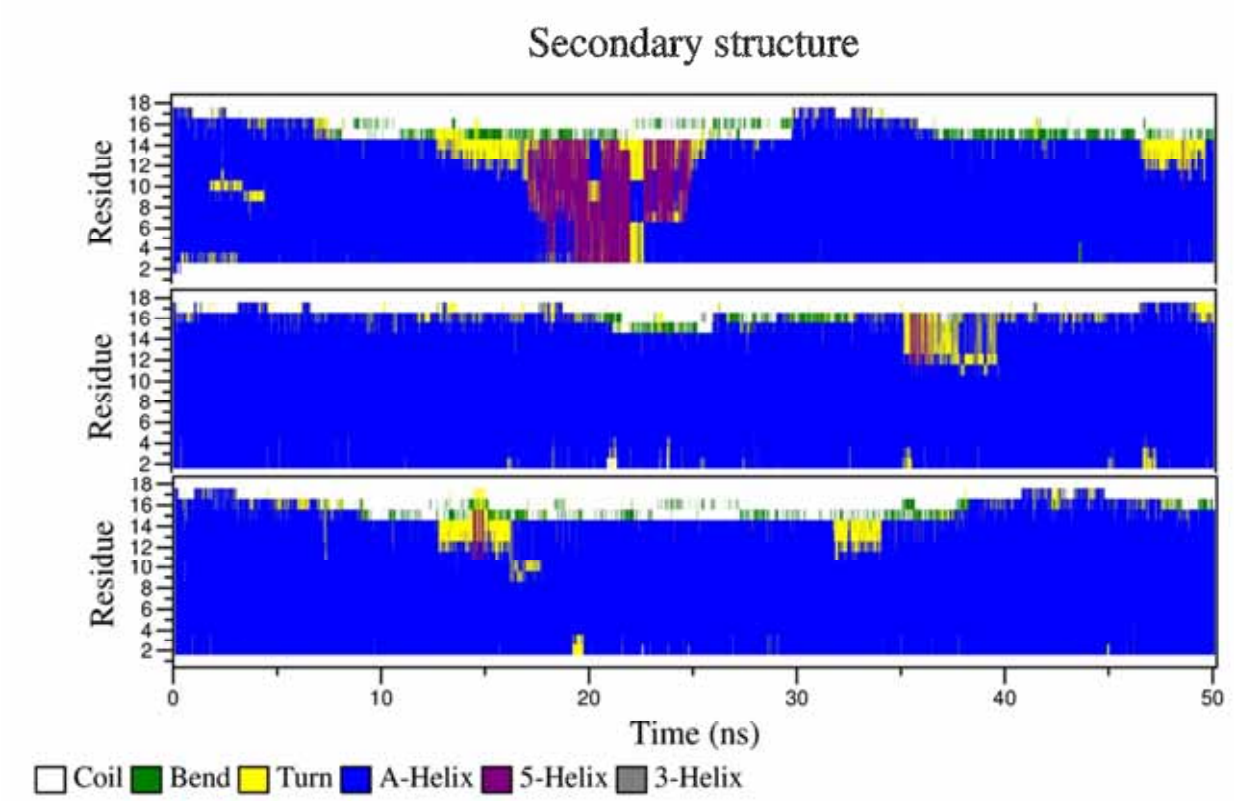

Fig. 3. The helical content obtained from MD simulations. Peptides: L1A (above), Ac-L1A (middle) and Abz-L1A-W8V (below).

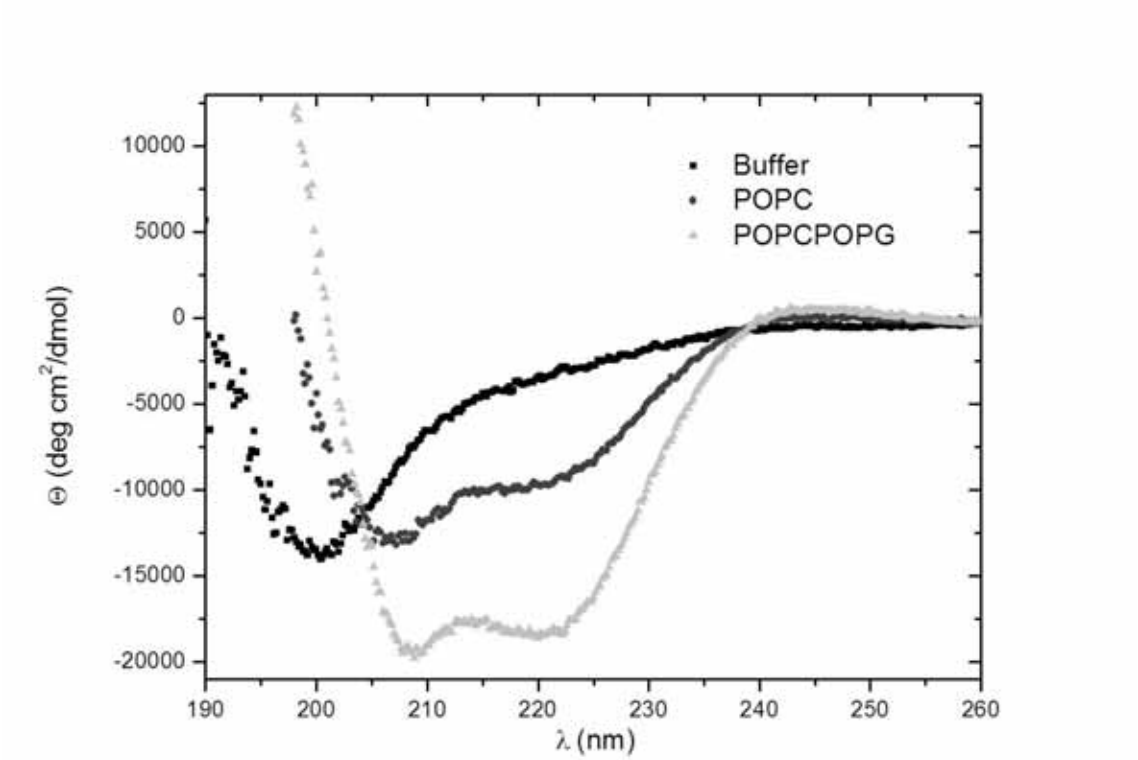

Fig. 4. Circular dichroism spectra of Abz-L1A-W8V at 20 μM in TRIS buffer in the absence and the presence of SUVs at 400 μM of vesicles POPC and POPC/POPG (80:20).

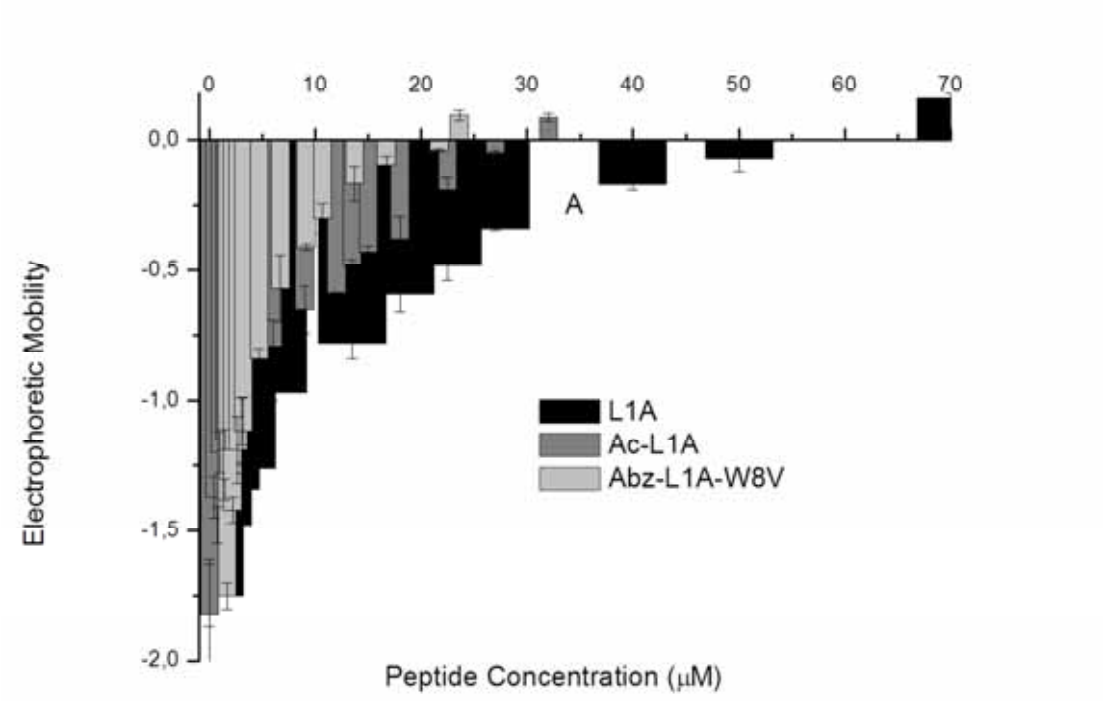

Fig. 5. Zeta potential of POC/POPG (8:2) large unilamellar vesicles (110 nm diameter) as a function of total peptide concentration when titrated with aliquots of L1A – (triangles), Ac-L1A (circles) and Abz-L1A-W8V (squares) at 40 μM total lipid concentration in Tris buffer 10 mM 150 mM NaCl.

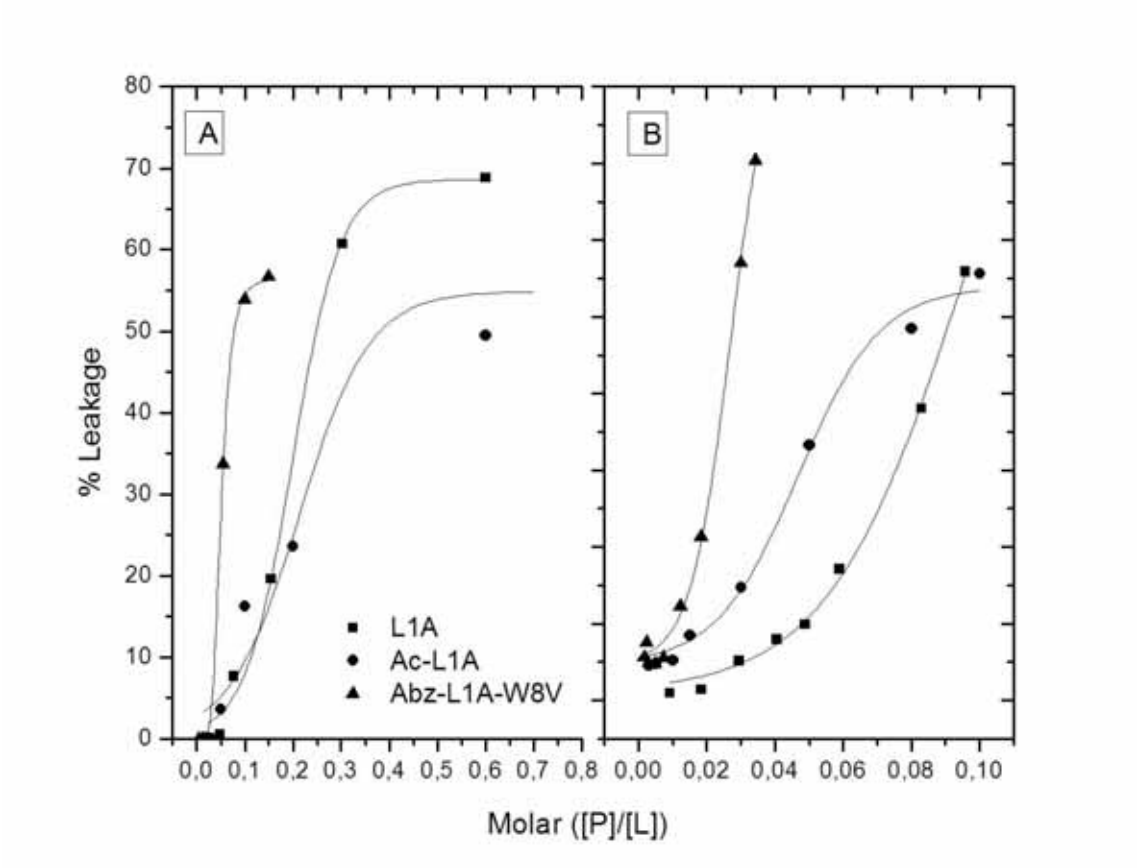

Fig. 6. Dose response curves for L1A and analogs induced leakage of carboxyfluorescein entrapped LUVs. The percentage of leakage is shown as a function of the ratio of peptide to total lipid molar concentrations after 1 minute of peptides action in A- POPC and B- POPC/POPG (8:2) LUVs for L1A (squares), Ac-L1A (up triangles) and Abz-L1A-W8V (circles). Total lipid concentration 100 µM.

Tables

Table 1. Average distance between charged groups. The selected groups for this calculation are: NH_3 side chains of lysine, NH_3 terminal connected to Ile1 and O side chains of aspartic acid.

	L1A		**Ac-L1A**		**Abz-L1A**	
Grupos de Cargas	Distância Média (Å)	Desvio Médio (Å)	Distância Média (Å)	Desvio Médio (Å)	Distância Média (Å)	Desvio Médio (Å)
ASP2:NH_3–Terminal	7.2	0.7	**-**	**-**	**-**	**-**
ASP2:LYS5	5.5	1.4	6.1	1.9	5.4	1.5
ASP2:LYS9	11.9	1.7	10.9	2.4	11.1	2.1
ASP2:LYS10	13.9	2.0	14.9	2.0	15.1	1.9
ASP2:LYS16	20.4	2.0	21.3	2.2	21.4	1.7
ASP13:NH_3–Terminal	17.8	1.5	-	-	-	-
ASP13:LYS5	16.2	2.1	16.5	1.8	16.7	1.7
ASP13:LYS9:	7.5	2.5	9.0	2.3	8.7	2.4
ASP13:LYS10	9.6	2.9	8.6	2.5	8.6	2.6
ASP13:LYS16	6.2	2.0	6.8	2.9	5.7	1.9
ASP13:ASN17	11.5	4.1	6.8	3.0	11.0	4.1

Table 2. Structural parameters and helix fractions in TFE, SDS and PC and PCPG vesicles for L1A, Ac-L1A, Abz-W8V-L1A, MP1, MPX.

	L1A		Ac-L1A		Abz-W8V-L1A		Polybia MP-1		MP-X	
Q	+3		+2		+2		+2 [c]		+4 [c]	
<H>	-0.11		-0.1		-0.1		-0.108 [c]		0.009 [c]	
μ	0.36		0.36		0.36		0.29 [c]		0.21 [c]	
Φ	140		140		140		120 [d]		100 [d]	
fα TFE 40%	0.45		-		0.45		0.41 [c]		0.61 [c]	
	PC [a]	PC/ PG [a]	PC [a]	PC/ PG [a]	PC [a]	PC/ PG [a]	PC	PC/ PG	PC	PC/ PG
f_h Vesicles	0.11	0.19	0.26	0.49	0.32	0.53	0.27[b,c]	0.36[b,c]	0.12[b,d]	0.4[b,d]
$\Delta\lambda_{max}$	28	32	34	35	6	6	19 [d]	22 [d]	18 [d]	21 [d]
K_{SVV}/K_{SVB}	0.6	0.27	0.31	0.15	0.28	0.11	0.32 [d]	0.27 [d]	0.38 [d]	0.28 [d]
[P]/[L] at EC_{50} vesicles	0.08	0.04	0.2	0.03	0.03	0.02	0.032	0.025	0.59	0.20

[a] vesicles POPC and POPCPOPG (80:2),

[b] vesicles of eggPC and egg PCPG (70:30)

[c] dos Santos Cabrera et al 2008

[d] Leite et al 2010

Table 3. Biological activities and hemolysis of synthetic peptides.

Peptides (μM)	**Gram -** *E. coli*	*P. aeruginosa*	**Gram +** *S. aureus*	Hemolysis (%)
IDGLKAIWKKVADLLKNT-NH_2	4.6	37.0	>74.0	4.0
Ac-IDGLKAIWKKVADLLKNT-NH_2	9.0	72.5	>72.5	5.0
Abz-IDGLKAIVKKVADLLKNT-NH_2	9.0	70.0	>70.0	46.0
Chloramphenicol	7.7	>124.0	30.9	
Polybia-MP1 / chloroamphenicol [a]	5.0/12.0	5.0/22.0	9.0/22.0	
Polybia-MP1	-	-	-	5
Melittin				100

*Percentage of hemolysis at a 300ug of the peptides or 148, 145, 140 and 110 μM of the L1A, Ac-L1A, Abz-L1A-W8V and melittin. Chloramphenicol and melittin were used as controls for antibacterial and hemolytic activities respectively.

[a] Souza et al, 2009.

REFERENCES

Berendsen HJC, Postma JPM, van Gunsteren WF, Hermans J. Interaction models for water in relation to protein hydration. In: Pullman B (ed) Intermolecular forces. Reidel, Dordrecht 1981; 331–342.

Berendsen HJC, Postma JPM, van Gunsteren WF, DiNola A, Haak JR (1984). Molecular dynamics with coupling to an external bath. The Journal of Chemical Physics 1984;81:3684–3690.

Darden T, York D, Pedersen L. Particle mesh Ewald: An N·log(N) method for Ewald sums in large systems. The Journal of Chemical Physics 1993;98:10089–10092.

Dathe M, Nikolenko H, Meyer J, Beyermann M, Bieneert M. Optimization of the antimicrobial activity of magainin peptides by modification of charge. FEBS Lett 2001;501:146-50.

Deber CM, Li S-C. Peptides in membranes: helicity and hydrophobicity. Biopolymers 1995;37:295-318.

Dos Santos Cabrera MP, Arcisio-Miranda M, Gorjão R, Leite NB, de Souza BM, Curi R, et al. Influence of the Bilayer Composition on the Binding and Membrane Disrupting Effect of Polybia-MP1, an Antimicrobial Mastoparan Peptide with Leukemic T-Lymphocyte Cell Selectivity. Biochemistry 2012;51(24):4898-908.

Dos Santos Cabrera MP, Costa STB, Souza BM, Palma MS, Ruggiero JR, Ruggiero Neto J. Selectivity in the mechanism of action of mastoparan antimicrobial peptide Polybia-MP1. Eur Biophys J 2008;37:879-91.

Eisenberg D. Three-dimensional structure of membrane and surface proteins. Annu Rev Biochem 1984;53:595–623.

Fairman R, Shoemaker KR, York EJ, Stewart JM, Baldwin RL. Further studies of the helix dipole model: effects of a free α-NH_3^+ or α-COO^- group on helix stability. Proteins 1989;5:1-7.

Fioroni M, Burger K, Mark AE, Roccatano D (2000) A new 2,2,2- trifluoroethanol model for molecular dynamics simulations. J Phys Chem B 104:12347–12354

Fjell CD, Hancock REW and Cherkasov A. AMPer: a database and an automated discovery tool for antimicrobial peptides. Bioinformatics 2007;23:1148–55.

Hamil P, Brown K, Jensen H, Hancock REW. Novel anti-infectives: is host defence the answer? Curr Opinion Biotechnol 2008;19:628-36.

Hess B, Bekker H, Berendsen HJC, Fraaije JGE (1997) LINCS: a linear constraint solver for molecular simulations. J Comp Chem 18:1463–1472

Korkmaz B, Attucci S, Juliano MA, Kalupov T, Jourdan ML, Juliano L, et al. Measuring elastase, proteinase 3 and cathepsin G activities at the surface of human neutrophils with fluorescence resonance energy transfer substrates. Nat Protoc 2008;3(6):991-1000.

Ladokhin AS, Jayasinghe S, White, SH. How to measure and analyze the tryptophan fluorescence in membrane properly and why bother. Anal Biochem 2000;285(2):235-45.

Leite NB, Costa LC, Alvares DS, dos Santos Cabrera MP, Souza BM, Palma MS, et al. The effect of acidic residues and amphipathicity on the lytic activities of mastoparan peptides studied by fluorescence and CD spectroscopy. Amino Acids 2011;40:91-100.

Lindahal E, Hess B, van der Spoel D (2001) Gromacs 3.0: a package for molecular simulations and trajectory analysis. J Mol Model 7:306–317

Malde AK, Zuo L, Breeze M, Stroet M, Poger D, Nair PC, Oostembrink C, Mark AE. An Automated Force Field Topology Builder (ATB) and Repository: Version 1.0. Journal of Chemical Theory and Computation 2011;7:4026–4037.

Marqusee S, Baldwin RL. Helix stabilization by $Glu^{-}\cdots Lys^{+}$ salt bridges in short peptides of de novo design. Proc. Acad. Sci. USA 1987;84:8898- 902.

Matsuzaki K. Control of cell selectivity of antimicrobial peptides. Biochim Biophys Acta 2009;1788:1687-92.

Miyamoto S, Kollman PA (1992) SETTLE: an analytical version of the SHAKE and RATTLE algorithm for rigid water models. J Comput Chem 13:952–962

Meletiadis J, Meis JGM, Mouton JW, Donnelly VPE. Comparison of NCLS and 3-(4,5-dimethyl-2-yhyazil)-2,5-diphenyl-2H tetrazolium bromide (MTT) method of in vitro susceptibility testing of filamentous fungi and development of a new simplified method. J Clin Microbiol 2000;38:2949-54.

Pronk S, Páll S, Schulz R, Larsson P, Bjelkmar P, Apostolov R, Shirts MR, Smith JC, Kasson PM, van der Spoel D, Hess B, Lindahl E. GROMACS 4.5: a high-throughput and highly parallel open source molecular simulation toolkit. Bioinformatics 2013;29: 845–854.

Raghuramanan H, Chattopadhyay A. Orientation and dynamics of melittin in membranes of varying composition utilizing NBD fluorescence. Biophys J 2007;92:1271-83.

Rouser G, Fleischer S, Yamamoto A. Two Dimensional Thin Layer Chromatographic Separation of Polar Lipids and Determination of Phospholipids by Phosphorus Analysis of Spots. Lipids 1970;5:494-96.

Schuler L, Daura X, Van GUNSTEREN WF. An improved GROMOS96 force field for aliphatic hydrocarbons in the condensed phase. Journal of computational chemistry 2001;22:1205–1218.

Sforça ML, Oyama Jr S, Canduri F, Lorenzi CCB, Pertinhez T, Konno K, et al. How C-terminus carboxyamidation alters the biological activity of peptides from the venon of the Eumenine solitary wasp. Biochemistry 2004;43:5608-17.

Souza BM, Silva AVR, Resende VMF, Arcuri HA, dos Santo Cabrera MP, Ruggiero Neto J, Palma, MS. Characterization of two novel polyfunctional mastoparan peptides from the venom of the social wasp Polybia paulista. Peptides 2009;30:1387-95.

Wang G, Watson KM, Peterkofsky A, Buckheit RW. Indentification of novel human immunodeficiency virus Type 1- inhibitory peptides based on the antimicrobial peptide database. Antimicrob Agents Chemother. 2010;53:1343-6.

Wang K, Yan J, Zhang B, Song J, Jia J, Jia P, et al. Novel mode of action of polybia-MP1 a novel antimicrobial peptide in multidrug resistant leukemic cells. Cancer Lett. 2009;278:65-72.

Wang KR, Zhang BZ, Zhang W, Yan JX, Li J, Wang R. Antitumor effects and cell selectivity and structure-activity relationship of a novel antimicrobial peptide Polybia-MP1. Peptides 2008;29:2320-7.

Wang Z, Wang G. APD: the Antimicrobial Peptide Database. Nucleic Acids Res 2004;32: D590–592.

Wieprecht T, Dathe M, Krause E, Beyermann M, Maloy WL, MacDonald DL, Bienert M. Modulation of membrane activity of amphipathic, antibacterial peptides by slight modifications of the hydrophobic moment. FEBS Lett 1997;417:135–40.

Zasloff M. Antimicrobial peptides of multicellular organisms. Nature 2002;415:389-95.

Zanin LM, Dos Santos Alvares D, Juliano MA, Pazin WM, Ito AS, Ruggiero Neto J. Interaction of a synthetic antimicrobial peptide with model membrane by fluorescence spectroscopy. Eur. Biophys 2013;42;819-831.

4 CONCLUSÃO

Nesse trabalho foi desenhado com auxílio da dinâmica molecular um novo peptídeo com potencial antimicrobiano e não hemolítico contendo dezoito resíduos de aminoácidos (L1A) com carga, Q=+3. Também foram desenvolvidos dois peptídeos análogos: Ac-L1A e Abz-L1A-W8V, com os quais foi possível estudar alterações na região do N-terminal.

Os peptídeos com a inserção do Abz ou acetil perderam a carga positiva proveniente do NH_3^+ do N-terminal livre em L1A, devido essa modificação a carga final dos peptídeos foi reduzida, Q=+2. Esses peptídeos apresentaram maior teor helicoidal se comparado ao peptídeo L1A, observados em dinâmica molecular e em dicroísmo circular.

Podemos concluir que os peptídeos interagem com vesículas lipídicas de caráter zwitterionico (POPC) e aniônico (POPC/POPG), com maior intensidade em vesículas aniônicas. Menores valores da constante de Ster-Volmer (Ksv) foram evidenciados para vesículas aniônicas, e sugere-se que os peptídeos análogos estão mais enterrados na bicamada lipídica, com menores valores para Abz-L1A-W8V. A eficiência na atividade lítica se apresentou na seguinte ordem: Abz-L1A-W8V>Ac-L1A>L1A para ambas vesículas, menores valores da razão $([P]/[L])_{50}$ foram encontrados para os análogos, corroborando os demais experimentos de fluorescência e potencial zeta.

As medidas de fluorescência resolvidas no tempo para os peptídeos com sonda Trp se apresentaram em três tempos de vida, atribuídos a diferentes conformações em torno do anel indol da ligação C_α-C_β da cadeia lateral da alanina (isômeros). A inserção do acetil no N-terminal do Ac-L1A alterou conformacionalmente a molécula ou o resíduo de Trp, visto pelo fator pré-exponencial. Os peptídeos aumentaram o tempo de vida na presença de vesículas com maiores valores para vesícula aniônica. O peptídeo com a sonda Abz se apresenta em dois tempos de vida e sua ligação nas vesículas, aniônica e zwitteriônica não altera o equilíbrio dos seus isômeros no peptídeo Abz-L1A-W8V.

No decaimento da anisotropia podemos observar que os peptídeos apresentam difusão rotacional reduzida com adição de vesícula, com menores valores para Abz-L1A-W8V em POPO/POPG. Esses resultados sugeriu que os peptídeos estão se deslocando para um meio menos polar e mais restrito.

Os testes de atividade biológica foram realizados com bactérias Gram positivo: *Staphylococcus aureus* (ATCC 25923) e Gram negativo: *Escherichia coli* (ATCC

35218) and *Pseudomonas aeruginosa* (ATCC 27853). O peptídeo L1A demonstra a melhor atividade antimicrobiana e melhor seletividade.

Os peptídeos L1A e Ac-L1A apresentaram 4 e 5% de hemólise, enquanto o Abz-L1A-W8V 46% de hemólise, pode ser atribuído a um efeito causado pela sonda extrínseca Abz ou a troca do resíduo de triptofano pela valina

REFERÊNCIAS

BABAKHANI, A.; GORFE, A. A.; KIM, J. E.; MCCAMMON, J. A. Thermodynamics of peptide insertion and aggregation in a lipid bilayer. *Phys Chem B*, v. 112, n. 34, p. 10528-10534, 2008.

BAGHERI, M. Cationic Antimicrobial Peptides: Thermodynamic Characterization of Peptide-Lipid Interactions and Biological Efficacy of Surface-Tethered Peptides. Tese (Doktors der Naturwissenschaften) Fachbereich Biologie, Chemie, Pharmazie der Freien Universität Berlin, Berlin 2010.

BECHINGER, B. E.; LOHNER, K. Detergent-like actions of linear amphipathic cationic antimicrobial peptides. *Biochimica et Biophysica Acta (BBA) - Biomembranes*, v. 1758, n. 9, p. 1529-1539, 2006.

BESSALLE, R.; HAAS, H.; GORIA, A.; SHALIT, I.; FRIDKIN, M. Augmentation of the antibacterial activity of magainin by positive-charge chain extension. *Antimicrob Agents Chemother*, v. 36, n. 2, p. 313–317, 1992.

BLONDELLE, S. E.; HOUGHTEN, R. A. Design of model amphipathic peptides having potent antimicrobial activities. *Biochemistry*, v. 31, n. 50, p. 12688–12694, 1992.

BROGDEN, K. A. Antimicrobial peptides: pore formers or metabolic inhibitors in bacteria? *Nature Reviews Microbiology*, v. 3, n. 3, p. 238-250, 2005.

CABIAUX, V.; AGERBERTH, B.; JOHANSSON, J.; HOMBLÉ, F.; GOORMAGHTIGH, E.; RUYSSCHAERT, J.-M. Secondary structure and membrane interaction of PR-39, a Pro+Arg-rich antibacterial peptide. *Eur. J. Biochem*, v. 224, n. 3, p. 1019-1027, 1994.

CRONAN, J. E. Bacterial membrane lipids: where do we stand? *Annu Rev Microbiol*, v. 57, p. 203–224, 2003.

DATHE, M.; WIEPRECHT, T. Structural features of helical antimicrobial peptides: their potential to modulate activity on model membranes and biological cells. *Biochim. Biophys. Acta,* v. 1462, n. 1-2, p. 71-87, 1999.

DATHE, M.; MEYER, J.; BEYERMANN, M.; MAUL, B.; HOISCHEN, C.; BIENERT, M. General aspects of peptide selectivity towards lipid bilayers and cell

membranes studied by variation of the structural parameters of amphipathic helical model peptides. *Biochimica et Biophysica Acta*, v. 1558, p. 171-186, 2002.

DENNISON, S. R.; WALLACE, J.; HARRIS, F.; PHOENIX, D. A. Amphiphilic alpha-helical antimicrobial peptides and their structure/function relationships. *Protein Pept Lett*, v. 12, n. 1, p. 31–39, 2005.

EISENBERG, D. Three-dimensional structure of membrane and surface proteins. *Annual Review of Biochemistry*, v. 53, p. 595–623, 1984.

FALLA, T. J.; KARUNARATNE, D. N.; HANCOCK, R. E. W. Mode of action of the antimicrobial peptide indolicidin. *J. Biol. Chem,* v. 271, p. 19298-19303, 1996.

GUDMUNDSSON, G. H.; AGERBERTH, B.; ODEBERG, J.; BERGMAN, T.; OLSSON, B. E SALCEDO, R. "The human gene FALL39 and processing of the cathelin precursor to the antibacterial peptide LL-37 in granulocytes". *European Journal of Biochemistry*, v. 238, n. 2, p. 325-332, 2004.

HARWIG, S. S.; SWIDEREK, K. M.; LEE, T. D.; LEHRER, R. I. Determination of disulphide bridges in PG-2, an antimicrobial peptide from porcine leukocytes. *J. Pept. Sci.* v. 1, n. 3, p. 207-215, 1995.

HANCOCK, R. E. W. Cationic peptide: effectors in innate immunity and novel antimicrobials. *Lancet Infect. Dis*, v. 1, n. 3, p. 156-164, 2001.

HANCOCK, R. E. W.; ROZEK, A. Role of membranes in the activities of antimicrobial cationic peptides. *FEMS Microbiol. Lett.* v. 206, n. 6, p. 143-149, 2002.

HELMERHORST, E. J.; BREEUWER, P.; VAN'T HOF, W.; WALGREEN-WETERINGS, E.; OOMEN, L. C.; VEERMAN, E. C.; AMERONGEN, A. V.; ABEE, T. The cellular target of histatin 5 on Candida albicans is the energized mitochondrion. *J. Biol. Chem*, v. 274, n. 11, p. 7286-7291, 1999.

HUANG, H. W. Free energies of molecular bound states in lipid bilayers: lethal concentrations of antimicrobial peptides. *Biophys J*, v. 96, n. 8, p. 3263–3272, 2009.

JENSSEN, H.; HAMILL, P.; HANCOCK, R. E. W. Peptide antimicrobial agents. *Clinical microbiology reviews*, v. 19, n. 3, p. 491-511, 2006.

JONES, E. M.; SMART, A.; BLOOMBERG, G.; BURGESS, L.; MILLAR, M. R. Lactoferricin, a new antimicrobial peptide. *J. Applied Bacteriol,* v. 77, n.2, p. 208-214, 1994.

KIKUKAWA, T.; ARAISO, T. Changes in lipid mobility associated with alamethicin incorporation into membranes. *Arch. Biochem. Biophys,* v. 405, n. 2, p. 214-222, 2002.

LINDE, C. M. A.; HOFFNER, S. E.; REFAI, E.; ANDERSSON, M. In vitro activity of PR-39, a proline-arginine-rich peptide, against susceptible and multi-drug-resistant Mycobacterium tuberculosis. *J. Antimicrob. Chemother,* v. 47**,** n. 5, p. 575-580, 2001.

MANGONI, M. L.; RINALDI, A. C.; DI GIULIO, A.; MIGNOGNA, G.; BOZZI, A.; BARRA, D.; SIMMACO, M. Structure-function relationships of temporins, small antimicrobial peptides from amphibian skin. *Eur. J. Biochem*, v. 267, n. 5, p. 1447-1454, 2002.

MATSUZAKI, K. Why and how are peptide-lipid interactions utilized for self-defense? Magainins and tachyplesins as archetypes. *Biochim. Biophys. Acta,* v. 1462, n. 1-2, p. 1-10, 1999.

MATSUZAKI, K. Control of cell selectivity of antimicrobial peptides. *Biochimica et Biophysica Acta*, v. 1788, n. 8, p. 1687-1692, 2009.

MONTVILLE, T. J.; CHEN, Y. Mechanistic action of pediocin and nisin: recent progress and unresolved questions. *Appl. Microbiol. Biotechnol.* v. 50, n. 5, p. 511-519. 1998.

PASUPULETI, M.; WALSE, B.; SVENSSON, B.; MALMSTEN, M., SCHMIDTCHEN A. Rational design of antimicrobial C3a analogues with enhanced effects against Staphylococci using an integrated structure and function-based approach. *Biochemistry*, v. 47, n. 35, 9057–9070, 2008.

PASUPULETI, M.; SCHMIDTCHEN, A.; MALMSTEN, M. Antimicrobial peptides: key components of the innate immune system. *Crit Rev Biotechnol*, v. 32, n. 2, p. 143-171, 2012.

PETERS, B. M.; SHIRTLIFF, M. E.; JABRA-RIZK, MA. Antimicrobial Peptides: Primeval Molecules or Future Drugs? *PLoS Pathog*, v. 6, n. 10, e1001067. doi:10.1371/journal.ppat.1001067

PRENNER, E. J.; LEWIS, R. N.; MCELHANEY, R. N. The interaction of the antimicrobial peptide gramicidin S with lipid bilayer model and biological membranes. *Biochim. Biophys. Acta*, v. 1462, n.1-2, p. 201-221, 1999.

POUNY, Y.; RAPAPORT, D.; MOR, A.; NICOLAS, P.; SHAI, Y. Interaction of antimicrobial dermaseptin and its fluorescently labeled analogues with phospholipid membranes. *Biochemistry*, v. 31, p. 12416-12423, 1992.

POKORNY, A.; ALMEIDA, P. F. Kinetics of dye efflux and lipid flipflop induced by delta-lysin in phosphatidylcholine vesicles and the mechanism of graded release by amphipathic, alpha-helical peptides. *Biochemistry*, v. 43, n. 27, p. 8846–8857, 2004.

PUKALA, T. L.; BOWIE, J. H.; MASELLI, V. M.; MUSGRAVE, I. F. E TYLER, M. J. Hostdefence peptides from the glandular secretions of amphibians: structure and activity. *Natural Product Reports*, v. 23, n. 3, p. 368-393, 2006.

RAUSCH, J. M.; MARKS, J. R.; RATHINAKUMAR, R.; WIMLEY, W. C. Beta-sheet pore-forming peptides selected from a rational combinatorial library: mechanism of pore formation in lipid vesicles and activity in biological membranes. *Biochemistry*, v. 46, n. 43, p. 12124–12139, 2007.

SANSOM, M. S. P. Alamethicin and related peptaibols-model ion channels. *Eur. Biophys. J*, v. 22, n. 2, p. 105-124, 1993.

SEELIG, J. Thermodynamics of lipid–peptide interactions. *Biochim. Biophys. Acta*, v. 1666, p. 40-50, 2004.

SELSTED, M. E.; NOVOTNY, M. J.; MORRIS, W. L.; TANG, Y. Q.; SMITH, W.; CULLEN, J. S. Indolicidin, a novel bactericidal tridecapeptide amide from neutrophils. *J. Biol. Chem*, v. 267, n. 7, p. 4292-4295, 1992.

SHAI, Y.; OREN, Z. From "carpet" mechanism to de-novo designed diastereomeric cell-selective antimicrobial peptides. *Peptides*, v. 22, n. 10, p. 1629–1641, 2001.

SHAI, Y. Mode of action of membrane active antimicrobial. *Biopolymers*, v. 66, n.4, p. 236–248, 2002.

TAMAMURA, H.; WAKI, M.; IMAI, M.; OTAKA, A.; IBUKA, T.; WAKI, K.; MIYAMOTO, K.; MATSUMOTO, A.; MURAKAMI, T.; NAKASHIMA, H.; YAMAMOTO, N.; FUJII, N. Downsizing of an HIV-cell fusion inhibitor, T22

([Tyr5,12, Lys7]-polyphemusin II), with the maintenance of anti-HIV activity and solution structure. *Bioorganic. Med. Chem.*, v. 6, n.4, p. 473-479, 1998.

TOSSI, A.; SANDRI, L.,; GIANGASPERO, A. Amphipathic, alpha-helical antimicrobial peptides. *Biopolymers*, v. 55, n. 1, p. 4-30, 2000.

TYTLER, E. M.; ANANTHARAMAIAH, G. M.; WALKER, D. E.; MISHRA, V. K.; PALGUNACHARI, M. N.; SEGREST, J. P. Molecular basis for prokaryotic specificity of magainin-induced lysis. *Biochemistry*, v. 34, n. 13, p. 4393-4401, 1995.

UEMATSU, N.; MATSUZAKI, K. Polar angle as a determinant of amphipathic alpha-helix-lipid interactions: a model peptide study. *Biophy. J*, v. 79, n. 4, p. 2075-2083, 2000.

VAN'T HOF, W.; VEERMAN, E. C. I.; HELMERHORST, E. J.; AMERONGEN, A. V. N. Antimicrobial peptides: properties and applicability. *Biol. Chem.* v. 382, n. 4, 597-619, 2001.

WANG, T.; ZHANG, J.; SHEN, J. H.; JIN, Y.; LEE, W. H. E ZHANG, Y. Maximins S, a novel group of antimicrobial peptides from toad Bombina maxima. *Biochemical and Biophysical Research Communications*, v. 327, n. 3, p. 945-951, 2005.

WIMLEY, W. C. Describing the mechanism of antimicrobial peptide action with the interfacial activity model. *ACS Che Biol*, v. 5, n. 10, p. 905–917, 2010.

YEAMAN, M. R.; YOUNT, N. Y. Mechanisms of antimicrobial peptide action and resistance. *Pharmacol. Rev*, v. 55, n. 1, p. 27–55, 2003.

YOUNT, N. Y.; YEAMAN, M. R. Immunocontinuum: perspectives in antimicrobial peptide mechanisms of action and resistance. *Protein Pept Lett*, v. 12, n. 1, p. 49–67, 2005.

ZALTASH, S.; PALMBLAD, M.; CURSTEDT, T.; JOHANSSON, J.; PERSSON, B. Pulmonary surfactant protein B: a structural model and a functional analogue. *Biochim. Biophys. Acta*, v. 1466, n. 1-2, p. 179-186, 2000.

ZASLOFF, M. Antimicrobial peptides of multicellular organisms. *Nature*, v. 415, n. 6870, p. 389-395, 2002.

ZHAO, H.; RINALDI, A. C.; RUFO, A.; BOZZI, A.; KINNUNEN, P. K. J.; DI GIULIO, A. Structural and charge requirements for antimicrobial peptide insertion into biological and model membranes. In Pore-Forming Peptides and Protein Toxins (Menestrina, G., Dalla Serra, M. and Lazarovici, P., eds.), pp. 151-177, Harwood Academic Publishers, Reading, UK, 2002.